ENCAPSULATION OF REACTIVE COMPONENTS IN POLYURETHANE SYSTEMS.

Quentin Bouvier

ADVERTIMENT. L'accés als continguts d'aquesta tesi doctoral i la seva utilització ha de respectar els drets de la persona autora. Pot ser utilitzada per a consulta o estudi personal, així com en activitats o materials d'investigació i docència en els termes establerts a l'art. 32 del Text Refós de la Llei de Propietat Intel·lectual (RDL 1/1996). Per altres utilitzacions es requereix l'autorització prèvia i expressa de la persona autora. En qualsevol cas, en la utilització dels seus continguts caldrà indicar de forma clara el nom i cognoms de la persona autora i el títol de la tesi doctoral. No s'autoritza la seva reproducció o altres formes d'explotació efectuades amb finalitats de lucre ni la seva comunicació pública des d'un lloc aliè al servei TDX. Tampoc s'autoritza la presentació del seu contingut en una finestra o marc aliè a TDX (framing). Aquesta reserva de drets afecta tant als continguts de la tesi com als seus resums i índexs.

ADVERTENCIA. El acceso a los contenidos de esta tesis doctoral y su utilización debe respetar los derechos de la persona autora. Puede ser utilizada para consulta o estudio personal, así como en actividades o materiales de investigación y docencia en los términos establecidos en el art. 32 del Texto Refundido de la Ley de Propiedad Intelectual (RDL 1/1996). Para otros usos se requiere la autorización previa y expresa de la persona autora. En cualquier caso, en la utilización de sus contenidos se deberá indicar de forma clara el nombre y apellidos de la persona autora y el título de la tesis doctoral. No se autoriza su reproducción u otras formas de explotación efectuadas con fines lucrativos ni su comunicación pública desde un sitio ajeno al servicio TDR. Tampoco se autoriza la presentación de su contenido en una ventana o marco ajeno a TDR (framing). Esta reserva de derechos afecta tanto al contenido de la tesis como a sus resúmenes e índices.

WARNING. Access to the contents of this doctoral thesis and its use must respect the rights of the author. It can be used for reference or private study, as well as research and learning activities or materials in the terms established by the 32nd article of the Spanish Consolidated Copyright Act (RDL 1/1996). Express and previous authorization of the author is required for any other uses. In any case, when using its content, full name of the author and title of the thesis must be clearly indicated. Reproduction or other forms of for profit use or public communication from outside TDX service is not allowed. Presentation of its content in a window or frame external to TDX (framing) is not authorized either. These rights affect both the content of the thesis and its abstracts and indexes.

UNIVERSITAT ROVIRA i VIRGILI

Encapsulation of reactive components for polyurethane systems

QUENTIN BOUVIER

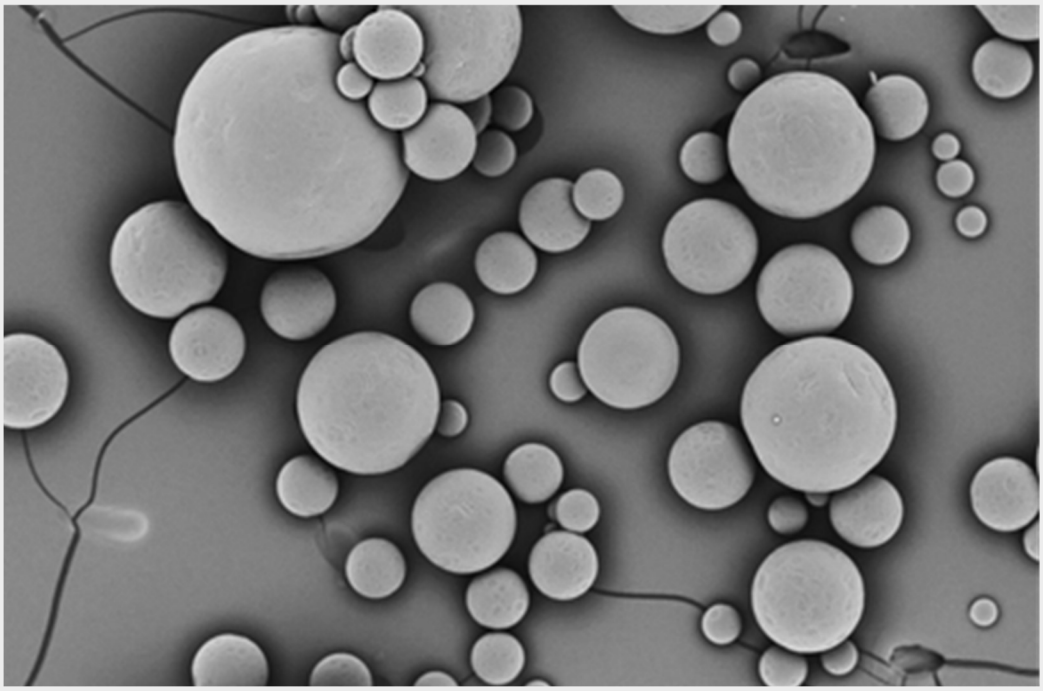

DOCTORAL THESIS

2021

Doctoral Thesis

Encapsulation of reactive components for polyurethane systems

Quentin Bouvier

supervised by Dr. Stefanie Eiden and Prof. Pablo Ballester

Tarragona

November 2021

Dr. Stefanie Eiden, Industrial Researcher, Project Manager and Senior Expert at Covestro Deutschland AG, and,

Prof. Pablo Ballester, Group Leader of the Institute of Chemical Research of Catalonia (ICIQ) and Research Professor of the Catalan Institution for Research and Advanced Studies (ICREA),

CERTIFY that the present study, entitled "Encapsulation of reactive components for polyurethane systems", presented by Quentin Bouvier to receive the degree of Doctor in Chemistry, has been carried out under our supervision in Covestro Deutschland AG and in the Institut Català d'Investigació Química, ICIQ, respectively.

Leverkusen, 05/11/2021

Doctoral Thesis Supervisor

Dr. Stefanie Eiden

Tarragona, 05/11/2021

Doctoral Thesis Supervisor

Prof. Pablo Ballester

This thesis is applying to the Industrial Doctorate mention. It is the result of the work done at Covestro Deutschland AG and at the Institut Català d'Investigació Química, ICIQ, in the framework of the NOAH-ITN supported by the European Union's Horizon 2020 research and innovation program under the Marie Sklodowska-Curie grant agreement No 765297.

Acknowledgements

The work in this thesis would not have been possible without the support and assistance of many other people, and some of them will be thanked here.

First and foremost, I would like to express my deepest gratitude to my industrial supervisors, Dr. Stefanie Eiden and Dr. Hans-Josef Laas, that have given me infinite guidance and support throughout my entire Ph.D. Thank you for the freedom you gave me to perform my research, and at the same time, being here as soon as I needed advices. I would also like to thank Dr. Raul Pires and Dr. Karsten Danielmeier, for welcoming me into their research unit at Covestro Deutschland AG, as well as all the other colleagues from Covestro that have been involved in the project. Especially Lars Fahrenkamp and Peter-Benno Klossek, for their day-to-day help in the lab, and my office partner, Dr. Veronika Eilermann, who was always kind and helpful to me.

I want to sincerely thank my academic supervisor Prof. Pablo Ballester for welcoming me in his group, as well as Dr. Gemma Aragay for her coordination of the Network of functional molecular containers with controlled switchable abilities (NOAH). Thank you both for your invaluable advices and help. Thank you also to the students I had the chance to collaborate with, Andrés Felipe Sierra, Andrea Rivoli, Chiara Mirabella, Dr. Dragos Dabuleanu, Pedro Ferreira, Dr. Qingqing Sun, Yifan Li and all the other students part of the NOAH network. I also want to thank the research units of ICIQ and URV for their help and availability, especially the URV microscopy unit.

I would also like to give special thanks to Prof. François Gabbaï (Texas A&M University) and Dr. Adrian Birch (The Dow Chemical Company), as the experience I gained while working with them has been vital for the success of this Ph.D.

Enfin et surtout, j'aimerais remercier mes parents pour leur soutien inconditionnel. Sans vous rien n'aurait été possible. Un grand merci à vous ! Merci aussi à mes amis qui m'ont soutenu durant ces trois années.

The NOAH project has received funding from the European Union's Horizon 2020 research and innovation program under the Marie Sklodowska-Curie grant agreement No 765297.

Abstract

Nowadays polyurethanes are widely used in the coating and adhesive industry. Many different technologies exist to apply coatings and adhesives on substrates and technologies in which crosslinking or adhesion could be controlled are of greatest interest. Indeed, this would offer new possibilities for complex coating/adhesive systems. For this purpose, special reagents called blocked polyisocyanates have already been developed; they are derivatives of isocyanates which can only be activated via thermal trigger. In a similar approach, the encapsulation and controlled release of polyurethane formulation components would offer new perspectives toward enhanced technologies. First, the nanoencapsulation of metal-based catalysts into polycaprolactone nanocapsules was successfully performed by emulsion-solvent diffusion and nanoprecipitation. An improved encapsulation efficiency was obtained when the nanocapsules were loaded with a mixture of the catalyst and glyceryl trioctanoate, as well as when the nanocapsules were synthesized with charged outer surfaces. The implementation of these nanocapsules into polyurethane coatings showed that they are suitable for the preparation of thermoresponsive coatings. Then, the encapsulation of aliphatic polyisocyanates was successfully achieved, either in polyurea microcapsules by interfacial polycondensation, or in polycaprolactone nanocapsules by nanoprecipitation. The encapsulation process and the long-term stability of the microcapsules was greatly improved by working on the polyurea shell properties, however, the microcapsules still remain fragile over time and could not be used industrially. The nanoencapsulation of polyisocyanates showed the isocyanate-water side-reaction is particularly challenging to prevent and it suggested that water-free encapsulation techniques, such as spray congealing, should be investigated.

Table of Content

List of Figures

List of Tables

List of Abbreviations

1K	-	One component
2K	-	Two components
BA	-	Butyl Acetate
BK22	-	Borchi Kat 22
BK24	-	Borchi Kat 24
CTAB	-	cetyltrimethylammonium bromide
DABCO	-	1,4-diazacyclo[2.2.2]octane
DBTL	-	Dibutyl tin laurate
DBU	-	1,8-diazabicyclo[5.4.0]undec-7-ene
DETA	-	Diethylenetriamine
DLS	-	Dynamic Light Scattering
DMA	-	Dynamic Mechanical Analysis
DMCHA	-	N,N-dimethylcyclohexylamine
DMF	-	Dimethylformamide
DN36	-	Desmodur N3600
DSC	-	Differential Scanning Calorimetry
EA	-	Ethyl Acetate
EAs-	-	Ethyl Acetate saturated-
EDX	-	Energy Dispersive X-Ray
EE	-	Encapsulation Efficiency
ESD	-	Emulsion Solvent-Diffusion
EW	-	Equivalent Weight
FESEM	-	Field Emission Scanning Electron Microscopy
FTIR	-	Fourier-Transform Infrared
GA	-	Gum Arabic
Gel	-	Gelatin type A
GTO	-	Glyceryl Trioctanoate
H_{12}MDI	-	Bis-(4-isocyanatocyclohexyl) methane
HD36	-	Hydrophilically-modified Desmodur N3600

HDI	-	Hexamethylene diisocyanate
IPDI	-	Isophorone diisocyanate
JT-403	-	Jeffamine T-403
MDI	-	Methylene diphenyl diisocyanate
MEK	-	Methyl Ethyl Ketone
MEKs-	-	Methyl Ethyl Ketone saturated-
MPA	-	Methoxypropyl Acetate
NCO	-	Isocyanate function N=C=O
NDBA	-	N-dibutylamine
PCL	-	Polycaprolactone
PCL-10	-	Polycaprolactone 10kDa
PCL-45	-	Polycaprolactone 45kDa
PCL-80	-	Polycaprolactone 80kDa
PDI	-	Polydispersity Index
PEG	-	Poly(ethylene glycol)
PEI	-	Poly(ethylene imine)
PGLA	-	Poly(glycolic-co-lactic acid)
PLA	-	Poly(lactic acid)
PVA	-	Poly(vinyl alcohol)
rpm	-	Rotation per minute
SDS	-	Sodium Dodecyl Sulfate
SEM	-	Scanning Electron Microscopy
TAP	-	2,4,6-triaminopyrimidine
TDI	-	Toluene diisocyanate
TEM	-	Transmission Electron Microscopy
TEPA	-	Tetraethylenepentamine
w/w	-	Weight by weight
v/v	-	Volume by volume
Ws-	-	Water saturated-

Chapter 1. General Introduction

1.1. From isocyanates to polyisocyanates

1.1.1. The isocyanate functional group

Organic compounds that contain the functional group R-N=C=O (NCO) are referred to as isocyanates. Compounds containing two or more NCO groups are respectively called diisocyanates or polyisocyanates. Such compounds are involved in a broad range of reactions due to the intrinsic reactivity of the functional group, which can be hinted from its resonance form (Fig. 1.1). The electrophilic carbon is able to react rapidly with various species containing hydrogen atoms. The reactivity of these compounds is also modified by the nature of the R group (mesomeric effect); therefore aromatic isocyanates are significantly more reactive than aliphatic isocyanates.

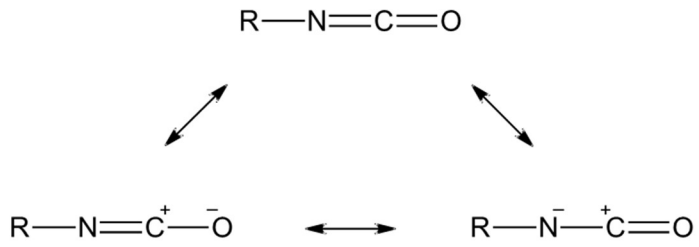

Figure 1.1. Isocyanate resonance

The first synthesis of aliphatic isocyanates was published by Wurtz in 1849 through a reaction between organic sulfates and cyanates[1]. The following year, Hofmann published a process to synthesize aromatic isocyanates by pyrolysis of symmetrical diphenyl oxamide[2]. In 1884, Hentschel discovered the synthesis process which is still used nowadays for the synthesis of isocyanates[3]. They are obtained by phosgenation of the corresponding primary amines (Fig. 1.2). The synthesis of diisocyanates/polyisocyanates is following the same path and using the corresponding polyamines as reagents.

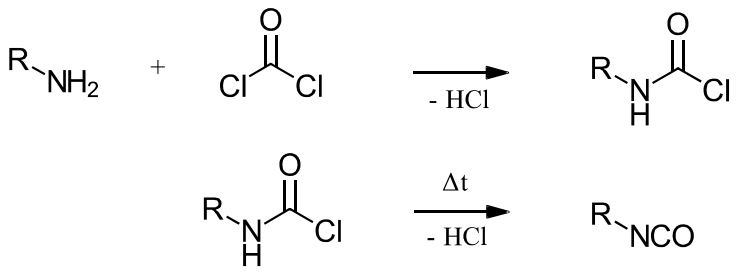

Figure 1.2. Synthesis of isocyanates by phosgenation of amines

Polyisocyanates are mostly used for the preparation of polyurethanes and polyureas by reaction with polyols and polyamines, respectively. Isocyanate compounds are defined by properties particularly employed in polyurethane chemistry:

- NCO content (%) defines the isocyanate content in the compound, as the weight percentage of isocyanate groups in the material. This value is mostly measured following the standard test method ASTM D2572-97. The isocyanate compound is allowed to react with an excess of N-dibutylamine. After the reaction has occurred, the remaining N-dibutylamine is determined by back titration with hydrochloric acid.
- Average functionality represents the average number of isocyanate groups per molecule.
- Viscosity ($mPa \cdot s$)
- Equivalent weight (g) corresponds to the mass of the compound for one equivalent of functional group (here the isocyanate group). In polyurethane chemistry, this value is mostly determined as the average molecular weight divided by the average functionality. The equivalent weight is linked to the NCO content via equation 1.1:

$$EW_{isocyanate} = \frac{42}{\%\ NCO} \times 100 \qquad (1.1)$$

A large number of polyisocyanates have been developed throughout the years. However, the standard commercial polyisocyanates of the polyurethane industry are all based on just few diisocyanates (Table 1.1).

These diisocyanates can be sorted into two categories based on their chemical structure: aromatic and aliphatic diisocyanates, the former being much more reactive than the latter. For that reason, MDI and TDI are extensively used in the polyurethane industry. In 2000, more than 95% of isocyanates sold were either MDI or TDI[4].

Table 1.1. Most common industrial diisocyanates

<table>
<tr><th colspan="3">Aromatic diisocyanates</th></tr>
<tr><td colspan="2">4,4' or 2,4’
Methylene diphenyl diisocyanate
MDI
 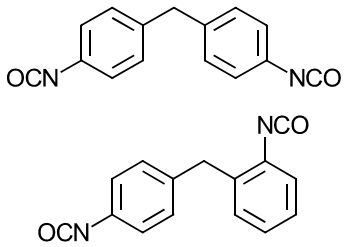 </td><td>2,4- or 2,6-
Toluene diisocyanate
TDI
 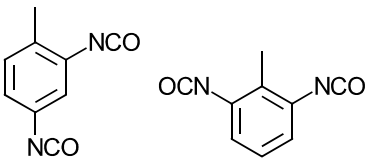 </td></tr>
<tr><th colspan="3">Aliphatic diisocyanates</th></tr>
<tr><td>Hexamethylene
diisocyanate
HDI
 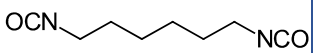 </td><td>Isophorone
diisocyanate
IPDI
 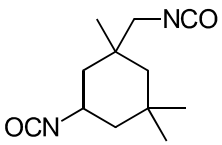 </td><td>Bis-(4-isocyanato-
cyclohexyl) methane
H₁₂MDI
 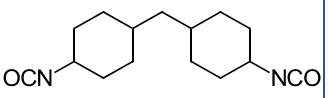 </td></tr>
</table>

Aromatic diisocyanates are frequently used for the preparation of polyurethane foams by reaction with polyols in the presence of a catalyst and a blowing agent. Depending on the formulation, rigid foams can be prepared for construction or insulation of buildings, as well as flexible foams for furniture, mattresses or automotive seats.

Despite their high reactivity, aromatic diisocyanates cannot be used for all applications as they undergo an oxidative degradation under UV radiation[5]. This leads to a yellowing of the polyurethane and can also reduce its lifetime. For these reasons, aromatic diisocyanates are not usable for other applications, such as most coatings. In this case, aliphatic isocyanates (HDI and IPDI) are preferred because they are offering a long-term stability as well as UV resistance.

Even though most of the commercial polyisocyanates are the ones previously described, other diisocyanates are still in development. One of the most recent ones being the pentamethylene diisocyanate (Table 1.2).

Table 1.2. Other types of diisocyanates

Pentamethylene diisocyanate	m-xylene diisocyanate	Tetramethylxylene diisocyanate
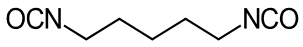	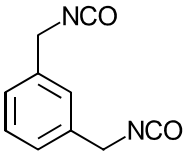	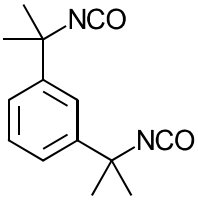

In 2015, Covestro AG has developed a polyurethane coating crosslinker based on pentamethylene diisocyanate, of which 70% of its carbon content is derived from biomass[6]. This material is able to exhibit the same properties as usual diisocyanates or even slightly better. Xylene diisocyanate and tetramethylxylene diisocyanate are also of great interest because they are combining properties of aromatic and aliphatic diisocyanates[6, 7].

1.1.2. The isocyanate chemistry

Isocyanates are able to react with many nucleophilic species, but the most important reactions are those leading to the formation of urethane and urea by reaction with alcohols and amines, respectively. Table 1.3 gives an overview of the basic reactions of the isocyanate group. The reaction with water produces an unstable carbamic acid which is converted in an amine via the release of carbon dioxide. The produced amine reacts rapidly with an isocyanate function yielding to the corresponding urea.

Table 1.3. Main reaction of isocyanates

Reaction with alcohol: formation of urethane
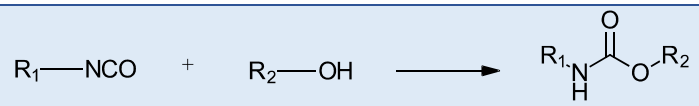
Reaction with amine: formation of urea
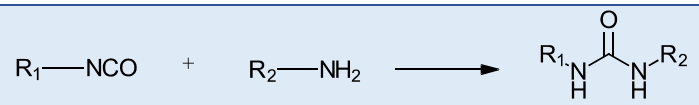
Reaction with water: formation of urea
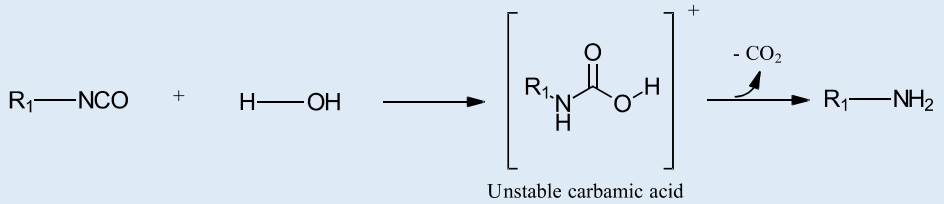 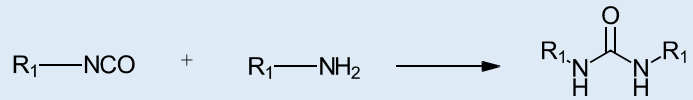
Reaction with urethane: formation of allophanate
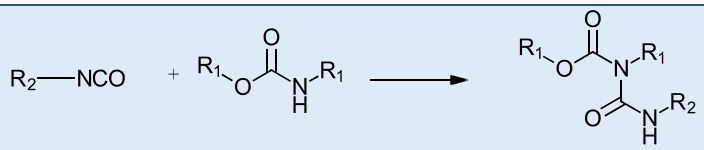
Reaction with urea: formation of biuret
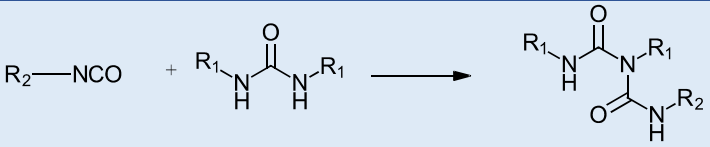

Even though the synthesis of compounds such as biurets or allophanates is possible, the kinetic of their reaction is significantly lower compared to initial reagents (amines and alcohols). The type of alcohol or amine (primary, secondary) and their chemical structure play an important role in the urethane/urea formation rate. Table 1.4 shows the relative uncatalyzed reaction rate of isocyanates with varying reaction partners, pointing out that the formation of urea with aliphatic amines is faster than any other reaction previously described. It is possible to observe a decrease of reactivity for more substituted amines or alcohols due to steric influence. Moreover, the reaction rate of primary alcohols are similar to the one of water, hence the reaction process and the solvent need to be carefully investigated to avoid, if necessary, the side reaction with water during the preparation of urethanes. This wide variation of kinetic rates and the large numbers of amines and alcohols offer a broad range of products based on urethanes and ureas, as well as a perfect control of the synthesis process.

Table 1.4. Relative reaction rates of isocyanates with varying reaction partners

Active H compound	Structure	Relative uncatalyzed reaction rate at 25°C
Primary aliphatic amine	R-N**H**$_2$	100,000
Secondary amine	R$_2$-N**H**	20,000-50,000
Primary aromatic amine	Ar-N**H**$_2$	200-300
Primary hydroxyl	R-CH$_2$-O**H**	100
Water	**H**$_2$O	100
Carboxylic acid	R-COO**H**	40
Secondary Hydroxyl	R$_2$CHO**H**	30
Urea	R-N**H**-CO-N**H**-R	15
Tertiary alcohol	R$_3$CO**H**	0.5
Urethane	R-N**H**-COOR	0.3
Amide	R-CO-N**H**$_2$	0.1

Reprinted with permission from [8]. Copyright © 2015 by John Wiley & Sons, Inc.

1.1.2.1. Polyisocyanates

Isocyanates are also able to react with each other as described in Table 1.5 with the help of a catalyst[9]. These reactions are gaining strong industrial significance if applied to diisocyanates since the synthesis of polyisocyanates becomes possible. Uretdione and isocyanurate polyisocyanates (based on HDI) are used since more than 50 years in the polyurethane industry, especially for coatings. Iminooxadiazinediones are more recent but still used since almost 20 years[10]. The conversion of diisocyanates into polyisocyanates via cyclopolymerization allows to obtain compounds with a higher isocyanate functionality, which are desirable for the preparation of cross-linked polyurethane. The reactivity of such compounds is, as before, influenced by the electronic effect, the steric effect and the nature of the carbon atom bearing the NCO group.

Table 1.5. Main cyclopolymerization of isocyanates

Synthesis of uretdione (dimer); applied to diisocyanates	
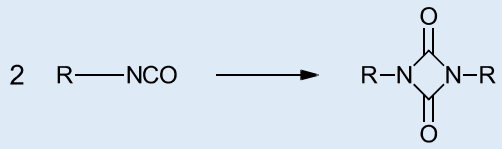	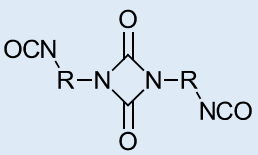
Synthesis of isocyanurate (trimer); applied to diisocyanates	
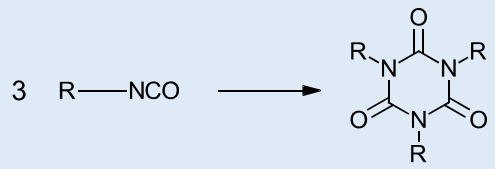	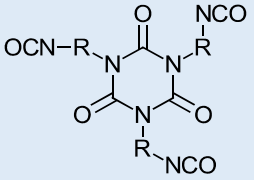
Synthesis of iminooxadiazinedione (asymmetric trimer); applied to diisocyanates	
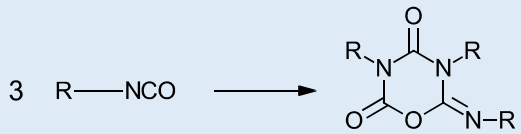	

1.1.2.2. Prepolymer

The term “prepolymer” refers to monomer which has been reacted to prepare a targeted compound with intermediate molecular weight. Typically, two or three molecules of monomer are reacting with one or two binding molecules. Prepolymers play a key role since they have been introduced in the polyurethane industry in 1947[11]. They are intermediates which can be both NCO-functional and OH-functional depending on their purpose. The most common prepolymer is made by reaction between three TDI molecules and one molecule of trimethylolpropane[10, 11] (Fig. 1.3).

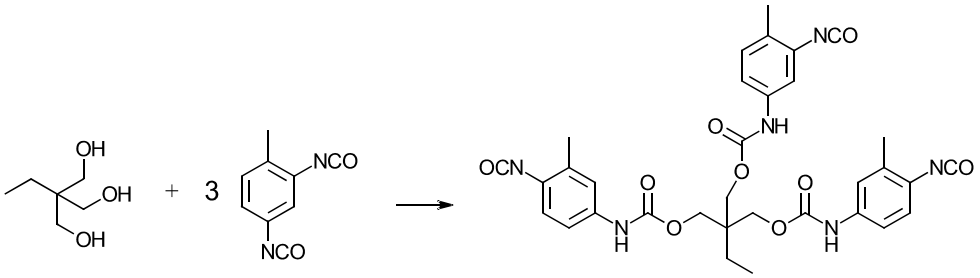

Figure 1.3. Synthesis of TDI prepolymer with trimethylolpropane (idealized structure)

1.1.2.3. Hydrophilically-modified polyisocyanates

In polyurethane coatings, some two-phase systems have been developed in which polyisocyanates are dispersed in an aqueous polyol solution. Most of the polyisocyanates are hydrophobic, which means another compound must be used to incorporate the polyisocyanate in the aqueous phase, such as a suitable organic co-solvent or an external emulsifier. However, the development of hydrophilically-modified polyisocyanates enables the preparation of a homogenous co-solvent-free mixture by a simple manual stirring. The reaction between aliphatic polyisocyanates, such as HDI, and a monofunctional polyethylene oxide polyether alcohol allows the synthesis of polyisocyanates bearing a hydrophilic polyether group. The mixture behaves like a non-ionic emulsifier and forms micelles when mixed with water (Table. 1.6. (a),(b))[12-14].

These types of molecules are standard NCO crosslinkers for waterborne coating and adhesive polyurethanes. The main difference between (a) and (b) is the final average functionality, which is directly correlated to the cross-linking density of the coating. The average functionality is lower than in the urethane (b) in comparison to the allophanate (a) which gives the latter an improved water and chemical resistance.

Table 1.6. Example of hydrophilically-modified polyisocyanate structures

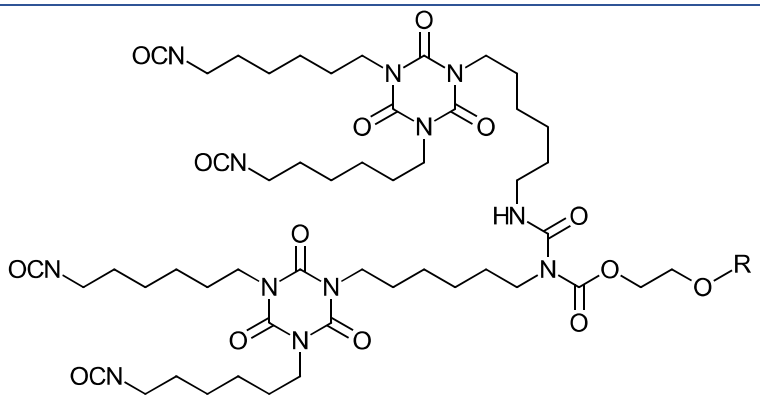

(a) Polyether Allophanate Hydrophilic Modification

(b) Polyether Urethane Hydrophilic Modification

(c) Ionic Sulfonate Hydrophilic Modification

Even though polyether-modified polyisocyanates are used in many applications, they still have some disadvantages. The emulsion prepared needs to have a long pot-life, and the coating prepared will be moisture-sensitive due to the hydrophilic polyether segments incorporated. To overcome these disadvantages, polyisocyanates hydrophilically modified with 3-(cyclohexylamino)-1-propane sulfonic acid (Fig. 1.4) were developed (Table 1.6, (c))[15]. Ionically modified-polyisocyanates are today the best hydrophilically modified polyisocyanates for use in two-component waterborne systems[5].

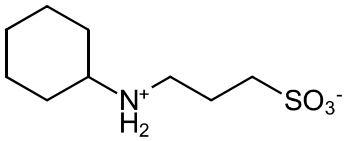

Figure 1.4. Structure of 3-(cyclohexylamino)-1-propane sulfonic acid

1.1.3. Health risks

Isocyanates such as diisocyanates are hazardous products that need to be manipulated with extreme care. Due to their vapor pressure and volatility, most of the common low molecular weight isocyanates are strongly irritating for eyes, intestines and respiratory tracts. A short term exposure to diisocyanates may cause sensitization (asthma, pulmonary malfunction), which can even lead to pulmonary failure in worst cases[16]. The toxicity of isocyanates has been studied for a long time, but even more intensively after the Bhopal (India) accident in 1984, when more than 3000 people died because of a large methylisocyanate leakage. Their death has been directly linked to the methylisocyanate toxicity[17]. Among diisocyanates, MDI has been proved to have the lower toxicity thanks to its very low vapor pressure. Despite this, MDI still remains a sensitizer and an allergen, exactly as other diisocyanates (TDI, HDI). To achieve a lower volatility and overcome hazards of diisocyanates, they are transformed into polyisocyanates with higher molecular weights. Polyisocyanates, prepolymers and hydrophilically-modified polyisocyanates previously introduced become highly relevant, especially for use in polyurethane coatings or adhesives, where normal diisocyanates cannot be used for obvious occupational health reasons.

1.2. Introduction to polyurethane

1.2.1. Historical and chemical aspect

Polyurethanes were discovered in 1937 by Heinrich Rinke and the development of the polyaddition process was made by Otto Bayer[11] in the early 1940s that resulted in the synthesis of many different polyurethanes and of the creation of the polyurethane industry. Then, fifty years ago, Otto Bayer and his team developed the first polyurethane coatings based on the combination between low molecular weight polyisocyanates (mainly TDI and HDI) called "Desmodur" and polyols called "Desmophen". Their outstanding properties (good chemical, corrosion and abrasion resistance, toughness, good mechanical strength) led to the replacement of alkyd coatings by polyurethane coatings through the next 30 years in all types of application: wood coating, corrosion protection, automotive, textile coating. Meanwhile, in 1951, the first polyurethane adhesive was produced to bond elastomers and metals[18], and in 1954, the production of polyurethane flexible foam started. Since then, polyurethanes success is unstoppable and their versatility offers new applications every year.

Nowadays, polyurethanes (PU) are very common polymeric materials that can be used in a broad range of fields via different forms, and be incorporated in various products[19, 20]:

- Polyurethane flexible foam is most common type of polyurethane. In addition of being extremely versatile, these foams are used in many applications such as furniture, carpet cushion, mattress, automotive seat and interior, packaging or textile fiber.
- Polyurethane rigid foam is the most common insulation material. It is today the best material for buildings and constructions in terms of energy efficiency and savings, due to very low heat-transfer properties, and also in terms of sound insulation.

- Coatings, adhesives, sealants and elastomers can be grouped as one type of polyurethane and are used in a broad of applications themselves. Polyurethane elastomers are rubber-like materials which can provide resistance to abrasion, temperature, aging, and many others depending on the expected use: valves, factory fixtures, wheels for shopping carts or skateboards and others.
- Thermoplastic polyurethanes are usually flexible and resistant to impact, abrasion and weather. Moreover, they offer a large combination of physical properties and processing applications. They are used in hundreds of products, e.g. sporting shoe soles, drive belts, medical tubing, and fire hose liner.
- Polyurethane binders provide a permanent bonding between different types of surfaces and fibers. Their main areas of use are wood panels, rubber or elastomeric flooring surfaces and sand casting for the foundry industry.
- Polyurethane dispersions consist of polyurethane/polyurea polymer particles suspended in water. They are used as starting material for different type of polyurethanes described before, such as adhesive or coating. They have the advantage of being ecologically friendly.

Polyurethanes are synthesized by reaction between a polyfunctional isocyanate and polyfunctional hydroxyl compound (Fig. 1.5). The main repeating unit is a urethane group but polyurethanes are also made of polyester, polyether or aromatic group for example, depending on the nature of the reagents. The structure of polyurethanes can be easily tailored due to different types of isocyanates, as previously described, but also due to a large number of hydroxyl compounds with different structures, molecular weights and functionalities.

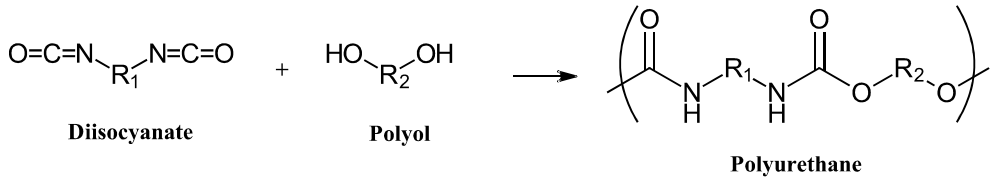

Figure 1.5. General route for the synthesis of polyurethane

The microscopic structure of the polyol (or polyamine, in case of polyurea) has a direct impact on the macroscopic properties of the polyurethane e.g., long and flexible polyols with low functionality (2-3) will lead to a soft elastic polyurethane. On the other hand, a short and rigid polyol with high functionality (3-8) will form a hard polyurethane due to a higher cross-linking in the material. The most important classes of polyols are polymers containing hydroxyl groups such as polyethers, polyesters or polyacrylates (Fig. 1.6). These polyols are widely used in coating and adhesive polyurethanes, which are the main areas of interest of this thesis.

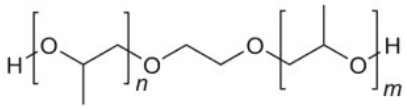

Polyether polyol

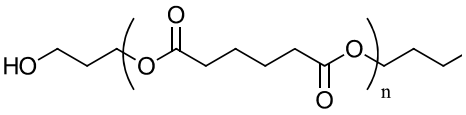

Polyester polyol

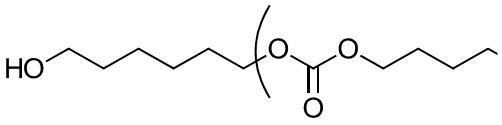

Polycarbonate polyol

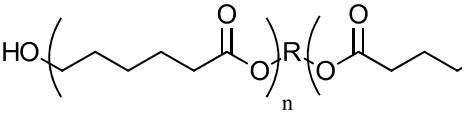

Polycaprolactone polyol

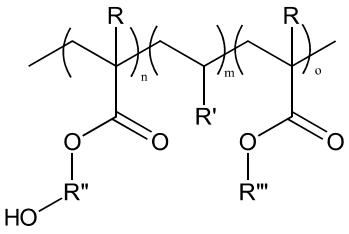

Polyacrylate polyol

Figure 1.6. General formula of commonly used polyols

1.2.2. Polyurethane coatings

Coating material refers to as liquid, pasty or powdery materials which are deposited on another material surface to protect it from the outside environment: corrosion, oxidation, wear and tear, and others. A coating formulation consists of many components, the most important ones being binders, pigments, colorants, fillers and solvents. An example of a coating formulation is shown in Table 1.7. In polyurethane coatings, the bond is made by reaction between polyols (in the example below, polyacrylate) and polyisocyanates. Colorants are all the color-bearing substances. Pigments can also influence the color (titanium dioxide pigment) or the physical properties of the coating. Fillers are also used to modify some physical properties, as well as increasing the volume (and therefore lowering the price). Many environmentally friendly and economical polyurethane coatings are available due to their overall performances that outpace others technologies without affecting the coated material. Polyurethane coatings are well-known for their efficiency in application: a short overall process which can be performed even at low temperatures[5]. Polyurethane coatings can be separated regarding different criterion: the nature of the system, its composition and its curing conditions.

Table 1.7. Solvent-borne two-component polyurethane formulation example

Component A	**Part by weight**
Polyols	33.80
Rheology modifiers *Thickener, Defoamer*	6.79
Fillers *Silica-based, Calcium carbonate, Barium sulfate*	22.52
Pigments *Titanium dioxide, Iron dioxide*	19.33
Solvents	8.00
Catalysts	0.78
Component B	
Polyisocyanates	8.78

Nature of the system

Polyurethanes can be sorted depending on the solvent used in their formulation. They can be solvent-free, no solvent are used in the formulation, water-borne, water is used as solvent in the formulation, or finally solvent-borne, which regroups all formulation including an organic solvent.

One- and two-component formulations

One-component polyurethane coatings (usually called 1K formulation; K stands for Komponente, which is the German for "component") often refers to as moisture-curing coatings. They can be divided into two groups depending on the curing temperature. They consist of isocyanate prepolymers which are able to react with moisture coming from the outside environment. This formulation has obvious advantages (one component, react with air) but they are counterbalanced by the fact that each component needs to be carefully dried to avoid internal moisture, which would lead the formulation to react by itself at any moment. This issue does not concern two-component polyurethane formulations (usually called 2K formulation). They are extensively used for many applications and also have the advantage to be bubble-free even at high film thickness. Two-component polyurethane coatings (example in Table 1.7) are made of a component A, containing polyols and additives, and a component B, the polyisocyanate(s). The reaction between these two components forms the polyurethane coating film. However, as the reaction rate is very high, two-component systems have a relatively short pot-life. The mixture becomes useless when its viscosity has doubled, which occurred in between 4 to 6 hours.

Curing conditions

Generally, the preparation of coatings involves two curing mechanisms that are overlapping: solvent removal, either by heating or at room temperature, followed by chemical cross-linking, offering to the coating hardness and other desired mechanical properties. All two-component formulations follow this path, but other curing processes also exist for one-component system:

- Physical drying can be solely used for some 1K-component coatings. It consists of polyurethane or polyurethane-urea chains (up to 150,000 g/mol) dissolved in an organic solvent. After solvent removal, no cross-linking is happening and the coating is creating by interactions between molecular chains.
- Chemical curing involves, as its name suggests, a chemical reaction which can happen at different temperatures.
    - Cross-linking at room temperature: the so-called moisture curing polyurethane coatings are polyisocyanate prepolymers able to react with the ambient humidity. The reaction with water produces amines, and then an urea network. This type of system is strongly dependent of the weather conditions (humidity) directly linked to the drying rate.
    - Cross-linking at higher temperature: stable unreactive systems (thermally reactive blocked-polyisocyanates[21, 22], solid-form powder coatings) containing both polyols and polyisocyanates are prepared and the cross-linking occurs as a consequence of the heating process. These systems are still considered as one-component formulations.
- Air-drying curing is using oxygen to cross-link the polyurethane with the help of catalysts, which can be done by introducing fatty acids or fatty alcohols in the polymer backbone.
- The curing can also be done by using UV-radiation as starting mechanism to engage a curing process, as previously described. This technology is strongly studied[23-25] because it offers several advantages, especially because even the areas not reachable by the UV-radiation device can be chemically cross-linked.

1.2.3. Polyurethane adhesives

Bonding is the surface-to-surface joining of similar or dissimilar materials using a substance which adheres to the surfaces of the two adherents to be joined, transferring the forces from one adherent to the other[26]. Adhesive bonding is one of many joining techniques, as well as screwing or welding. An adhesive is a non-metallic component that uses internal strength (cohesion) and surface bonding (adhesion) to join materials. This technique is offering several advantages: no holes need to be done in the material (screwing), the material is not damaged by stress (welding) and adhesives allow the repartition of the strength all along the material.

Polyurethane is one of the polymers used as adhesive for bonding, as well as epoxy resins, silicones, acrylic based polymers and others. Similarly to polyurethane coatings, polyurethane adhesives can be sorted in various forms in view of their formulation (1K or 2K adhesives), their joining technique (physical setting, chemical curing) and their solvent system (solvent-borne, water-borne and solvent-free). They are either containing urethane groups in their polymer backbone or these urethane groups are synthesized during curing. Polyurethane adhesives are able to adhere properly to many surfaces, not only because of their strong physical bonding force, but also because of polar affinity between the polymer and the nature of the surface[26]. Moreover, isocyanates are able to react with moisture present on the surface, purposely or not, which also increases the joining strength.

Polyurethane coatings and adhesives are very similar in terms of chemistry, manufacture and technology, however they differ heavily on one main point: their optical properties. Polyurethane coatings have strong limitations on their optical properties as it modifies directly the aspect of the product. Any changes in the coating formulation can affect its quality. On the other side, optical properties are only secondary preoccupation because most of the adhesives are not meant to be viewed in the final product.

1.2.4. Polyurethane catalysis

In the polyurethane industry, it is well-known that the reaction between aliphatic polyisocyanates and nucleophilic species is slower in comparison to aromatic polyisocyanates systems, thus it is necessary to use catalysts in aliphatic systems. To be effective, polyurethane catalysts have to satisfy a wide range of characteristics: high reactivity at low concentration, high selectivity towards the urethane reaction against the side reactions, low toxicity and good availability at low cost[5]. Two main classes of catalysts exist for polyurethane formulations: tertiary amines and Lewis acidic metal-based catalysts[27-29] (Table 1.8).

Table 1.8. Most common polyurethane polymerization catalysts

Tertiary amines		
1,4-diazacyclo-[2.2.2]octane **DABCO** 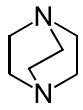	1,8-diazabicyclo-[5.4.0]undec-7-ene **DBU** 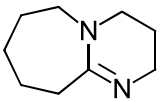	N,N-dimethyl-cyclohexylamine **DMCHA** 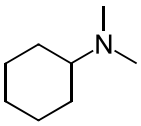
Lewis acidic metals		
Dibutyl tin laurate **DBTL** 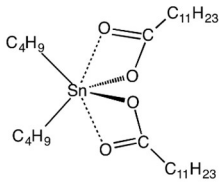	Bismuth tri(2-ethylhexanoate) 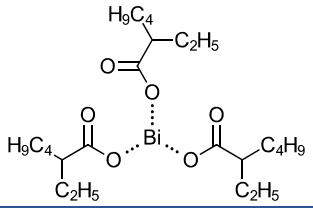	Zinc bis(2-ethylhexanoate) 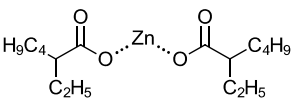

Dibutyl tin dilaurate (DBTL) is the most widespread metal-based catalyst due to its outstanding catalytic properties[30, 31], however, it has been classified as reproductively toxic by the European Commission in 2017. Since then, and despite being known for more than 30 years[32, 33], zinc and bismuth carboxylates, among many others[5, 29, 34-37], keep on gaining interest as DBTL-alternatives. Indeed, they have replaced DBTL in many formulations and will therefore be actively used in this thesis.

1.3. Encapsulation

1.3.1. Definition and general purpose

Encapsulation is a process in which a material (or a mixture of materials) is surrounded and protected by a thin protective film of other materials, temporarily or permanently. The encapsulated material might be tiny solid particles, liquid droplets or gas bubbles and can be referred to as various names such as core material, payload, actives, fill, inner or internal phase. The protective material can be made of a wide range of materials, for instance, metals, ceramics, lipids[38], as well as polymers, and can be referred to as wall, membrane, coating, shell or carrier[39]. In this work, only polymers will be investigated as encapsulating material.

They are two main types of encapsulation that are distinguished by the size of the synthesized particles: micro- and nano-encapsulation. The former leads to microparticles which are between 1 to $1000 \mu m$ in size, whereas the latter forms nanoparticles which are between 1 to $1000 nm$ in size. The microencapsulation process is attributed to Bungen Burg de Jon and Kanin 1931 and their idea has been adapted for many applications in different areas such as food industry[40-42], medical and pharmaceutical[43-45], agricultural[46, 47] or textiles[48]. Thanks to the technological progress, some nanoencapsulation techniques were developed based on existing microencapsulation techniques, and since 20 years, nanoencapsulation is increasingly studied. Most of the nanoencapsulation research is performed for the food industry[49, 50] or the pharmaceutic industry (drug delivery systems)[51, 52]. The purposes of all those particles are directly linked to their application, but they can be sum up as following[53, 54]:

- Separation or mixture of incompatible components
- Modification of the physical character of a material (use of liquids as solids)
- Protection of the immediate environment (degradation reaction, oxidation, dehydration for example) and/or increase of the stability
- Masking of odor, taste and activity of core materials
- Controlled and/or targeted release of core materials
- Safe and convenient handle of toxic material

The morphology of the synthesized particles depends on the core material but more particularly on the shell material, as well as the encapsulation technique selected. Some of the different structures obtained during the synthesis are presented in Fig. 1.7. One of the most frequent structure is the core-shell structure (a) in which the core material is perfectly surrounded by the shell material, such structure are called capsules. But the particles can also have several shells and therefore be called multi-shell particles (b).

These first two structures are mononuclear, i.e. they contain only one core. However, it is also possible to prepare particles with several cores, which are referred to as polynuclear particles, such as matrix particles (frequently called spheres, c), in which the core material is homogeneously distributed in a matrix of the shell material. Multi-core particles (d) and irregular particles (e) are rarer, but are also possible outcomes of the encapsulation process.

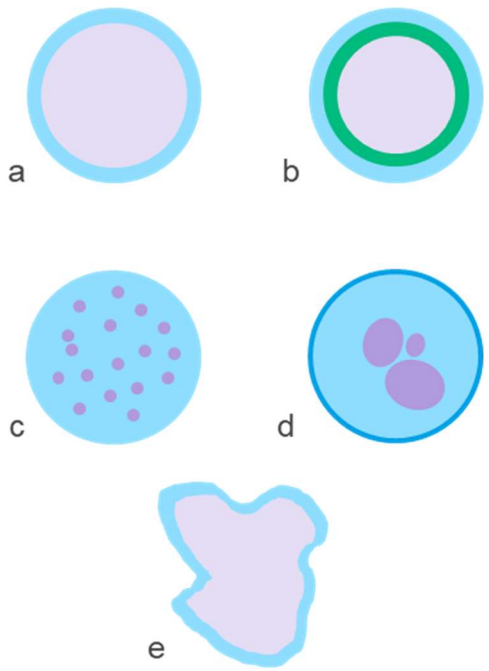

Figure 1.7. Types of particle structures: (a) core-shell; (b) multi-shell; (c) matrix; (d) multi-core; (e) irregular

The particles are also distinguished via their release mechanisms which depend on the physical and chemical properties of the shell material. The permeability of the shell especially plays an important role and leads to three main release mechanisms of the core: diffusion, shell rupture or shell dissolution (Fig 1.8). If the shell is permeable to the liquid in which microcapsules are immersed, the solvent is able to go in and out of the shell inducing a slow diffusion of the core in the media. The release rate can be controlled by modifying the physical and chemical properties of the wall. For example, aspirin is a well-known medicine against fever, inflammation and arthritis, but a direct ingestion of aspirin can provoke secondary effects, such as peptic ulcers and bleeding[55]. The microencapsulation of aspirin in semi-permeable cellulose shells prevents the secondary effects just mentioned[56, 57]. To be perfectly effective, the core release of micro- and nanoparticles must occur at the appropriate time and place. It is possible to achieve such performance especially with shell dissolution or rupture core-release process. The particle shells can be prepared in order to answer to an external stimulus such as temperature[58], pH[59], pressure[60] or UV light[61].

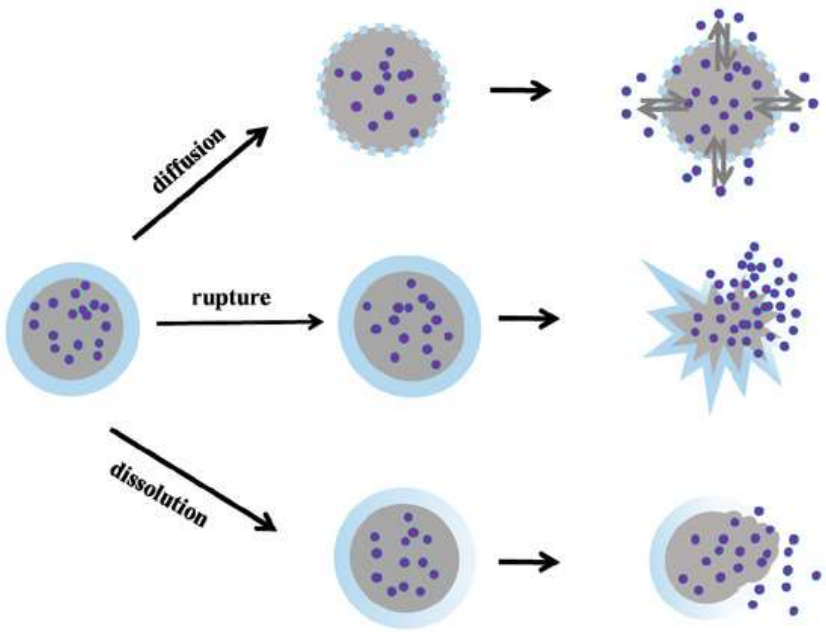

Figure 1.8. Main release mechanisms[62]

1.3.2. Review of polymeric encapsulation techniques

Many encapsulation techniques have been developed throughout the years and some of them will be described here. Encapsulation knowledge and methods are at the intersection of several fields: colloid chemistry, physical chemistry, polymer chemistry, biochemistry, physics, and biotechnology and material science[63]. Moreover, the preferred micro/nanoparticles with desired properties can only be prepared while using the suitable technique (Table 1.9) in view of the core material physical state, the particle size range, the payload and the capsule morphology. Studying extensively many reaction parameters such as core-to-shell ratio, capsule size, shell thickness or shell permeability is also important to obtained the desired particles. Some techniques are based on chemical reactions, while, on the other side, some are based on physical principles. Therefore, they are usually divided in three categories: chemical, physico-chemical and physico-mechanical techniques.

Table 1.9. Process parameters of common microencapsulation techniques

	Type of particle	Payload	Particle structure
Physico-mechanical processes			
Air Suspension	Microparticle	Medium, High	Core-shell
Centrifugal Extrusion	Microparticle	Medium, High	Core-shell, Matrix
Pan Coating	Microparticle	Medium, High	Core-shell
Spinning Disk	Microparticle	Low, Medium, High	Core-shell, Matrix
Spray Congealing	Micro- and Nanoparticle	Low, Medium, High	Matrix
Spray Drying	Micro- and Nanoparticle	Low, Medium, High	Matrix
Physico-chemical processes			
Coacervation	Micro- and Nanoparticle	Medium, High	Core-shell, Matrix
Emulsion-Solvent Diffusion	Nanoparticle	High	Core-shell, Matrix
Ionotropic Gelation	Micro- and Nanoparticle	Medium, High	Core-shell, Matrix
Layer-by-Layer Absorption	Micro- and Nanoparticle	High	Core-shell
Nanoprecipitation	Micro- and Nanoparticle	High	Core-shell, Matrix
Salting Out	Nanoparticle	High	Core-shell, Matrix
Solvent Evaporation	Micro- and Nanoparticle	Low, Medium, High	Core-shell, Matrix
Suprecritical Fluid Precipitation	Micro- and Nanoparticle	Low, Medium, High	Core-shell, Matrix
Chemical processes			
Dispersion Polymerization	Micro- and Nanoparticle	High	Core-shell
Emulsion Cross-Linking	Micro- and Nanoparticle	High	Core-shell, Matrix
Emulsion Polymerization	Micro- and Nanoparticle	Low, Medium, High	Core-shell
In-situ Polymerization	Micro- and Nanoparticle	High	Core-shell
Interfacial Polycondensation	Micro- and Nanoparticle	High	Core-shell
Suspension Polymerization	Micro- and Nanoparticle	High	Core-shell, Matrix

Adapted with permission from [64]. Copyright © 2016 by Taylor & Francis Group, LLC

It is important to note that many other microencapsulation techniques exist, such as annular jet process or vacuum encapsulation[40, 54, 55, 64-69], and they cannot all be described here.

The encapsulation techniques based on physico-mechanical properties are often restricted to the synthesis of microparticles due to the instruments limitations. However, thanks to the technological progress, these encapsulation techniques become more and more adaptable for the synthesis of nanoparticles, spray drying being the most relevant example. Many of the physico-chemical and chemical encapsulation methods are based on the formation of an emulsion or a dispersion. As the size of emulsion droplets or dispersion particles can be easily controlled, those methods are easily adaptable for the synthesis of both micro- and nanoparticles.

1.3.2.1. Physico-mechanical techniques

Air suspension

The air suspension process is also called fluidized-bed coating. This is one of the most efficient techniques for microencapsulation of solids for food and pharmaceutical applications because it offers a good control of the microparticle properties. In a coating chamber (Fig. 1.9), a controlled air stream goes upward through a perforated plate and creates a suspension of particles. The shell material is sprayed on the suspended particles, either from the top or the bottom (or eventually from the side). Then, the particles settle down and go again through the same path several times until the desired thickness is achieved. Usually, the shell material is a polymer solution and the solvent evaporates by using a hot air stream. This process generally prepares particles from few micrometers to 250μm but it can eventually be modified to reach few millimeters. The obtained particles have a narrow size distribution[55].

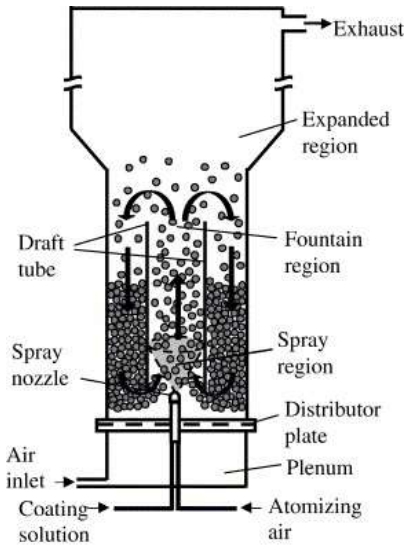

Reprinted with permission from [70]. Copyright © 2006 Elsevier B.V.

Figure 1.9. Scheme of air suspension encapsulation process: bottom spray (left) and top spray (right)

Centrifugal Extrusion

The centrifugal extrusion is one among many other extrusion techniques, such as melt injection or melt intrusion, and uses a rotating extrusion head containing concentric nozzles. The process is described in Figure 1.10 (top) and is mostly employed to encapsulate flavor oils. The core material is pumped through the inner orifice and a liquid shell material through the outer orifice forming a coextruded rod of core material surrounded by shell material. As the device rotates, the extruded rod breaks into droplets[67]. The shell material can be hardened by cooling during the time droplets are in flight or by using a melt material as shell. Droplets can also be immerged into a solvent to cool them down faster or a dryer can be used to evaporate the solvent in which the shell material is dissolved.

Finally, the centrifugal extrusion can be used in combination with other encapsulation techniques such as ionic gelation[39]. The particles frequently have a size range from 100 to 2000μm and can be filled with up to 80% of core material.

Spinning Disk

This technique, also called centrifugal suspension separation, is simple, rapid and cost effective, as well as very similar to the centrifugal extrusion described above. Core particles are suspended in the liquid shell material, and the mixture is then poured on the rotating disk (Fig. 1.10, bottom). Due to rotations and the centrifugal forces, the mixture is thrown out of the disk as droplets. These droplets have a range size of $1\mu m$ to $2mm$ and are solidified most of the time by cooling, even though other techniques can be performed, similarly to the centrifugal extrusion[64].

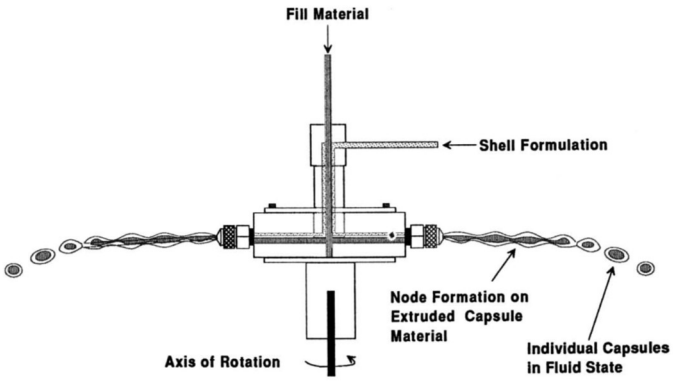

Reprinted with permission from [39]. Copyright © 1995 American Chemical Society

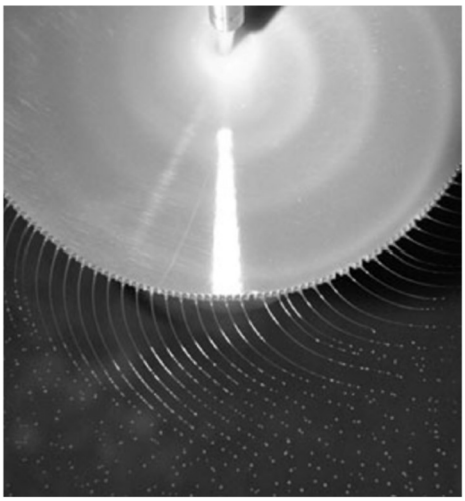

Reprinted with permission from [71]. Copyright © 2012 Woodhead Publishing Limited

Figure 1.10. Scheme of centrifugal extrusion process (top) and picture of a spinning disk (bottom)

Pan coating

This process is one of the oldest encapsulation methods as it has been developed in the 1880s. The microparticles obtained via pan coating are referred to as pellets[72]. The scheme of the process is shown in Figure 1.11. The particles are tumbled in a pan while the coating material is applied. The coating material is made of a shell material dissolved in a solvent. To remove this solvent, warm air is going through the pellets. Particles from few micrometers to few millimeters can be coated with this process, however, the coating is considered efficient only for a particle size greater than $600\mu m$. This technique is mostly applied to the preparation of controlled-release medical drugs.

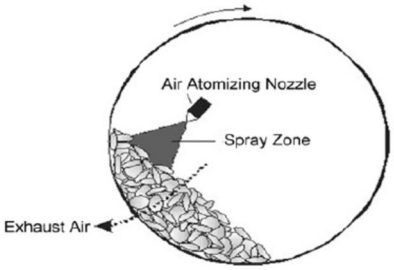

Reprinted with permission from [73]. Copyright © American Association of Pharmaceutical Scientists 2006

Figure 1.11. Scheme of pan coating encapsulation

Spray Drying

This is the most common microencapsulation technique because it offers several advantages such as low-cost and simple process, broad range of shell material and easy equipment availability. This process is still extensively studied and reviews on this single technique have already been published[74]. Lots of compounds are encapsulated by spray drying since decades, e.g., flavors, drugs and many others. This technique is based on the preparation of a solution, emulsion or suspension of the encapsulated material in a polymer solution, followed by the atomization (also called nebulization) of the mixture as small droplets. These droplets go through a drying chamber where a hot gas (usually air) stream is circulating. The solvent evaporates which leads to the formation of dried microparticles. A scheme of spray drying process is shown below in Figure 1.12.

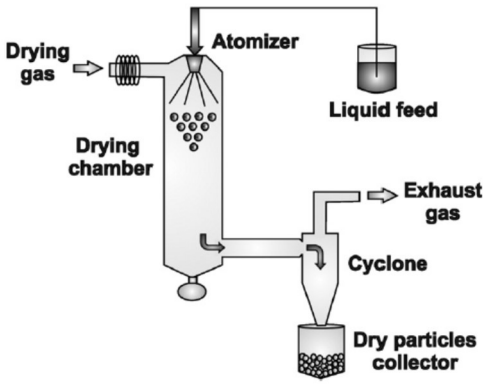

Reprinted with permission from [74]. Copyright © 2015 Elsevier B.V.

Figure 1.12. Scheme of the spray drying process

The size of the synthesized microparticles varies from a few micrometers to a few millimeters. Thanks to the technological progress, nanoparticles of a few hundred nanometers can nowadays be obtained[75]. The required time to encapsulate a single particle is very short, from millisecond to few seconds, therefore the encapsulation of heat non-resistant material can even be considered. Spray drying still has some disadvantages: low yield due to material lost on the drying chamber walls, non-uniformity of particle sizes and relatively porous shell due to quick solvent evaporation.

Spray Congealing

This versatile technique is also referred to as spray cooling and spray chilling in the literature. The principle is very similar to spray drying i.e. the same spraying device can be used. The core material is mixed with a melt material to obtain a solution, an emulsion or a suspension. Then the mixture is atomized and goes through the drying chamber. Cool gas stream circulates in the drying chamber to solidify the droplets. The particles are then collected at room temperature. The shell material must be solid at room temperature to avoid unwanted release of the core material. Spray congealing is a process even cheaper than spray drying as it only uses cold air. Moreover, spray cooling offers a precise control of the particle size which can be very useful for solid dosage of drugs[76]. This technique can also be used for food applications, such as the encapsulation of vitamins, minerals or acidulants[39].

1.3.2.2. Physico-Chemical techniques

Coacervation

This technique is based on the desolvation of one or several polymers in a solution leading to a phase separation. Polymers end up coating the material due to lower solubility. If only one polymer is used, the process is called simple coacervation but if more than one polymer are involved in the wall preparation, it is referred to as complex coacervation. For both processes, the core material has to be dispersed in a solvent in which its solubility is very low (typically no more than 2%). In simple coacervation, the polymer is generally dissolved in an aqueous solution and the phase separation can be induced by several methods:

- Addition of a water-miscible non-solvent, such as acetone or ethanol.
- Addition of inorganics salts, such as sodium sulfate, to salt-out the polymer
- Decrease of the temperature to lower the polymer solubility

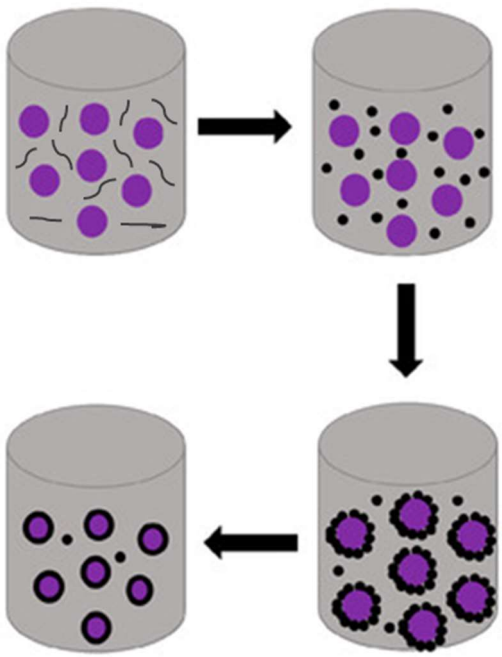

Figure 1.13. Scheme of complex coacervation process[62]

Complex coacervation is more developed compare to simple coacervation and its process is described in Fig. 1.13. At first, two ionic water-soluble polymers bearing different charges are introduced into the dispersed solution of core material. Typical polymers for such applications are gelatin (positively charged when the pH is lower than 7) and gum Arabic (always negatively charged). Then, the pH is adjusted in sort of having both polymers as ionic form, able to interact with each other. This interaction leads to a lower solubility and to a phase separation.

Therefore, there is a deposition of the polymers at the surface of the droplet leading to its encapsulation. The obtained capsule shell is highly water-swollen and possibly heat-dissoluble, which is not desired. To overcome this problem, the shell is covalently cross-linked with chemicals such as formaldehyde. Microcapsules produced by coacervation have a size range from $2\mu m$ to $1200\mu m$ and can have a payload up to 95%. The coacervation pH zone might be hard to find and the used salts must be completely removed. Also, coacervation encapsulation can be tricky for the encapsulation of pH sensitive material[64]. Complex coacervation is a very common method to prepare nanoparticles from 100 to $1000nm$ as well[77].

Layer-by-layer adsorption

Also referred to as layer-by-layer deposition, this technique is based on the successive addition of shell materials (layers) until the desired thickness is reached. Particle sizes are easily controllable with this process, as well as properties because the shell can be easily functionalized. The layers are made of compounds with affinity toward each other: positively and negatively charged polyelectrolyte solutions or proteins and polyphenols[78].

Supercritical fluid precipitation

This technique is based on the properties of supercritical fluids. Hardly compressed gasses behave both as liquids and gasses when they reach their supercritical fluid state (Fig. 1.14). Carbon dioxide (CO_2) and nitrogen dioxide (NO_2) are good candidates because they can reach their supercritical fluid state with moderate temperatures and pressures (for CO_2, $Tc = 304.2\ K$ and $Pc = 7.38\ MPa$)[66].

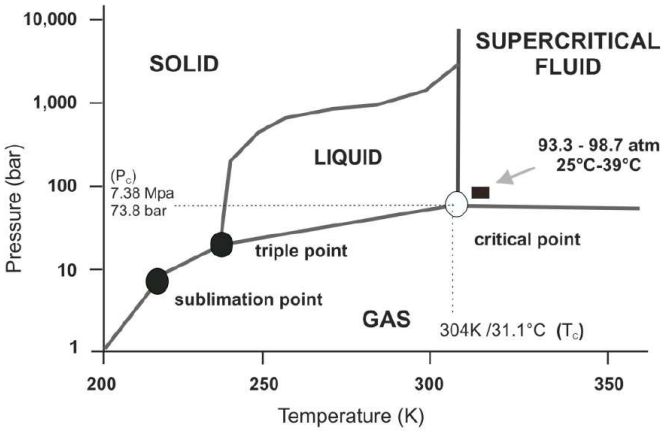

Figure 1.14. Pressure-Temperature phase diagram of CO_2[79]

With supercritical fluids, and especially carbon dioxide, several precipitation processes are available which depend on the role played by the supercritical CO_2: as solvent, in the *rapid expansion of supercritical solutions* process, as antisolvent, in the *supercritical antisolvent* process, or as solute, in the *gas antisolvent* process[64]. As solvent, the supercritical fluid, containing both core and shell materials, is released through a small nozzle at atmospheric temperature. Due to the fast pressure drop in the droplets, a desolvation of the shell material is occurring around the core material, and is forming a coating layer.

As antisolvent, core and shell material are mixed together and dispersed in an organic liquid. CO_2 has a large solubility in organic solvents but a very low solubility in high molecular weight substrates. The liquid mixture is saturated with CO_2; the solubility of the materials in the organic solvent is decreased, which causes supersaturation quickly followed by precipitation and formation of microcapsules.

As solute, CO_2 is dissolved in a melted solid, and the mixture is expanded through a nozzle to form small droplets. The expansion causes the vaporization of the dissolved CO_2, which has an intense cooling effect on the liquid droplets and they turn quickly into solid particles. Supercritical fluid precipitation has several advantages such as no toxicity, no flammability, possibility to encapsulate heat-sensitive compounds. However, the core and shell material must be soluble in one of the available supercritical fluids. This process is convenient for the preparation of both microparticles and nanoparticles[80].

Solvent evaporation

The polymeric shell material is dissolved in a volatile organic solvent. The core is subsequently dissolved, dispersed or eventually emulsified in the same solution. This solution is itself dispersed or emulsified in a second solution, most frequently a water solution. The mixture (dispersion, emulsion or double-emulsion) is heated to evaporate the volatile organic solvent and solid particles are formed. Many types of particles can be obtained depending on the formulation. The particles are obtained as a suspension or as a powder, after washing and drying. This technique is very easily performed and is therefore widely investigated for the preparation of nanoparticles[81]. This is also a very common technique for the synthesis of microparticles[67].

Ionotropic gelation

Also referred to as ionic gelation, this is one the easiest encapsulation method and frequently used in molecular gastronomy with a higher particle size (up to few centimeters). Ionotropic gelation, also called ionic gelation, consists in preparing polymer spheres containing the core ingredient. Calcium alginate is the most famous example. The alginate polymer is dissolved in an aqueous solution, and the core is put in suspension in this same solution. Through an extruding device, such as a spraying nozzle, or even simply a syringe, size-controlled droplets are prepared and dropped into an ionic solution.

These droplets are hardened by cross-linking of the wall material or polymer chain by using di- or multivalent metal ion (such as calcium chloride) aqueous solutions. Reversibly, micro/nanospheres can also be made by mixing the metal ion solution with the core ingredient and dropping the spheres into an alginate solution[64, 82]. This technique is adaptable to other natural polymers such as chitosan or polysaccharides and suitable for both microparticles and nanoparticles (Fig. 1.15)[83, 84].

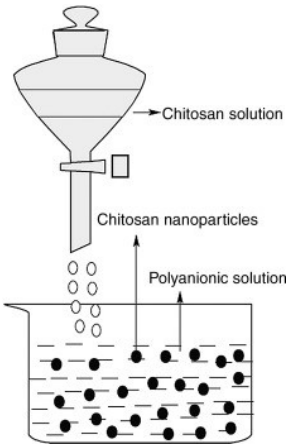

Reprinted with permission from [85]. Copyright © 2016 Elsevier Inc.

Figure 1.15. Scheme of the synthesis of chitosan nanoparticles by ionic gelation

Emulsion-Solvent Diffusion

As its name suggests, the emulsion-solvent diffusion consists in two steps. The polymer and the material to encapsulate are dissolved in water-partially soluble solvent, such as ethyl acetate or propylene carbonate. Beforehand, the organic solvent is saturated with water and reversely, the aqueous phase, which can contain a surfactant, is saturated with the organic solvent. Therefore, the oil-in-water emulsion prepared with these solutions is stable and solvent exchanges from one phase to another are not permitted. The thermodynamic equilibrium between the two phases is disrupted by addition of a large amount of non-saturated water. This causes the organic phase to diffuse into the aqueous phase, the polymer precipitates and a nanoparticle suspension is obtained[51]. Microparticles are very rarely prepared via this method.

Salting-out

The salting-out procedure is an adaptation of the emulsion-solvent diffusion method. Instead of being saturated with an organic solvent, the aqueous phase is saturating with electrolytes, such as magnesium chloride or calcium chloride. Due to this saturation, the water-miscible, or partially miscible, solvent is separated from the aqueous phase. After preparation of a stable oil-in-water emulsion, the addition of non-saturated water modifies the equilibrium (Fig. 1.16). The solvent diffuses into the aqueous phase, the polymer precipitates and nanoparticles are formed. More solvents are usable for this procedure than for the emulsion-solvent diffusion, however, more efforts to purify the nanoparticles are required[51, 86]. As for the emulsion-solvent diffusion method, this technique is almost exclusively employed for the synthesis of nanoparticles.

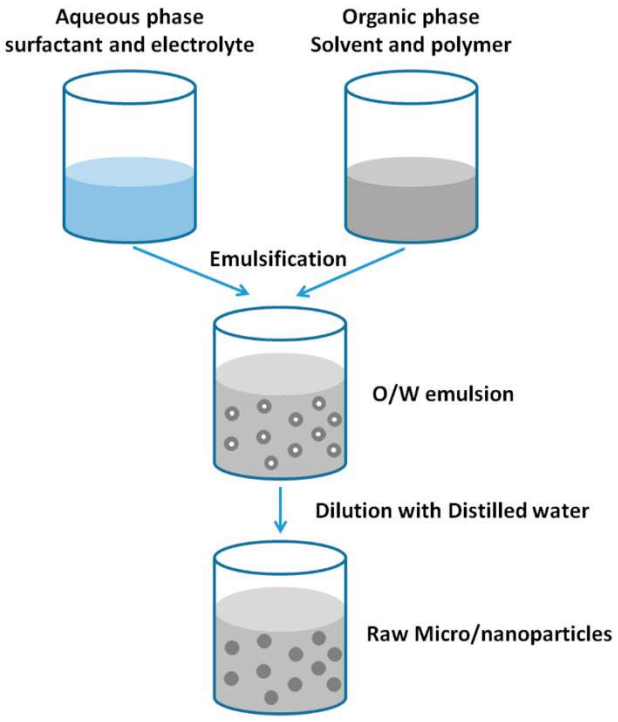

Figure 1.16. Scheme of the salting-out encapsulation procedure[87]

Nanoprecipitation

This method has many names and is also referred to as solvent displacement method, anti-solvent precipitation or solvent shifting method. This technique produces is mainly used to prepare nanoparticles, even though a few microparticles have been synthesized as well[88]. The polymer and the core material are dissolved into a water-soluble solvent, such as acetone or ethanol. This mixture is added dropwise to water solution or directly injected in the solution as shown in Figure 1.17.

Due to the fast diffusion of the organic solvent in the water, the polymer precipitates at the water-organic solvent interface and nanoparticles are formed. The nanoparticles can have different structures depending on the synthesis formulation. Synthetic preformed polymers are most commonly employed, such as poly(lactic acid)[51, 89].

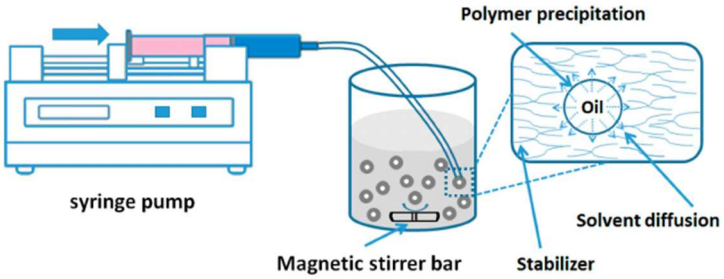

Figure 1.17. Scheme of the nanoprecipitation method[87]

1.3.2.3. Chemical techniques

Chemical microencapsulation techniques are mostly based on polymerization and can be divided in five types: dispersion polymerization, suspension polymerization, in-situ polymerization, emulsion polymerization and interfacial polycondensation, depending on where the polymerization reaction occurs and on the shell arrangement. The particles prepared via these polymerization techniques can have a lot of different sizes as they are directly related to the emulsion/dispersion preparation (mixing rate, droplet material). All the chemical techniques presented here can synthesize both micro- and nano-particles

Dispersion polymerization

This encapsulation consists in the polymerization of a monomer at the surface of particles dispersed in an organic solvent. The prepared polymer is, however, not soluble in the continuous phase. Some functional groups grafted on the polymer backbone, or on the particle surface, allow the insoluble polymer to position itself around the particles and form a protective shell (Fig. 1.18). This technique frequently encapsulates inorganic compounds and could be seen as a standard dispersion polymerization in which flocculation is avoided and micro/nanoparticles are created instead.

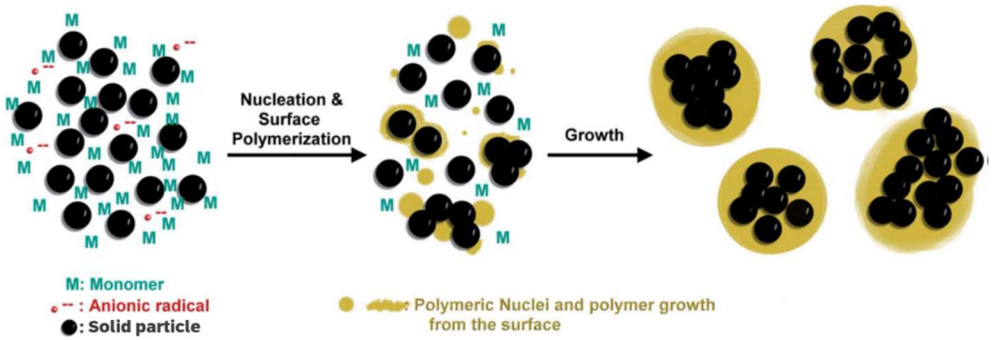

Adapted with permission from [90]. Copyright © The Royal Society of Chemistry 2014

Figure 1.18. Scheme of dispersion polymerization encapsulation

Suspension polymerization

This encapsulation is based on the dispersion of an organic solvent containing the monomers, the initiator and eventually a small amount of suspending agent. This dispersion is obtained and maintained by a high and constant shearing. At a certain temperature, the initiators are starting the polymerization reaction which occurs inside the droplets. The formed polymer precipitates in the organic solvent and forms the micro/nanoparticle shell (Fig. 1.19).

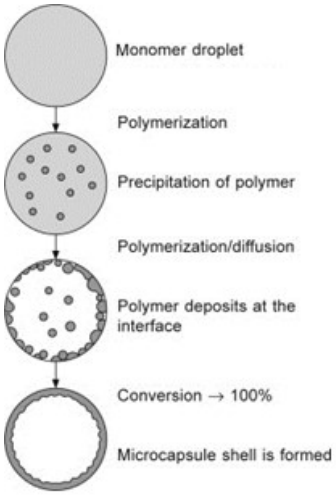

Reprinted with permission from [91]. Copyright © 2015 Elsevier Ltd.

Figure 1.19. Scheme of suspension polymerization encapsulation

Emulsion polymerization

This encapsulation leads more frequently to the preparation of nanoparticles from 10 to 1000nm. Different types of emulsions are prepared (water-in-oil (w/o), oil-in-water (o/w), double emulsion (w/o/w or o/w/o)) containing a mixture of monomer and core material. Contrarily to the in-situ polymerization (see after), the polymerization occurs within the emulsion droplet to create the particles. The size of the emulsion droplets has a direct impact on the size of the particles, which means all the parameters influencing the emulsion are of high importance (surfactant concentration, water to oil ratio). Polyacrylate and polycyanoacrylate are the two main classes of nanoparticles obtained via this technique[51].

In-situ polymerization

It consists in a formation of a wall as described in Figure 1.20. A mixture of monomer is dissolved in the continuous phase (generally water) leading to a pre-crosslinking. Then, the oil phase (core material) is added and an emulsion is created by stirring. The pre-crosslinked polymer is deposed on the surface of the droplet and complete polymerization is achieved by heating or changing the pH. In this technique, the polymerization occurs exclusively in the continuous phase.

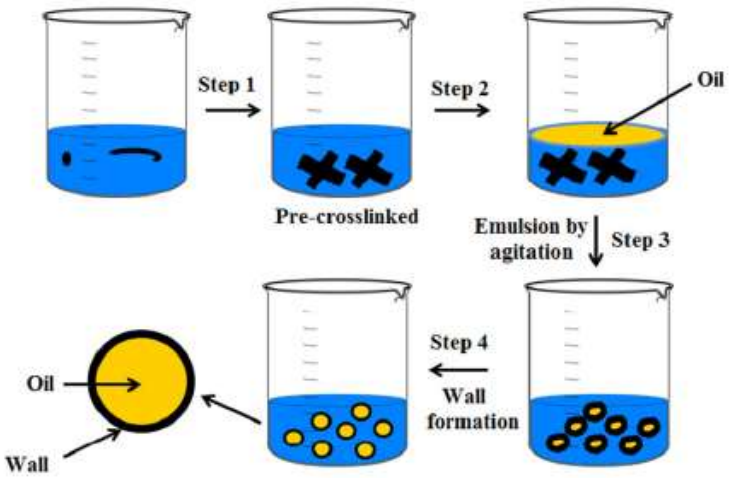

Adapted with permission from [55]. Copyright © 2015 Institute of Food Technologists®

Figure 1.20. Scheme of in-situ polymerization encapsulation

Emulsion cross-linking

The emulsion cross-linking method consists in the preparation of a water-in-oil emulsion. The aqueous phase contains the polymer as well as the material to encapsulate and is emulsified in the organic phase made of an immiscible organic solvent and a surfactant. The droplets are converted into micro/nanoparticles via covalent cross-linking of the polymer, which can occur thermally (over 500°C) or using a cross-linking agent. This technique is most frequently used for natural polymers, for example, glutaraldehyde is famous for cross-linking chitosan particles[83, 92].

Interfacial polycondensation

Polycondensation is a type of polymerization, more precisely a polyaddition, which releases small molecules during the synthesis (such as water or hydrochloric acid). This technique is very similar in its preparation to the in-situ polymerization and the emulsion polymerization, except the two monomers are not soluble in the same phase. Two solutions are prepared: one contains the core material and a monomer dissolved in a solvent; the other one is generally a water solution containing a surfactant. Both solutions are mixed to obtain an emulsion. The second monomer (water-soluble) is then added to the mixture. It reacts quickly with the first monomer at the interface of the droplets, which forms a strong polymer surrounding the core material[93] (Fig. 1.21).

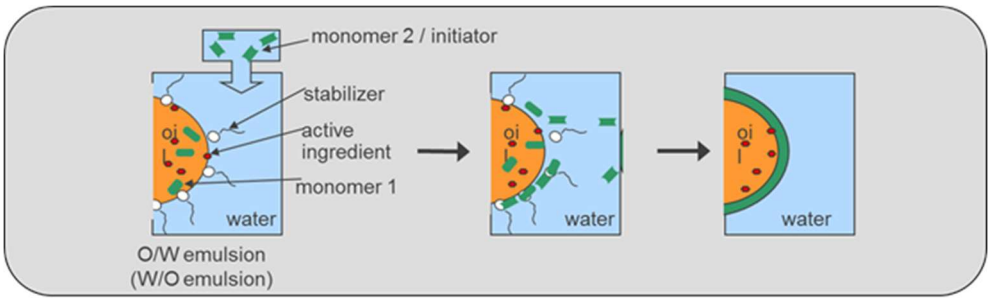

Figure 1.21. Scheme of interfacial polycondensation encapsulation

1.4. Aim and outline of the thesis

Nowadays polyurethanes are widely used in the coating and adhesive industry. Many different technologies exist to apply coatings and adhesives on substrates, and technologies in which crosslinking or adhesion could be controlled are of greatest interest. This would offer new possibilities for complex coating/adhesive system. Indeed, it would improve their pot-life which is the main drawback of polyurethane formulations. For this purpose, so-called blocked isocyanates have already been developed; they are derivatives of isocyanates which can only be activated via thermal trigger. In a similar approach, the encapsulation and controlled release of catalysts or reactive polyisocyanates would offer new perspectives toward enhanced technologies. Therefore, the work presented in this thesis focuses on the encapsulation of polyurethane formulation components, especially for application in coatings and adhesives, with the objective to develop new products gathering both triggered activation and long-term stability.

In the first part, the nanoencapsulation of polyurethane polymerization catalysts, namely zinc bis(2-ethylhexanoate) and bismuth tri(2-ethylhexanoate), will be discussed. The syntheses of catalyst-loaded polycaprolactone nanoparticles will be studied via two different synthesis methods: emulsion-solvent diffusion and nanoprecipitation (Chapter 2), followed by a thorough optimization up to the early steps of the implementation of nanoparticles into an existing polyurethane coating formulation (Chapter 3). In the second part, the encapsulation of polyisocyanates to be utilized as cross-linkers will be investigated through two different approaches. The microencapsulation of polyisocyanates in a polyurea and/or a polyurethane shell – obtained by interfacial polycondensation – will be examined (Chapter 4). Afterwards, the knowledge acquired from the previous studies will be used to briefly explore the nanoencapsulation of polyisocyanates into a polycaprolactone shell by nanoprecipitation (Chapter 5).

Lastly, the general conclusion will summarize the obtained results and the learnt concepts. It will also discuss the future of catalyst-loaded nanoparticles and will debate the possibilities regarding the encapsulation of polyisocyanates (Chapter 6).

1.5. References

1. von Wurtz, A., *Ueber die Verbindungen der Cyanursäure und Cyansäure mit Aethyloxyd, Methyloxyd, Amyloxyd und die daraus entstehenden Producte; Acetyl- und Metacetylharnstoff, Methylamin, Aethylamin, Valeramin.* Justus Liebigs Annalen der Chemie, 1849. **71**(3): p. 326-342 DOI: 10.1002/jlac.18490710308.
2. Hofmann, A.W., *Beiträge zur Kenntniss der flüchtigen organischen Basen).* Justus Liebigs Annalen der Chemie, 1850. **74**(1): p. 1-33 DOI: 10.1002/jlac.18500740102.
3. Hentschel, W., *Notizen.* Berichte der deutschen chemischen Gesellschaft, 1884. **17**(1): p. 1284-1289 DOI: 10.1002/cber.188401701333.
4. Randall, D.L.S., *The polyurethanes book*. 2002: Huntsman Polyurethanes, Everberg, Belgium.
5. U. Meier-Westhues, et al., *Polyurethanes: Coatings, Adhesives and Sealants*. 2nd Revised Edition. 2019: Vincentz Network GmbH & Co. KG, Hanover, Germany.
6. Golling, F.E., et al., *Polyurethanes for coatings and adhesives – chemistry and applications.* Polymer International, 2019. **68**(5): p. 848-855 DOI: 10.1002/pi.5665.
7. Pilch-Pitera, B., *Chapter 13 - Polyurethane Blends for Powder Clear Coatings*, in *Polyurethane Polymers*, S. Thomas, et al., Editors. 2017, Elsevier, Amsterdam, The Netherlands. p. 305-321.
8. Sonnenschein, M., *Polyurethanes: Science, Technology, Markets, and Trends*. 2015: Wiley, Hoboken, New Jersey, USA.
9. Laas, H.J., R. Halpaap, and J. Pedain, *Zur Synthese aliphatischer Polyisocyanate – Lackpolyisocyanate mit Biuret-, Isocyanurat- oder Uretdionstruktur.* Journal für Praktische Chemie/Chemiker-Zeitung, 1994. **336**(3): p. 185-200 DOI: 10.1002/prac.19943360302.
10. Mundstock, H., et al., *New low viscous polyisocyanates for VOC compliant systems.* Macromolecular Symposia, 2002. **187**(1): p. 281-292 DOI: 10.1002/1521-3900(200209)187:1<281::AID-MASY281>3.0.CO;2-H.
11. Bayer, O., *Das Di-Isocyanat-Polyadditionsverfahren (Polyurethane).* Angew. Chemie, 1947. **59**(9): p. 257-288 DOI: 10.1002/ange.19470590901.
12. Hombach, R., H. Reiff, and M. Dollhausen, *Water-dispersible polyisocyanate composition and its use as additive for aqueous adhesives* 1985. **EP0206059B1**.
13. Laas, H.-J., et al., *Water-dispersible polyisocyanate mixtures* 1991. **EP0540985B1**.
14. Laas, H.-J., R. Halpaap, and C. Wamprecht, *Water-dispersable polyether-modified mixtures of polyisocyanates.* 1998. **EP0959087B1**.
15. Laas, H.-J. and R. Halpaap, *Modified Polyisocyanates.* 2001. **WO2001088006A1**.
16. Karol, M.H., *Respiratory effects of inhaled isocyanates.* Crit Rev Toxicol, 1986. **16**(4): p. 349-79 DOI: 10.3109/10408448609037467.
17. Varma, D.R. and I. Guest, *The Bhopal accident and methyl isocyanate toxicity.* Journal of Toxicology and Environmental Health, 1993. **40**(4): p. 513-529 DOI: 10.1080/15287399309531816.
18. *Bonding Elastomers to Metals with MDI-50*, in *Elastomers Division Bulletin*, W. E. I. du Pont de Nemours & Co., Del., Editor. 1951.
19. Akindoyo, J.O., et al., *Polyurethane types, synthesis and applications – a review.* RSC Advances, 2016. **6**(115): p. 114453-114482 DOI: 10.1039/C6RA14525F.
20. American Chemistry Council. October 2021; Available from: americanchemistry.com/industry-groups/center-for-the-polyurethanes-industry-cpi/applications-benefits/polyurethane-applications.

21. Blomeyer, F., et al., *Improvements relating to lacquer solutions.* 1967. **GB1071930A**.
22. Durot, L., et al., *Mask Polyisocyanates and Uses Thereof.* 2011. **FR2981649B1**.
23. Patel, M., et al., *UV-curable Polyurethane Coatings Derived from Cellulose.* Iranian Polymer Journal, 2009. **18**: p. 903-915.
24. Kunwong, D., N. Sumanochitraporn, and S. Kaewpirom, *Curing behavior of a UV-curable coating based on urethane acrylate oligomer: The influence of reactive monomers.* Songklanakarin Journal of Science and Technology, 2011. **33**(2): p. 201-207.
25. Mishra, V., et al., *Development of Green Waterborne UV-Curable Castor Oil-Based Urethane Acrylate Coatings: Preparation and Property Analysis.* International Journal of Polymer Analysis and Characterization, 2015. **20**(6): p. 504-513 DOI: 10.1080/1023666X.2015.1050852.
26. Brockmann, W., et al., *Adhesive bonding : materials, applications and technology*. 2009: Wiley-VCH Verlag, Weinheim, Germany.
27. J. H. Saunders and K.C. Frisch, *Polyurethanes: Chemistry and Technology*. High Polymers. Vol. XVI. 1962: Interscience, New York, USA.
28. de Lima, V., et al., *Kinetic study of polyurethane synthesis using different catalytic systems of Fe, Cu, Sn, and Cr.* Journal of Applied Polymer Science, 2010. **115**(3): p. 1797-1802 DOI: 10.1002/app.31298.
29. Guhl, D., *Alternatives to DBTL catalysts in polyurethanes – a comparative study*. 2008: European Coatings Conference.
30. A. J. Bloodworth and A.G. Davies, *N-Stannylcarbamates, and their Role as Possible Intermediates in the Formation of Urethanes.* Proceedings of the Chemical Society, 1963(September): p. 264 DOI: 10.1039/PS9630000253.
31. Delebecq, E., et al., *On the Versatility of Urethane/Urea Bonds: Reversibility, Blocked Isocyanate, and Non-isocyanate Polyurethane.* Chemical Reviews, 2013. **113**(1): p. 80-118 DOI: 10.1021/cr300195n.
32. Spector, R.J., *Rigid polyurethane foam process using lithium/zinc catalyst.* 1981. **US4256847A**.
33. R. Leckart Arthur and V.H. H., *Catalysts containing metal compounds of antimony, bismuth or arsenic.* 1986. **US4584362B1**.
34. Silva, A.L. and J.C. Bordado, *Recent Developments in Polyurethane Catalysis: Catalytic Mechanisms Review.* Catalysis Reviews, 2004. **46**(1): p. 31-51 DOI: 10.1081/CR-120027049.
35. Belmokaddem, F.-Z., et al., *Novel nucleophilic/basic and acidic organocatalysts for reaction between poorly reactive diisocyanate and diols.* Designed Monomers and Polymers, 2016. **19**(4): p. 347-360 DOI: 10.1080/15685551.2016.1152545.
36. Sardon, H., et al., *Organic Acid-Catalyzed Polyurethane Formation via a Dual-Activated Mechanism: Unexpected Preference of N-Activation over O-Activation of Isocyanates.* Journal of the American Chemical Society, 2013. **135**(43): p. 16235-16241 DOI: 10.1021/ja408641g.
37. Sardon, H., et al., *Synthesis of Polyurethanes Using Organocatalysis: A Perspective.* Macromolecules, 2015. **48**(10): p. 3153-3165 DOI: 10.1021/acs.macromol.5b00384.
38. Khan, I., K. Saeed, and I. Khan, *Nanoparticles: Properties, applications and toxicities.* Arabian Journal of Chemistry, 2019. **12**(7): p. 908-931 DOI: 10.1016/j.arabjc.2017.05.011.
39. Risch, S.J. and A.G. Reineccius, *Encapsulation and controlled release of food ingredients*. 1995: American Chemical Society, Washington DC, USA.
40. Jackson, L.S. and K. Lee, *Microencapsulation and the food industry.* Lebensmittel-Wissenschaft & Technologie, 1991. **24**: p. 289-297.

41. Fávaro-Trindade, C.S., S.C.d. Pinho, and G.A. Rocha, *Revisão: microencapsulação de ingredientes alimentícios.* Brazilian Journal of Food Technology, 2008. **11**(2): p. 103-112.
42. Nazzaro, F., et al., *Microencapsulation in food science and biotechnology.* Curr Opin Biotechnol, 2012. **23**(2): p. 182-6 DOI: 10.1016/j.copbio.2011.10.001.
43. Orive, G., et al., *History, challenges and perspectives of cell microencapsulation.* Trends in Biotechnology, 2004. **22**(2): p. 87-92 DOI: 10.1016/j.tibtech.2003.11.004.
44. Mukherji, S. and V. Nalawade, *Microencapsulation: A review on polymers and correlation with BCS classification of drugs.* International Journal of Pharma and Bio Sciences, 2015. **6**: p. P305-P317.
45. Park, J.K. and H.N. Chang, *Microencapsulation of microbial cells.* Biotechnol Adv, 2000. **18**(4): p. 303-19 DOI: 10.1016/s0734-9750(00)00040-9.
46. Wilkins, R.M., H.S. Kas, and A.A. Hincal, Minutes Int. Symp. Encapsulation, 1994: p. 171-186.
47. John, R.P., et al., *Bio-encapsulation of microbial cells for targeted agricultural delivery.* Crit Rev Biotechnol, 2011. **31**(3): p. 211-26 DOI: 10.3109/07388551.2010.513327.
48. Nelson, G., *Application of microencapsulation in textiles.* Int J Pharm, 2002. **242**(1-2): p. 55-62 DOI: 10.1016/s0378-5173(02)00141-2.
49. Kumar, P., et al., *Nanotechnology and its challenges in the food sector: a review.* Materials Today Chemistry, 2020. **17**: p. 100332 DOI: 10.1016/j.mtchem.2020.100332.
50. González-Reza, R.M., M.L. Zambrano-Zaragoza, and H. Hernández-Sánchez, *Polymeric Nanoparticles in Foods*, in *Plant Nanobionics: Volume 2, Approaches in Nanoparticles, Biosynthesis, and Toxicity*, R. Prasad, Editor. 2019, Springer International Publishing: Cham. p. 217-233.
51. Reis, C.P., et al., *Nanoencapsulation I. Methods for preparation of drug-loaded polymeric nanoparticles.* Nanomedicine, 2006. **2**(1): p. 8-21 DOI: 10.1016/j.nano.2005.12.003.
52. Castro, K.C.d., J.M. Costa, and M.G.N. Campos, *Drug-loaded polymeric nanoparticles: a review.* International Journal of Polymeric Materials and Polymeric Biomaterials, 2020: p. 1-13 DOI: 10.1080/00914037.2020.1798436.
53. Dubey, R., T.C. Shami, and K.U. Rao, *Microencapsulation Technology and Applications.* Defence Science Journal, 2009. **59**: p. 82-95 DOI: 10.14429/dsj.59.1489.
54. Das, S., et al., *Microencapsulation techniques and its practices.* International Journal of Pharmaceutical Science and Technology, 2011. **6**: p. 1-23.
55. Bakry, A.M., et al., *Microencapsulation of Oils: A Comprehensive Review of Benefits, Techniques, and Applications.* Comprehensive Reviews in Food Science and Food Safety, 2016. **15**(1): p. 143-182 DOI: 10.1111/1541-4337.12179.
56. Yang, C.-Y., S.Y. Tsay, and R.C.C. Tsiang, *Encapsulating aspirin into a surfactant-free ethyl cellulose microsphere using non-toxic solvents by emulsion solvent-evaporation technique.* Journal of Microencapsulation, 2001. **18**(2): p. 223-236 DOI: 10.1080/026520401750063937.
57. Pathak, Y.V., M. Shingatgiri, and A.K. Dorle, *In vivo performance of pentaestergum-coated aspirin microcapsules.* Journal of Microencapsulation, 1987. **4**(2): p. 107-110 DOI: 10.3109/02652048709021804.
58. Mak, W.C., et al., *Controlled Delivery of Human Cells by Temperature Responsive Microcapsules.* Journal of functional biomaterials, 2015. **6**(2): p. 439-453 DOI: 10.3390/jfb6020439.

59. Abbaspourrad, A., S.S. Datta, and D.A. Weitz, *Controlling Release From pH-Responsive Microcapsules.* Langmuir, 2013. **29**(41): p. 12697-12702 DOI: 10.1021/la403064f.
60. Zhen, Z.H. and Z.S. Wang, *Pressure Sensitive Essence Microcapsules with MF-UF Resin as Double Wall.* Advanced Materials Research, 2013. **746**: p. 106-109 DOI: 10.4028/www.scientific.net/AMR.746.106.
61. Dispinar, T., C.A.L. Colard, and F.E. Du Prez, *Polyurea microcapsules with a photocleavable shell: UV-triggered release.* Polymer Chemistry, 2013. **4**(3): p. 763-772 DOI: 10.1039/C2PY20735D.
62. Hu, M., et al., *Research Advances of Microencapsulation and Its Prospects in the Petroleum Industry.* Materials, 2017. **10**(4): p. 369 DOI: 10.3390/ma10040369.
63. Somasundaran, P., *Encyclopedia of surface and colloid science*. 2006: Taylor & Francis, New York, USA.
64. Mishra, M., *Handbook of Encapsulation and Controlled Release*. 2015: CRC Press, New York, USA.
65. da Silva, P.T., et al., *Microencapsulation: concepts, mechanisms, methods and some applications in food technology.* Ciencia Rural, 2014. **44**: p. 1304-1311 DOI: 10.1590/0103-8478cr20130971.
66. Mishra, D., A. Jain, and P. Jain. *A Review on Various Techniques of Microencapsulation*. 2013.
67. Bansode, S., et al., *Microencapsulation: A review.* International Journal of Pharmaceutical Sciences Review and Research, 2010. **1**.
68. Achinna, P. and A. Kuna, *Microencapsulation technology: A review.* J Res Angrau, 2010. **38**.
69. Poncelet, D. *Microencapsulation: fundamentals, methods and applications*. 2006. Dordrecht: Springer Netherlands.
70. KuShaari, K., et al., *Monte Carlo simulations to determine coating uniformity in a Wurster fluidized bed coating process.* Powder Technology, 2006. **166**(2): p. 81-90 DOI: 10.1016/j.powtec.2006.05.001.
71. Oxley, J.D., *5 - Spray cooling and spray chilling for food ingredient and nutraceutical encapsulation*, in *Encapsulation Technologies and Delivery Systems for Food Ingredients and Nutraceuticals*, N. Garti and D.J. McClements, Editors. 2012, Woodhead Publishing. p. 110-130.
72. Augsburger, L.L.H.S.W.P., *Pharmaceutical dosage forms tablets. Volume 1, Volume 1*. 2008: Informa Healthcare, New York, USA.
73. Pandey, P., et al., *Scale-up of a pan-coating process.* AAPS PharmSciTech, 2006. **7**(4): p. 102-102 DOI: 10.1208/pt0704102.
74. Sosnik, A. and K.P. Seremeta, *Advantages and challenges of the spray-drying technology for the production of pure drug particles and drug-loaded polymeric carriers.* Adv Colloid Interface Sci, 2015. **223**: p. 40-54 DOI: 10.1016/j.cis.2015.05.003.
75. Chopde, S., et al., *Nanoparticle formation by nanospray drying & its application in nanoencapsulation of food bioactive ingredients.* Journal of Agriculture and Food Research, 2020. **2**: p. 100085 DOI: 10.1016/j.jafr.2020.100085.
76. Oh, C.M., P.W.S. Heng, and L.W. Chan, *A study on the impact of hydroxypropyl methylcellulose on the viscosity of PEG melt suspensions using surface plots and principal component analysis.* AAPS PharmSciTech, 2015. **16**(2): p. 466-477 DOI: 10.1208/s12249-014-0204-x.

77. Sinha, V.R., et al., *6 - Current Polyesteric Systems for Advanced Drug Delivery*, in *Nanoarchitectonics for Smart Delivery and Drug Targeting*, A.M. Holban and A.M. Grumezescu, Editors. 2016, William Andrew Publishing. p. 143-168.
78. Caruso, F., et al., *Enzyme Encapsulation in Layer-by-Layer Engineered Polymer Multilayer Capsules.* Langmuir, 2000. **16**(4): p. 1485-1488 DOI: 10.1021/la991161n.
79. Budisa, N. and D. Schulze-Makuch, *Supercritical Carbon Dioxide and Its Potential as a Life-Sustaining Solvent in a Planetary Environment.* Life, 2014. **4**(3): p. 331-340.
80. Soh, S.H. and L. Lee, *Microencapsulation and Nanoencapsulation Using Supercritical Fluid (SCF) Techniques.* Pharmaceutics, 2019. **11**: p. 21 DOI: 10.3390/pharmaceutics11010021.
81. Deshmukh, R., P. Wagh, and J. Naik, *Solvent evaporation and spray drying technique for micro- and nanospheres/particles preparation: A review.* Drying Technology, 2016. **34**(15): p. 1758-1772 DOI: 10.1080/07373937.2016.1232271.
82. Hariyadi, D.M. and N. Islam, *Current Status of Alginate in Drug Delivery.* Advances in pharmacological and pharmaceutical sciences, 2020. **2020**: p. 8886095-8886095 DOI: 10.1155/2020/8886095.
83. Naskar, S., K. Koutsu, and S. Sharma, *Chitosan-based nanoparticles as drug delivery systems: a review on two decades of research.* J Drug Target, 2019. **27**(4): p. 379-393 DOI: 10.1080/1061186x.2018.1512112.
84. Idrees, H., et al., *A Review of Biodegradable Natural Polymer-Based Nanoparticles for Drug Delivery Applications.* Nanomaterials (Basel, Switzerland), 2020. **10**(10): p. 1970 DOI: 10.3390/nano10101970.
85. Giri, T.K., *5 - Nanoarchitectured Polysaccharide-Based Drug Carrier for Ocular Therapeutics*, in *Nanoarchitectonics for Smart Delivery and Drug Targeting*, A.M. Holban and A.M. Grumezescu, Editors. 2016, William Andrew Publishing. p. 119-141.
86. Lim, K. and Z.A.A. Hamid, *10 - Polymer nanoparticle carriers in drug delivery systems: Research trend*, in *Applications of Nanocomposite Materials in Drug Delivery*, Inamuddin, A.M. Asiri, and A. Mohammad, Editors. 2018, Woodhead Publishing, Sawston, UK. p. 217-237.
87. Wang, Y., et al., *Manufacturing Techniques and Surface Engineering of Polymer Based Nanoparticles for Targeted Drug Delivery to Cancer.* Nanomaterials, 2016. **6**: p. 26 DOI: 10.3390/nano6020026.
88. Barreras-Urbina, C.G., et al., *Nano- and Micro-Particles by Nanoprecipitation: Possible Application in the Food and Agricultural Industries.* International Journal of Food Properties, 2016. **19**(9): p. 1912-1923 DOI: 10.1080/10942912.2015.1089279.
89. Martínez Rivas, C.J., et al., *Nanoprecipitation process: From encapsulation to drug delivery.* International Journal of Pharmaceutics, 2017. **532**(1): p. 66-81 DOI: 10.1016/j.ijpharm.2017.08.064.
90. Chou, I.C., S.-I. Chen, and W.-Y. Chiu, *Surfactant-free dispersion polymerization as an efficient synthesis route to a successful encapsulation of nanoparticles.* RSC Advances, 2014. **4**(88): p. 47436-47447 DOI: 10.1039/C4RA07475K.
91. Al-Shannaq, R. and M. Farid, *Microencapsulation of phase change materials (PCMs) for thermal energy storage systems*, in *Advances in Thermal Energy Storage Systems*. 2015, Woodhead Publishing, Sawston, UK. p. 247-284.

92. K.M, D.M., B. Shivakumar, and P. Kumar, *Microencapsulation: An Acclaimed Novel Drug-Delivery System for NSAIDs in Arthritis.* Critical reviews in therapeutic drug carrier systems, 2010. **27**: p. 509-45 DOI: 10.1615/CritRevTherDrugCarrierSyst.v27.i6.20.
93. Yow, H.N. and A.F. Routh, *Formation of liquid core–polymer shell microcapsules.* Soft Matter, 2006. **2**(11): p. 940-949 DOI: 10.1039/B606965G.

Part 1. Encapsulation of polyurethane polymerization catalysts

Chapter 2. Synthesis of catalyst-loaded nanoparticles

2.1. Introduction

Two-component (2K) formulations represent most of the polyurethane coatings nowadays. Despite their excellent properties, 2K formulations still have one main disadvantage: their pot-life. The pot-life, also called gel time, refers to as the time in which the coating formulation is applicable. Indeed, the polyisocyanates and the polyols react with each other as soon as they are mixed, until they reach a too high viscosity to be processed. By general agreement, 2K polyurethane coatings become useless after they double their viscosity, typically within 4 to 6 hours[1].

To remedy this problem, photolatent[2] and thermolatent[3] catalysts have been developed. The polymerization reaction of the formulations remains uncatalyzed until light or heat are applied as external trigger to activate the catalyst release. In a similar approach, the use of catalyst-loaded thermoresponsive nanoparticles would significantly improve the formulation pot-lifes and offer new possibilities in the preparation of polyurethane coatings.

Nanoparticles can display different morphologies as described in Chapter 1. However, the two most common structural types are nanocapsules and nanospheres. The former consists in an encapsulated core surrounded by a polymer shell, while the latter possesses a polymer matrix in which the encapsulated material is dispersed, as illustrated in Figure 2.1. Such nanoparticles can be synthesized either by the polymerization of monomers, or obtained directly from a preformed polymer – the second approach has the advantage to avoid the use of toxic compounds (monomers, organic solvents) and to be simple in terms of production[4] (Table 2.1).

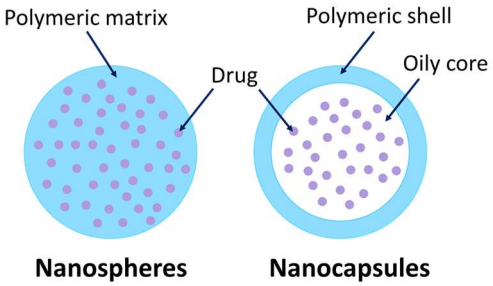

Figure 2.1. Structure of nanospheres and nanocapsules

Alginate and chitosan are naturally occurring polymers which are very commonly used for the synthesis of nanoparticles[5-7]. These polymers however contain polar groups which are involved in ionic interactions and due to the ionic nature of the compound to be encapsulated in this work – carboxylic metal salts – the use of non-ionizable (neutral but polar) synthetic polymers was preferred for the synthesis of the shell and the matrix of the nanoparticles.

The synthetic polymers more frequently used include polylactic acid (PLA), polyethylene glycol (PEG), poly(lactic-co-glycolic acid) (PLGA) and polycaprolactone (PCL)[4, 8, 9]. Moreover, encapsulations with a combination of the aforementioned polymers are also regularly performed, for example, PLA-PGLA[10], PCL-PEG-PCL or PGLA-PEG[11]. They all are biodegradable and biocompatible polymers which make them usable for plenty of applications.

As the investigated thermoresponsive nanoparticles are intended to be used in polyurethane coatings, PCL has been determined as the most appropriate polymer due to its melting point of $60°C$. As polyurethane coatings are typically cured between 80 and $120°C$[1], PCL-based nanoparticles are, by their nature, very convenient for the thermally triggered catalysts' release. To synthesize such nanoparticles, four techniques are described in the literature[4, 8]. Namely, solvent evaporation, emulsion-solvent diffusion (ESD), salting out and nanoprecipitation. Table 2.1. has been adapted from a table available in the nanoencapsulation review of C. Pinto Reis and coworkers[4].

Table 2.1. Advantages and drawbacks of common nanoencapsulation methods

Method	Simplicity of procedure	Need for purification	Facility Scaling-Up	Encapsulation Efficiency	Safety of Compounds
Emulsion Polymerization	Low to High[a]	High	High	Low to High[a]	Low to Medium[a]
Interfacial Polymerization	Low	High	Medium	High	Low
Solvent Evaporation	High	Low	Low	Medium	Medium
Nanoprecipitation	High	NR[b]	NR[b]	High	Medium
Emulsion-Solvent Diffusion	Medium	Medium	High	High	Medium
Salting Out	High	High	High	High	Low
Ionotropic Gelation	Medium to High[c]	Medium to High[c]	High	Medium to High[c]	Low to High[c]
Coacervation	NR[b]	High	NR[b]	Low	Low

a: depending on the emulsion; b: NR= non referenced; c: depending on the polymer
Adapted with permission from [4]. Copyright © 2006 Elsevier Inc.

It summarizes the advantages and drawbacks of each technique. The solvent evaporation method is not suitable for this project, as even today, its scale-up remains challenging. The ESD and the salting out technique are very similar, however the latter involves the use of electrolytes that could adversely affect the encapsulation of ionic species. Thus, the aim of this part is to synthesize and characterize polycaprolactone nanoparticles containing zinc or bismuth salts – via nanoprecipitation and ESD – aiming at the obtention of new polyurethane formulations.

2.2. Materials & Methods

2.2.1. Materials

Several types of material are involved in the synthesis of nanoparticles. First, the synthetic polymer poly(ε-caprolactone) (PCL) with different molecular weights (M_n= $10\,kDa$ (PCL-10), $45\,kDa$ (PCL-45), $80\,kDa$ (PCL-80)) was supplied by Sigma Aldrich. PCL is a polyester (Fig. 2.2) which, thanks to its biocompatibility and its biodegradability, is approved by the US Food and Drug Administration. Therefore, PCL is very frequently used for biomedical applications[12] such as polymeric nanoparticles.

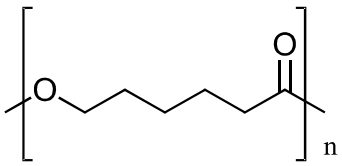

Figure 2.2. Polycaprolactone structure

The surfactants play a key role in the synthesis of nanoparticles, as they prevent the nanoparticles to agglomerate. The non-ionic surfactants Pluronic F-68 (triblock copolymer poly(ethylene glycol)-poly(propylene glycol)-poly(ethylene glycol); M_w=8.4 kDa), Pluronic L-35 (triblock copolymer poly(ethylene glycol)-poly(propylene glycol)-poly(ethylene glycol); M_w= $1.9\,kDa$), poly(vinyl alcohol) (PVA; M_w=$31kDa$) and Tween 80 (Polysorbate 80) were supplied by Sigma Aldrich (Table 2.2). Pluronic F-68 and Pluronic L-35 have the same general structure but they differ in terms of molecular weight and poly(ethylene glycol) (PEG) part, as they are made of 80% and 50% of PEG respectively. All those non-ionic surfactants stabilize the emulsions and/or the nanoparticle dispersions by steric repulsion. The catalyst Borchi Kat 22 (BK22) (zinc bis(2-ethylhexanoate); 21.8 – 22.6 % zinc content) was kindly donated by Borchers and previously described (Table 1.8). Water was purified with a $0.22\mu m$ Milipak® membrane filter. All other solvents and reagents were of analytical grade. All chemicals and materials were used as received.

Table 2.2. Surfactant structures

Pluronic F-68 & Pluronic L-35 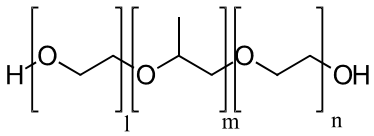
Poly(vinyl alcohol) **PVA** 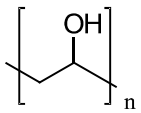
Tween 80 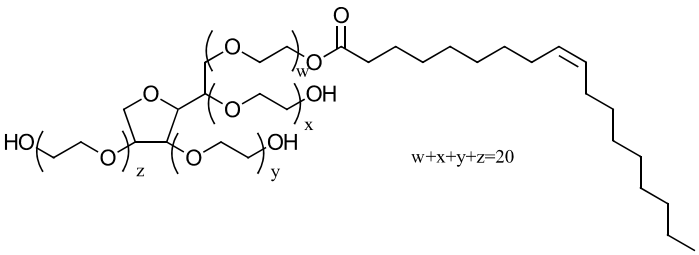

2.2.2. Synthesis methods

2.2.2.1. Emulsion Solvent-Diffusion

Nanoparticles containing BK22 (zinc-based catalyst) were synthesized via emulsion-solvent diffusion (ESD), firstly described by Quintanar-Guerrero and coworkers[13, 14] (Fig. 2.3). This method is based on the partial solubility of organic solvents in water. Therefore, water and ethyl acetate (EA) or methyl ethyl ketone (MEK) were mixed in large amounts to prepare saturated solutions: organic solvent-saturated with water (EAs-water and MEKs-water) and water-saturated with the organic solvent (Ws-EA and Ws-MEK). At 20°C, water is saturated with 8.7% and 24.0% of EA and MEK respectively. In turn, EA and MEK are saturated with 3.3% and 10.0% of water respectively.

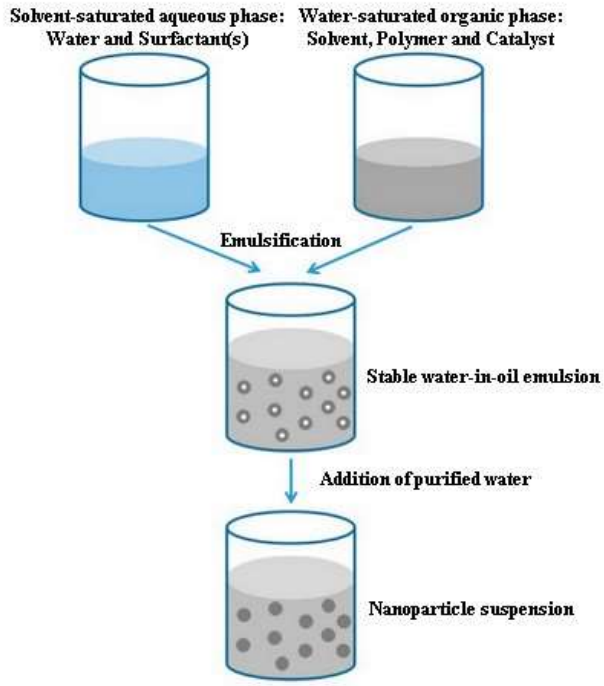

Figure 2.3. Nanoencapsulation of catalyst via emulsion-solvent diffusion technique (adapted from [15])

The PCL (100-400mg) was dissolved in the Ws-organic solvent (10mL) at 50°C and the zinc-based catalyst (100-800mg) was added subsequently. The resulting organic solution was added to an aqueous phase (40mL) containing different surfactants, as well as at different concentrations of the surfactant (0.1 to $2_{w/w}\%$). The mixture was emulsified using a high-speed mixer (Ultra-Turrax T25, IKA) rotating at 10,000rpm during 10 minutes. The resulting emulsion is stable and no solvent exchange is possible from one phase to another due to their respective saturation. A large amount of pure water was added at once to the emulsion to displace the equilibrium and induce the precipitation of the PCL nanoparticles. The amount of added water needs to be sufficiently large to extract entirely the solvent outside of the emulsion droplets, i.e. 200mL and 100mL when EA and MEK were used respectively. The nanoparticle suspension was mixed under moderate stirring for 30 minutes, followed by removal of the solvent and part of the water under vacuum.

2.2.2.2. Nanoprecipitation

Nanoparticles containing BK22 (zinc-based catalyst) were synthesized via nanoprecipitation as firstly described by Fessi and coworkers[16] (Figure 1.17). First, the polycaprolactone (50-150mg) was dissolved in acetone (10mL) at 50°C under moderate stirring and the catalyst (15-200mg) was added subsequently. This mixture was slowly added with a syringe pump (NE-1000, New Era Pump Systems Inc) to a water solution, containing a surfactant (0.1 to $2_{w/w}\%$), under magnetic stirring. After the addition was completed, the nanoparticle suspension was stirred 10 more minutes and filtered.

2.2.3. Characterization

2.2.3.1. Particle size analysis

The particle size was measured by Dynamic Light Scattering (DLS) using a Zetasizer Nano ZS (Malvern Instruments). All samples were diluted (1:10, v/v) in water and analyzed in triplicate at 25 °C. Particle size measurements were conducted in disposable polystyrene cells and the scattered light was collected at 173°. All data were analyzed with the Zetasizer software.

2.2.3.2. Morphology

Transmission Electron Microscopy (TEM; JEM-1011, Jeol) was used to study the morphology of the nanoparticles in suspension. One drop of sample was placed on a copper grid and the excess was removed with filter paper. The grid was dried overnight at room temperature. Field Emission Scanning Electron Microscopy (FESEM; Scios2, Thermo Fischer Scientific) was also used to observe the nanoparticles suspension. One drop of liquid sample was placed on an aluminum or silica support and dried overnight at room temperature. Samples were observed at an accelerated voltage of 5kV.

FESEM differs from the more common Scanning Electron Microscopy (SEM) by its electron emission source. SEMs are usually equipped with thermionic emitters, which means the material filament, typically made of tungsten or lanthanum hexaboride, is heated to create the electron beam. The FESEM uses a pointed emitter (FEG) of a few nanometers (Fig. 2.4), which, when heated, provides a much narrower electron beam, and therefore, a significantly better resolution can be obtained. FESEM also has the advantage to not require to coat the material for the analysis.

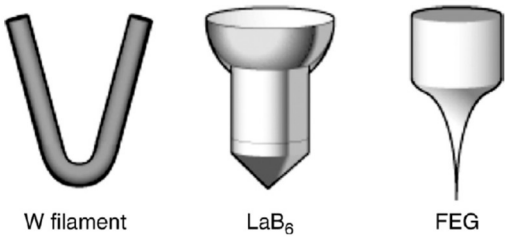

Reprinted with permission from [17]. Copyright © 2017 Elsevier Inc.

Figure 2.4. Electron sources for electron microscopy

2.2.3.3. X-Ray microanalysis

Field Emission Scanning Electron Microscopy with Energy Dispersive X-Ray (FESEM-EDX; Scios2, Thermo Fischer Scientific) was used to qualitatively detect metals inside the nanoparticles and in solution, in order to estimate the encapsulation efficiency. Samples were placed on an aluminum or a silica support as previously described. X-Ray microanalyses were performed at an accelerated voltage of $15kV$. Peaks were automatically assigned by the Pathfinder X-Ray Microanalysis Software (Thermo Fischer Scientific). No peak assignments were deleted, added or modified, unless told otherwise. All samples were analyzed in duplicate and at two different spots within the same sample.

2.3. Results and Discussion

The present chapter investigates the nanoencapsulation of polyurethane polymerization catalysts for uses in polyurethane coatings. For a proper efficiency of such system, the catalyst needs to be homogenously dispersed in the coating. This can be achieved by using nanoparticles of reduced size as it would allow a better dispersion in the formulation. The key parameters affecting the size of nanoparticles are known to be the surfactant nature and concentration, as well as the polymer, but process parameters can also make a significant difference.

2.3.1. Emulsion-Solvent Diffusion Encapsulation (ESD)

Parameters influencing the particle size

Not many organic solvents were suitable for the ESD encapsulation, as they needed to be partially soluble in water and to solubilize the PCL. Only two common solvents seemed appropriate: ethyl acetate (EA) and methyl ethyl ketone (MEK). Among those, EA is a largely and cheaply available and a smaller amount of EA than MEK is needed to perform the synthesis (due to higher solubility of MEK in water). Therefore, EA has been selected as the organic solvent for the ESD encapsulation. It is also important to precise that all ESD encapsulations were performed with PCL-80.

PVA and Pluronic-F68 are two of the most common types of surfactant used in ESD, in order to stabilize the emulsion during the first step of the synthesis[14, 18, 19]. Firstly, PVA ($1_{w/w}\%$) was investigated as surfactant for the encapsulation of metal salts, however, it led to formation of large white aggregates after the high speed mixing. PVA protected nanoparticles are known to have a negative zeta potential (-20mV to -25mV)[20, 21], therefore this aggregation might be explained by an ionic interaction between the encapsulated metal salts and the PVA surfactant[22]. On the other side, nanoparticles stabilized with Pluronic F-68 were successfully synthesized. The influence of the concentration of surfactant has been investigated (Fig. 2.5). The amount of surfactant impacts the size of the emulsion droplets, thus the size of the nanoparticles in solution.

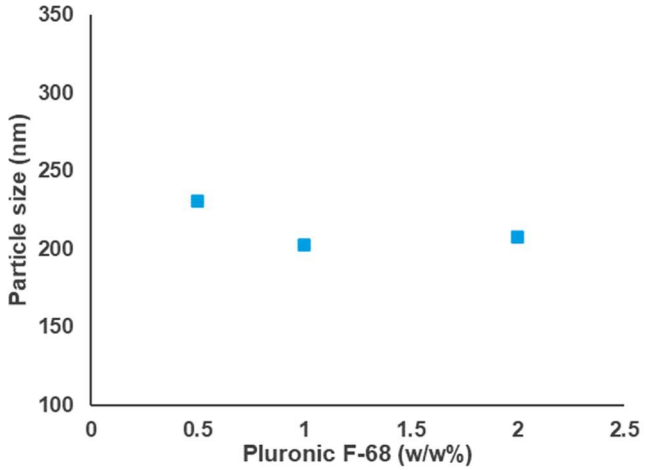

Figure 2.5. Effect of the surfactant concentration on the nanoparticle size (ESD)

Less surfactant can only stabilize a smaller surface, hence larger nanoparticles are normally formed, and this is what have been observed when increasing the surfactant concentration from 0.5 to 1.0$_{w/w}$%. On the opposite side, high concentrations of surfactant (>1.0$_{w/w}$%) led to a slightly higher particle size. These phenomenon have also been reported in other works, as the results of a higher viscosity in the aqueous phase, meaning a lower solvent diffusion rate[14, 18]. In addition, the effect of the concentration of PCL on the particle size was studied. It has been observed that an increase of the PCL concentration implies an increase of the particle size (Fig. 2.6).

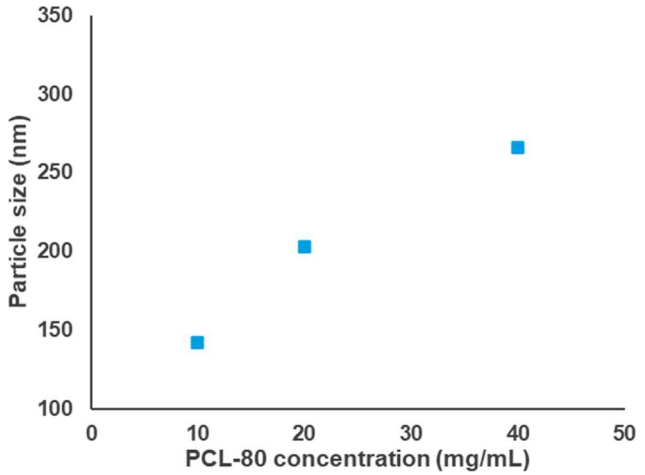

Figure 2.6. Effect of the polymer concentration on the nanoparticle size (ESD)

With a similar approach, an increase of the metal salt (BK22; zinc-based catalyst) concentration in the emulsion droplets should lead to a larger particle size, which is indeed what has been detected (Fig. 2.7). A larger BK22 ratio in the nanoparticle would be relevant, but this advantage is compensated by an increase in particle size, and, at too high concentrations of catalyst (>150mg/mL), small aggregates are formed in the solution and the non-aggregated particles were bigger than 1μm, which is not suitable for uses in polyurethane coatings.

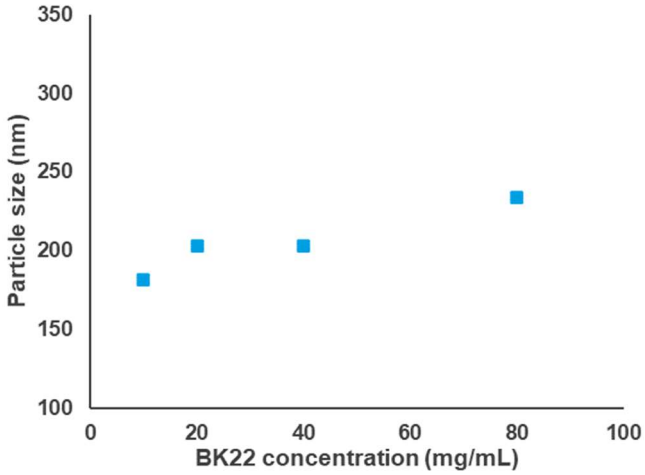

Figure 2.7. Effect of the catalyst concentration on the nanoparticle size (ESD)

Those first investigations have shown that the formulation parameters are important to control the size of the nanoparticles synthesized via ESD. However, it is well known that the process parameters can impact the size of the nanoparticles, especially those affecting the size of the emulsion droplets, such as the mixing time and speed[23-25].

Nanoparticles obtained from smaller emulsion droplets would logically be smaller as well. Therefore, it can be hypothesized that an increase of the mixing time or of the mixing speed should provide a decrease of the particle size. Firstly, the mixing time has been investigated at constant stirring (10,000rpm) during 5 to 20 minutes and the results are presented in Figure 2.8.

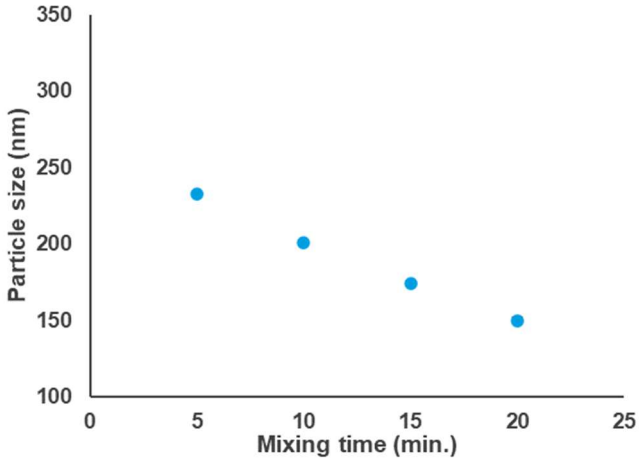

Figure 2.8. Effect of the mixing time (minutes) on the nanoparticle size (ESD)

As expected, the particle size clearly decreases proportionally to the increase of the mixing time. In the same way, Figure 2.9 illustrates that the increase of the mixing rate at constant time (10 min.) causes a decrease of the particle size, thus confirming the previously made assumption. Those observations are notable, as it means that the particle size is tunable by simply varying the mixing time and speed. It is worth mentioning that a high mixing rate during a prolonged period of time will lead to an increase of temperature of the solution, which could cause problems with the organic solvent and the emulsion stability.

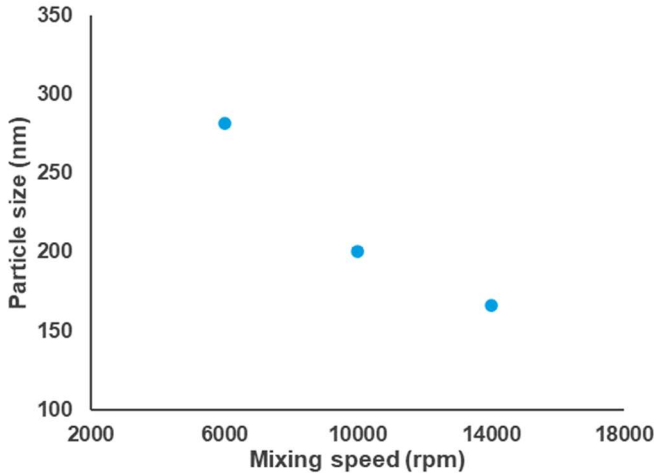

Figure 2.9. Effect of the mixing speed on the nanoparticle size (ESD)

One last process parameter was studied: the purified-water addition. The amount of added water was varied between $150mL$ and $250mL$, however a very small decrease was observed on the particle size of the nanoparticles, from $174nm$ to $156nm$, respectively. The volume of added water needs logically to be sufficient to extract entirely the EA from the emulsion droplet (about $111mL$ of water theoretically). This was expected, as with a larger amount of water, the diffusion rate of the EA into the water increases, therefore the particles should be smaller.

Lastly, EA was replaced by MEK in a few syntheses to evaluate the impact of the solvent on the particle size. For the same formulation, EA and MEK led to nanoparticles of $191nm$ and $142nm$ respectively. This significant difference remains so far unexplained but it could be due to the difference of solubility of water in the solvents or to a difference of affinity between the solvent and the surfactant. Studying more solvents would be necessary to draw conclusions, however, as mentioned earlier, suitable surfactants are rare.

Nevertheless, due to the boiling point of MEK ($99.0°C$) being close to the one of water, MEK cannot be fully removed by evaporation under vacuum. Therefore, MEK-based nanoparticles are not appropriate samples for the next purification step, lyophilization (Chapter 3), in which only water can be removed. On the other side, this is not an issue for EA-based nanoparticles, as the boiling point of EA is lower ($77.1°C$) and it can be properly removed under vacuum.

Reproducibility of the experiment

Nanoparticles were successfully obtained with a variety of formulations, however, the synthesis needs to be reproducible in order to confirm the previously drawn conclusions. To study this parameter, the exact same synthesis was performed five times. The nanoparticle size of each sample was measured three times and compared in Table 2.3 below. It is interesting to see that all the experiments are within a less than 20nm range. The experiment averages are all within about ± 5% from the total average, which is a good reproducibility in terms of particle size. Moreover, the polydispersity index (PDI) was studied during these reproducibility experiments.

The PDI is used to define the particle size distribution within a single sample. Usually, a PDI below 0.1 is considered as a highly monodispersed system[26] and it can be seen in Table 2.3 that the average PDI of the five experiments is actually of 0.100. Those results indicate that the ESD technique has a very good reproducibility.

Table 2.3. Study of the reproducibility of the ESD nanoencapsulation

Experiment number	Particle size (nm)				Polydispersity Index			
	Measurements	*Experiment average*	*Total average*	*Maximum difference to average*	*Measurements*	*Experiment average*	*Total average*	*Maximum difference to average*
1	171.1	170.4	174.9	± 9.2	0.103	0.106	0.100	± 0.025
	171.0				0.119			
	169.0				0.097			
2	168.7	165.8			0.111	0.120		
	165.3				0.120			
	163.4				0.128			
3	174.9	174.4			0.111	0.100		
	173.8				0.090			
	174.4				0.099			
4	185.2	184.2			0.104	0.101		
	183.6				0.087			
	183.9				0.113			
5	179.4	179.6			0.103	0.075		
	180.6				0.063			
	178.9				0.058			

Microscopy

The nanoparticle solutions were observed by Transmission Electron Microscopy (TEM) (Fig. 2.10) and by Field Emission Scanning Electron Microscopy (FESEM) (Fig. 2.11). The synthesized nanoparticles seem to be nanospheres (Fig. 2.1), as nanospheres are made of a polymer matrix (light gray area) in which the metal salt is dispersed (darker area).

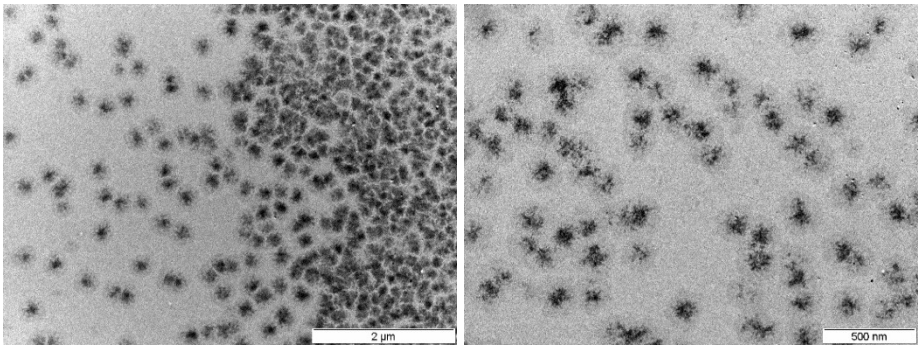

Figure 2.10. TEM pictures of nanoparticle suspensions at x20k (left) and x50k (right) (ESD)

Moreover, standard ESD encapsulations generally form nanospheres[8, 27]. Nanosphere sizes observed by TEM are in accordance with the DLS measurements, as well as the sizes observed by FESEM. FESEM pictures show white spherical nanospheres with a smooth external surface. High resolution pictures are difficult to obtain as the polymer material can easily melt.

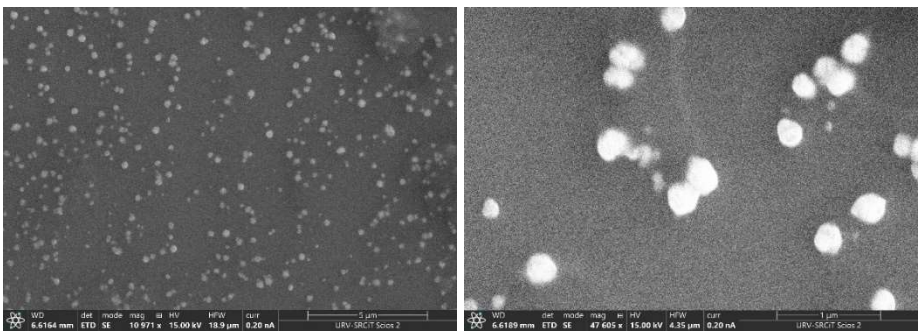

Figure 2.11. FESEM pictures of nanoparticle suspensions: ~x11k (left) and ~x48k (right) (ESD)

The FESEM device is equipped with an EDX (Energy Dispersive X-Ray) which allows to perform X-Ray microanalyses on the sample. The X-Ray microanalysis can even be focused on a selected spot, as shown in Figure 2.12 below (orange spot). It is then possible to get an idea of the chemical composition on a certain point of the sample. The results presented here show that the synthesized particles contain carbon, oxygen and zinc, which is the central element of the catalyst. The detected silica is in fact the support on which the sample is observed. Therefore, with the TEM pictures, the FESEM pictures and the X-Ray microanalysis, it can be confirmed that the nanoencapsulation of catalyst into PCL is successful via the emulsion-solvent diffusion technique.

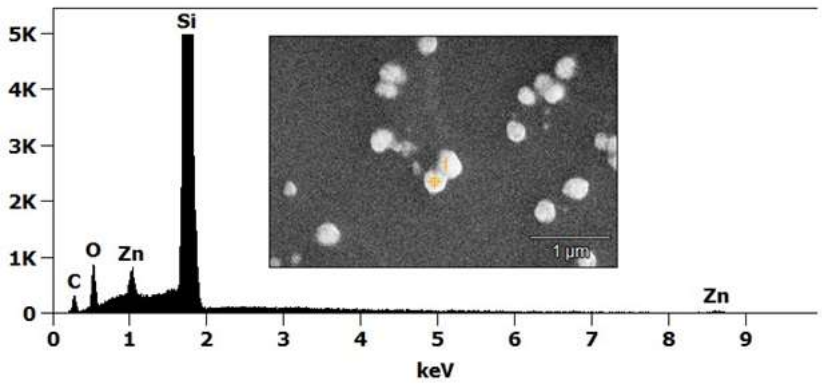

Figure 2.12. X-Ray microanalysis of ESD nanospheres

2.3.2. Nanoprecipitation encapsulation

Parameters influencing the particle size

PVA and Pluronic F-68 are also some of the most common surfactants for nanoprecipitation[28-31]. Tween 80 is, as well, used very often[30, 32, 33]. Even some surfactant-free nanoprecipitations are also described[34, 35] which is what have been firstly investigated in this work. Nanoprecipitation without surfactant led to stable nanoparticles only for a short amount of time. After the addition of half of the organic phase, the aggregation started and, by the end of the addition, the polymeric material had aggregated entirely. It shows that the addition of a surfactant in the aqueous phase is necessary towards the synthesis of BK22-loaded nanoparticles.

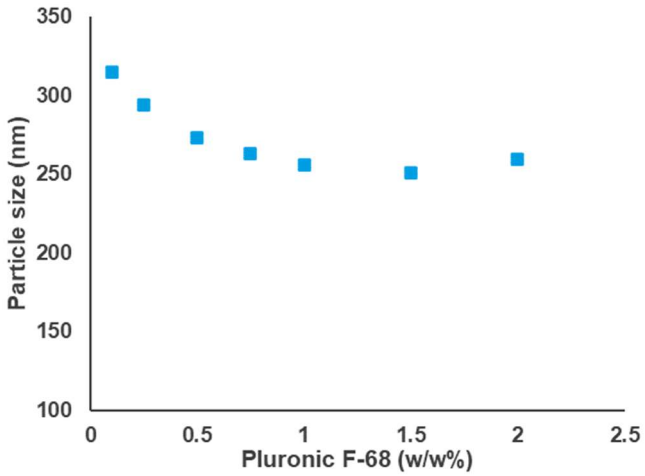

Figure 2.13. Effect of the surfactant on the nanoparticle size (nanoprecipitation)

It has been evaluated that PVA as a surfactant would not be suitable, as the same aggregates as for the ESD method were observed. Stable nanoparticles were successfully synthesized with Pluronic F-68 at different concentrations (from $0.1_{w/w}$% to $2.0_{w/w}$%). The results of the particle size measurements are shown in Figure 2.13. It can observed that a decrease of the particle size is detected when the surfactant concentration increases.

Above 1.0$_{w/w}$% of Pluronic F-68, the particle size is slightly increasing, as the increase of viscosity in the aqueous phase slows down the diffusion of the acetone into the water[36], but this could also be due to the deposition of extra surfactant at the surface of the nanoparticles[37]. In addition, Pluronic L-35 was tested. It is triblock copolymer just as Pluronic F-68, but with a lower molecular weight and slightly more hydrophobic. Syntheses of nanoparticles using Pluronic L-35 were attempted, however, the results were similar to the surfactant-free experiments yielding to an agglomeration of the nanoparticles. Lastly, nanoparticles stabilized with Tween 80 were synthesized. Although stable nanoparticles were properly produced, their sizes were too large. Nanoparticles of 578nm and 922nm were obtained with 1.0$_{w/w}$% and 2.0$_{w/w}$% Tween 80 solution respectively. Tween 80 is more frequently used in combination with a second surfactant[30, 32, 33], which might explain such a difference in terms of particle size. After that, the effect of the catalyst concentration was studied (Fig. 2.14). At low concentrations, it seems that the catalyst concentration does not affect the particle size[30, 38]. An increase in the particle size is observed when reaching relatively high catalyst concentration. It is therefore possible to increase the catalyst concentration in the nanoparticles up to 10-15mg/mL without negatively impacting the particle size.

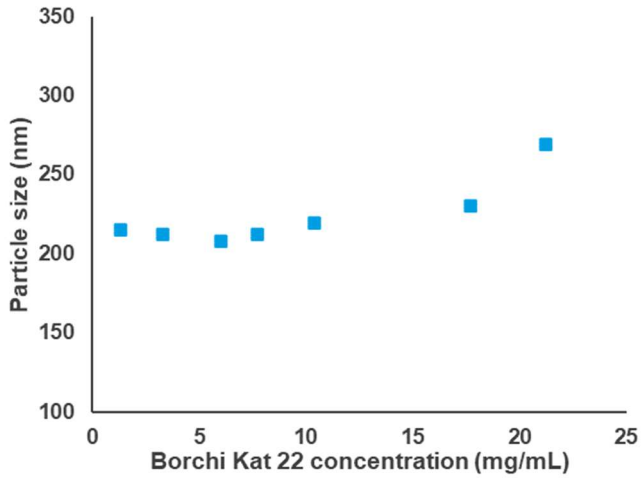

Figure 2.14. Effect of the catalyst concentration of the nanoparticle size (nanoprecipitation)

The effects of the PCL concentration and molecular weight on the size of particles were investigated (Fig. 2.15). The increase of the polymer concentration led to an increase of the particle size, as observed for the ESD method and in other works[32, 39, 40]. On the other side, the impact of the PCL molecular weight on the nanoparticle size has been rarely studied. The results shows that PCL-80 nanoparticles are larger than PCL-45 and PCL-10 nanoparticles whereas PCL-45 and PCL-10 nanoparticles are very similar in size. It is here important to consider the hydrodynamic volume of the PCL. The hydrodynamic volume of a polymer is the volume it occupies in solution. This volume increases when the polymer molecular weight increases, which explains why larger nanoparticles were obtained when using PCL-80. The hydrodynamic volume is also affected by the affinity between the polymer and the solvent; a good affinity will lead to a higher hydrodynamic volume. PCL happens to bear hydroxy groups at the end of its backbone. Those hydroxy groups are negligeable in PCL-80 and PCL-45, which are highly hydrophobic. However, PCL-10 bears significantly more hydroxy groups, which makes it slightly more hydrophilic. PCL-10 hydrodynamic volume is therefore slightly increased and this could explain why, in water, no size differences were measured between PCL-45 and PCL-10 nanoparticles.

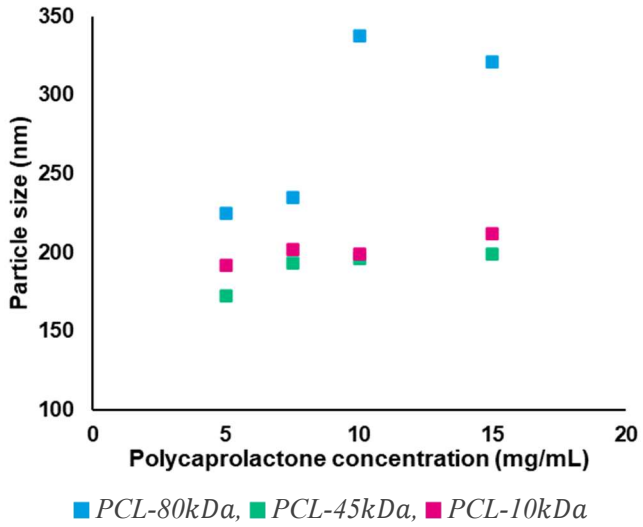

Figure 2.15. Effect of the PCL concentration on the particle size (nanoprecipitation)

Both the PCL concentration and its molecular weight have an impact on the particle size, but they affect much more the amount of aggregates formed. During the syntheses of nanoparticles via nanoprecipitation, a small amount of aggregates was always formed, which was subsequently removed by filtration.

Figure 2.16 shows the amount of weighted aggregates as a function of the PCL concentration and molecular weight. The amount of aggregates increases as the polymer concentration increases, for all molecular weights[41]. This is explained by the fact that nanoprecipitation depends on the quick transfer of acetone into to the aqueous phase. A higher PCL concentration and/or molecular weight is slowing down the diffusion of the acetone, generating aggregates[40]. PCL-80 nanoparticles produce therefore bigger particles and much more aggregates than PCL-45 and PCL-10 nanoparticles. Those results led to the selection of PCL-45 as polymer material for the next experiments.

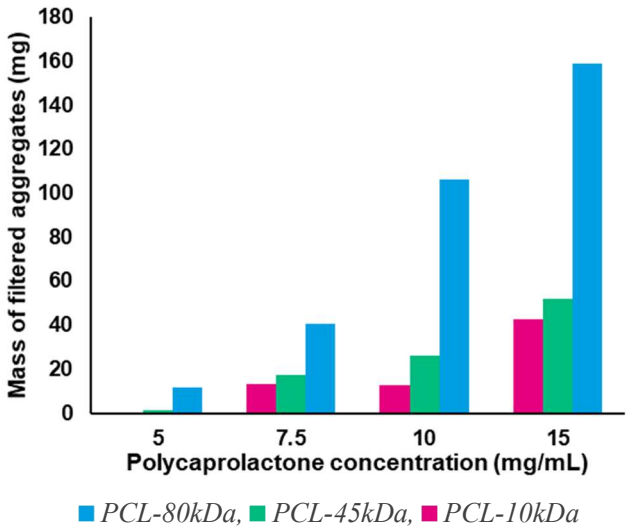

Figure 2.16. Effect of the PCL concentration on the amount of formed aggregates (nanoprecipitation)

Similarly to the previous method, the process parameters were studied to evaluate their impact on the particle size of the nanoparticles prepared via nanoprecipitation. The first investigated parameter was the addition speed, controlled with the syringe pump from $0.5 mL/min$ to $4 mL/min$. However, no clear tendency was observed (Annex A.1) and the addition speed was kept as it was, i.e. $0.5 mL/min$. Badri and coworkers[37] studied the same parameter and showed that the particle size decreases proportionally to the increase of the addition speed, but this decrease is minor as a less than 5% difference was noticed between the slowest ($1.67 mL/min.$) and the fastest addition ($3.67 mL/min.$). Then, the impact of the mixing speed on the particle size was determined. As for the ESD method and foreseeably, the increase of the mixing speed shows a decrease of the particle size (Fig. 2.17).

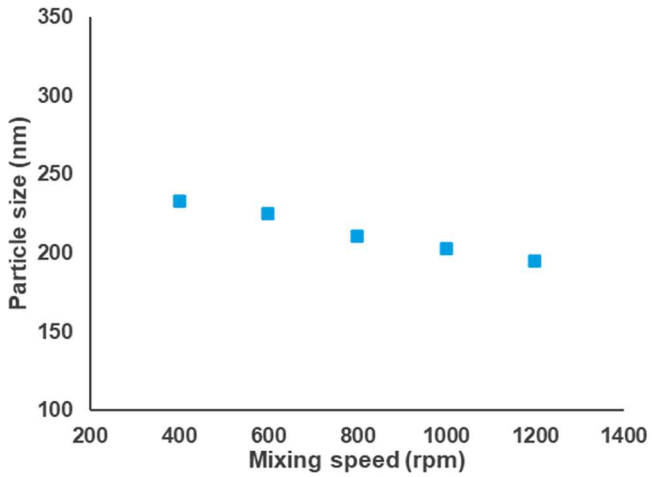

Figure 2.17. Effect of the mixing speed on the particle size (nanoprecipitation)

Finally, the influence of the aqueous phase to organic phase ratio was controlled. The increase of this ratio means that the organic phase is added in a larger amount to the aqueous phase (water and surfactant), which, at first glance, seems that it should not impact the particle size. However, the data show that a larger aqueous phase creates slightly larger nanoparticles (Fig. 2.18). This might be due to the mixing speed just described before. An aqueous phase of $150 mL$ magnetically stirred ($600 rpm$) behaves differently of a $20 mL$-aqueous phase. This difference of mixing efficiency could lead to this slight increase of the nanoparticle size.

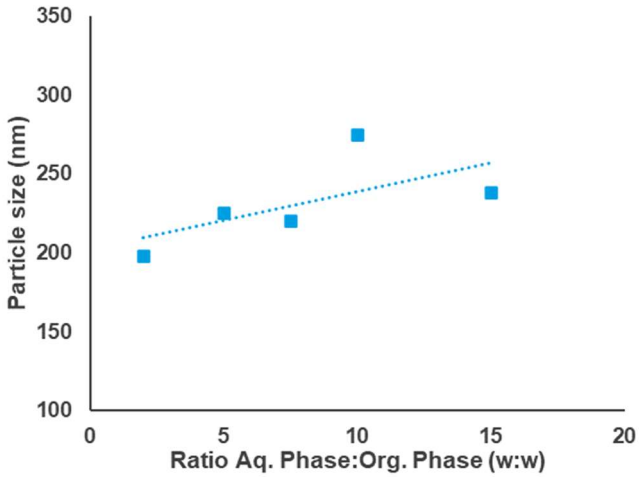

Figure 2.18. Effect of the Aqueous:Organic Phase ratio on the particle size (nanoprecipitation)

Reproducibility

The reproducibility of the nanoprecipitation encapsulation has been tested by preparing three times the exact same experiment. The particle size and PDI of each sample was measured three times by DLS and the results are compared in Table 2.4 below. It can be seen that the experiment has a very good reproducibility as the particle size did not vary of more than 3% overall and the PDI remains relatively low.

Table 2.4. Study of the reproducibility of the nanoprecipitation encapsulation

Experiment number	Particle size (nm)				Polydispersity Index			
	Measurements	*Experiment average*	*Total average*	*Maximum difference to average*	*Measurements*	*Experiment average*	*Total average*	*Maximum difference to average*
1	194.6	195.6	193.4	± 2.2	0.115	0.114	0.124	± 0.014
	197.1				0.129			
	195.0				0.097			
2	190.9	191.3			0.123	0.120		
	191.7				0.120			
	191.3				0.118			
3	193.1	193.4			0.164	0.138		
	193.2				0.120			
	194.0				0.129			

Microscopy

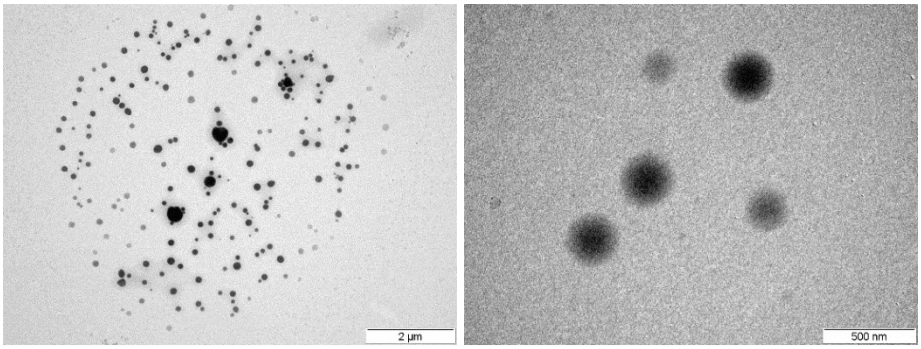

Figure 2.19. TEM pictures of nanoparticle suspensions at x12k (left) and x120k (right) (nanoprecipitation)

The nanoparticle suspensions were analyzed by TEM (Fig. 2.19) and FESEM (Fig. 2.20). According to the TEM pictures, the nanoparticles seem to be nanocapsules, but the darker core could also be due to the higher thickness of the particle in the center. Nevertheless, the TEM pictures look very similar to nanocapsules obtained in other projects[37, 42]. Nanocapsules sizes are overall consistent with the DLS measurements.

FESEM pictures are showing white spherical nanocapsules, which are very similar to the nanospheres obtained by ESD. It is worth mentioning that the nanoparticle are melting at high magnifications due to the electron beam (Fig. 2.20, right).

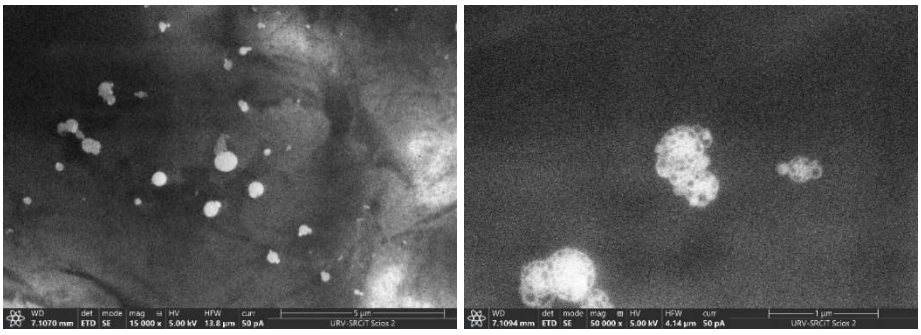

Figure 2.20. FESEM pictures of nanoparticle suspensions at x15k (left) and x50k (right) (nanoprecipitation)

Lastly, the nanoparticles were analyzed by FESEM-EDX to determine if the zinc-based catalyst could be detected inside the nanoparticles. To be able to perform the microanalysis, the electric current and voltage need to be increase. This results in, most of the time, a poor image quality as seen in Figure 2.21, in which it can also be observed that zinc was indeed detected inside the capsule. This confirms the successful encapsulation of BK22 catalyst into PCL nanoparticles via the nanoprecipitation technique.

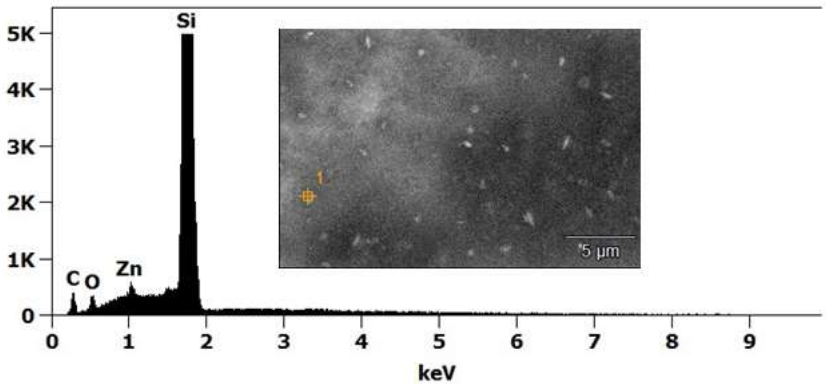

Figure 2.21. X-Ray microanalysis of nanocapsules obtained by nanoprecipitation

2.4. Conclusion

Both ESD and nanoprecipitation produced stable nanoparticles with high reproducibility. They respond similarly to a lot of parameters, such as the catalyst, surfactant and polymer concentration or the mixing speed. Smaller nanoparticles could be more homogenously dispersed in a polyurethane coating, ensuring an even distribution of the catalyst and ESD-nanoparticles are tunable in terms of sizes, as the mixing speed and time allow to tailor easily the droplet sizes, whereas the nanoparticles prepared by nanoprecipitation are more dependent on the formulation, especially the polymer concentration. On the other side, the nanoparticles obtained via nanoprecipitation are much easier to synthesize in terms of process and, at the end of the synthesis, concentrated nanoparticle suspensions are obtained in about $20mL$ of water whereas ESD-nanoparticles are obtained in an aqueous phase of about $240mL$. This makes the next step, lyophilization, significantly faster.

However, the main difference between the two synthesis methods is the structure of the nanoparticles. As a hydrophobic liquid molecule (BK22) is encapsulated, it could be hypothesized that either nanocapsules or nanospheres would be formed, depending on the catalyst-polymer affinity, but it was also expected that the same type of particles would be obtained, regardless of the synthesis methods, as suggested in other works comparing these techniques[43, 44]. Why nanospheres and nanocapsules were obtained remains unclear so far, but the work of C. Mora-Huertas and coworkers[44] can help to give a tentative answer. They showed that nanoparticles with different zeta-potentials were obtained depending on the technique, and more generally, depending on the solvent. They explained this difference by the orientation of the PCL molecules in the droplets, which could indeed play a role on the location of the catalyst when the polymer precipitates, and therefore to the final structure of the nanoparticles. This could be investigated in future work by performing the syntheses with different solvents. Finally, nanocapsules are preferred over nanospheres because they have a higher loading capacity[45]. This, in addition to a much easier process, led to the selection of nanoprecipitation as the most convenient method for the synthesis of catalyst-loaded nanoparticles and will be the main focus of Chapter 3.

2.5. References

1. U. Meier-Westhues, et al., *Polyurethanes: Coatings, Adhesives and Sealants*. 2nd Revised Edition. 2019: Vincentz Network GmbH & Co. KG, Hanover, Germany.
2. Carroy, A., et al., *Novel latent catalysts for 2K-PUR systems.* Progress in Organic Coatings, 2010. **68**(1): p. 37-41 DOI: 10.1016/j.porgcoat.2009.10.007.
3. F. Richter, et al., *Use of Tin Catalysts for the Production of Polyurethane Coatings.* 2012. **US 2012/0220717 A1**.
4. Reis, C.P., et al., *Nanoencapsulation I. Methods for preparation of drug-loaded polymeric nanoparticles.* Nanomedicine, 2006. **2**(1): p. 8-21 DOI: 10.1016/j.nano.2005.12.003.
5. Idrees, H., et al., *A Review of Biodegradable Natural Polymer-Based Nanoparticles for Drug Delivery Applications.* Nanomaterials (Basel, Switzerland), 2020. **10**(10): p. 1970 DOI: 10.3390/nano10101970.
6. Hariyadi, D.M. and N. Islam, *Current Status of Alginate in Drug Delivery.* Advances in pharmacological and pharmaceutical sciences, 2020. **2020**: p. 8886095-8886095 DOI: 10.1155/2020/8886095.
7. Naskar, S., K. Koutsu, and S. Sharma, *Chitosan-based nanoparticles as drug delivery systems: a review on two decades of research.* J Drug Target, 2019. **27**(4): p. 379-393 DOI: 10.1080/1061186x.2018.1512112.
8. Zielińska, A., et al., *Polymeric Nanoparticles: Production, Characterization, Toxicology and Ecotoxicology.* Molecules (Basel, Switzerland), 2020. **25**(16): p. 3731 DOI: 10.3390/molecules25163731.
9. Sinha, V.R., et al., *Poly-ϵ-caprolactone microspheres and nanospheres: an overview.* International Journal of Pharmaceutics, 2004. **278**(1): p. 1-23 DOI: 10.1016/j.ijpharm.2004.01.044.
10. Barichello, J.M., et al., *Encapsulation of hydrophilic and lipophilic drugs in PLGA nanoparticles by the nanoprecipitation method.* Drug Dev Ind Pharm, 1999. **25**(4): p. 471-6 DOI: 10.1081/ddc-100102197.
11. Avramović, N., et al., *Polymeric Nanocarriers of Drug Delivery Systems in Cancer Therapy.* Pharmaceutics, 2020. **12**(4) DOI: 10.3390/pharmaceutics12040298.
12. Malikmammadov, E., et al., *PCL and PCL-based materials in biomedical applications.* J Biomater Sci Polym Ed, 2018. **29**(7-9): p. 863-893 DOI: 10.1080/09205063.2017.1394711.
13. Quintanar-Guerrero, D., et al., *Influence of stabilizing agents and preparative variables on the formation of poly(d,l-lactic acid) nanoparticles by an emulsification-diffusion technique.* International Journal of Pharmaceutics, 1996. **143**(2): p. 133-141 DOI: 10.1016/S0378-5173(96)04697-2.
14. Quintanar-Guerrero, D., et al., *A mechanistic study of the formation of polymer nanoparticles by the emulsification-diffusion technique.* Colloid and Polymer Science, 1997. **275**(7): p. 640-647 DOI: 10.1007/s003960050130.
15. Wang, Y., et al., *Manufacturing Techniques and Surface Engineering of Polymer Based Nanoparticles for Targeted Drug Delivery to Cancer.* Nanomaterials, 2016. **6**: p. 26 DOI: 10.3390/nano6020026.
16. Fessi, H., et al., *Nanocapsule formation by interfacial polymer deposition following solvent displacement.* International Journal of Pharmaceutics, 1989. **55**(1): p. R1-R4 DOI: 10.1016/0378-5173(89)90281-0.

17. de Assumpção Pereira-da-Silva, M. and F.A. Ferri, *1 - Scanning Electron Microscopy*, in *Nanocharacterization Techniques*, A.L. Da Róz, et al., Editors. 2017, William Andrew Publishing. p. 1-35.
18. Zambrano-Zaragoza, M.L., et al., *Optimization of nanocapsules preparation by the emulsion–diffusion method for food applications.* LWT - Food Science and Technology, 2011. **44**(6): p. 1362-1368 DOI: 10.1016/j.lwt.2010.10.004.
19. Guinebretière, S., et al., *Study of the emulsion-diffusion of solvent: preparation and characterization of nanocapsules.* Drug Development Research, 2002. **57**(1): p. 18-33 DOI: 10.1002/ddr.10054.
20. Hernández-Giottonini, K.Y., et al., *PLGA nanoparticle preparations by emulsification and nanoprecipitation techniques: effects of formulation parameters.* RSC Advances, 2020. **10**(8): p. 4218-4231 DOI: 10.1039/c9ra10857b.
21. Tham, C.Y., et al., *Poly (Vinyl Alcohol) in Fabrication of PLA Micro- and Nanoparticles Using Emulsion and Solvent Evaporation Technique.* Advanced Materials Research, 2014. **1024**: p. 296-299 DOI: 10.4028/www.scientific.net/AMR.1024.296.
22. Zhao, B., et al., *Permeation and diffusion of nutrient ions in poly (vinyl alcohol) hydrogel membrane.* Chemical Papers, 2020. **74**(11): p. 3913-3923 DOI: 10.1007/s11696-020-01210-5.
23. Mulia, K., et al., *Effect of High Speed Homogenizer Speed on Particle Size of Polylactic Acid.* Journal of Physics: Conference Series, 2019. **1198**(6): p. 062006 DOI: 10.1088/1742-6596/1198/6/062006.
24. Moreira, J.B., et al., *Preparation of beta-carotene nanoemulsion and evaluation of stability at a long storage period.* Food Science and Technology, 2019. **39**(3): p. 599-604 DOI: 10.1590/fst.31317.
25. Pengon, S., et al., *Development of Nanoemulsions Containing Coconut Oil with Mixed Emulsifiers: Effect of Mixing Speed on Physical Properties.* Key Engineering Materials, 2019. **819**: p. 181-186 DOI: 10.4028/www.scientific.net/KEM.819.181.
26. Ardani, H.K., et al., *Enhancement of the stability of silver nanoparticles synthesized using aqueous extract of Diospyros discolor Willd. leaves using polyvinyl alcohol.* IOP Conference Series: Materials Science and Engineering, 2017. **188**: p. 012056 DOI: 10.1088/1757-899x/188/1/012056.
27. Guterres, S.S., M.P. Alves, and A.R. Pohlmann, *Polymeric nanoparticles, nanospheres and nanocapsules, for cutaneous applications.* Drug target insights, 2007. **2**: p. 147-157 DOI: 10.1177/117739280700200002.
28. Siqueira-Moura, M.P., et al., *Development, characterization, and photocytotoxicity assessment on human melanoma of chloroaluminum phthalocyanine nanocapsules.* Mater Sci Eng C Mater Biol Appl, 2013. **33**(3): p. 1744-52 DOI: 10.1016/j.msec.2012.12.088.
29. Lebouille, J.G.J.L., et al., *Nanoprecipitation of polymers in a bad solvent.* Colloids and Surfaces A: Physicochemical and Engineering Aspects, 2014. **460**: p. 225-235 DOI: 10.1016/j.colsurfa.2013.11.045.
30. Fraj, A., et al., *A comparative study of oregano (Origanum vulgare L.) essential oil-based polycaprolactone nanocapsules/ microspheres: Preparation, physicochemical characterization, and storage stability.* Industrial Crops and Products, 2019. **140**: p. 111669 DOI: 10.1016/j.indcrop.2019.111669.
31. Jummes, B., et al., *Antioxidant and antimicrobial poly-ε-caprolactone nanoparticles loaded with Cymbopogon martinii essential oil.* Biocatalysis and Agricultural Biotechnology, 2020. **23**: p. 101499 DOI: 10.1016/j.bcab.2020.101499.

32. Venturini, C.G., et al., *Formulation of lipid core nanocapsules.* Colloids and Surfaces A: Physicochemical and Engineering Aspects, 2011. **375**(1-3): p. 200-208 DOI: 10.1016/j.colsurfa.2010.12.011.
33. Granata, G., et al., *Essential oils encapsulated in polymer-based nanocapsules as potential candidates for application in food preservation.* Food Chem, 2018. **269**: p. 286-292 DOI: 10.1016/j.foodchem.2018.06.140.
34. Nguyen, C.A., et al., *Preparation of surfactant-free nanoparticles of methacrylic acid copolymers used for film coating.* AAPS PharmSciTech, 2006. **7**(3): p. 63 DOI: 10.1208/pt070363.
35. Crucho, C.I.C. and M.T. Barros, *Surfactant-free polymeric nanoparticles composed of PEG, cholic acid and a sucrose moiety.* Journal of Materials Chemistry B, 2014. **2**(25): p. 3946-3955 DOI: 10.1039/C3TB21632B.
36. Guhagarkar, S., V. Malshe, and P. Devarajan, *Nanoparticles of Polyethylene Sebacate: A New Biodegradable Polymer.* AAPS PharmSciTech, 2009. **10**: p. 935-42 DOI: 10.1208/s12249-009-9284-4.
37. Badri, W., et al., *Elaboration of Nanoparticles Containing Indomethacin: Argan Oil for Transdermal Local and Cosmetic Application.* Journal of Nanomaterials, 2015. **2015**: p. 1-9 DOI: 10.1155/2015/935439.
38. Alshamsan, A., *Nanoprecipitation is more efficient than emulsion solvent evaporation method to encapsulate cucurbitacin I in PLGA nanoparticles.* Saudi Pharmaceutical Journal, 2014. **22**(3): p. 219-222 DOI: 10.1016/j.jsps.2013.12.002.
39. Lepeltier, E., C. Bourgaux, and P. Couvreur, *Nanoprecipitation and the "Ouzo effect": Application to drug delivery devices.* Advanced Drug Delivery Reviews, 2014. **71**: p. 86-97 DOI: 10.1016/j.addr.2013.12.009.
40. Beck-Broichsitter, M., et al., *Preparation of nanoparticles by solvent displacement for drug delivery: A shift in the "ouzo region" upon drug loading.* European Journal of Pharmaceutical Sciences, 2010. **41**(2): p. 244-253 DOI: 10.1016/j.ejps.2010.06.007.
41. Legrand, P., et al., *Influence of polymer behaviour in organic solution on the production of polylactide nanoparticles by nanoprecipitation.* International Journal of Pharmaceutics, 2007. **344**(1): p. 33-43 DOI: 10.1016/j.ijpharm.2007.05.054.
42. Reimondez-Troitiño, S., et al., *Polymeric nanocapsules: a potential new therapy for corneal wound healing.* Drug Delivery and Translational Research, 2016. **6**(6): p. 708-721 DOI: 10.1007/s13346-016-0312-0.
43. Mora-Huertas, C.E., et al., *Nanocapsules prepared via nanoprecipitation and emulsification-diffusion methods: comparative study.* Eur J Pharm Biopharm, 2012. **80**(1): p. 235-9 DOI: 10.1016/j.ejpb.2011.09.013.
44. Mora-Huertas, C.E., H. Fessi, and A. Elaissari, *Influence of process and formulation parameters on the formation of submicron particles by solvent displacement and emulsification–diffusion methods: Critical comparison.* Advances in Colloid and Interface Science, 2011. **163**(2): p. 90-122 DOI: 10.1016/j.cis.2011.02.005.
45. Deng, S., et al., *Polymeric Nanocapsules as Nanotechnological Alternative for Drug Delivery System: Current Status, Challenges and Opportunities.* Nanomaterials, 2020. **10**(5) DOI: 10.3390/nano10050847.

Chapter 3. Improvement of the encapsulation efficiency of catalyst-loaded nanocapsules

3.1. Introduction

Nanospheres and nanocapsules were successfully synthesized via the emulsion-solvent diffusion encapsulation technique and the nanoprecipitation technique respectively. Both techniques showed interesting results but the nanoprecipitation has been selected as the most convenient due to a much easier process and to its ability to form nanocapsules. The obtained nanocapsules contain a common polyurethane polymerization catalyst, namely Borchi Kat 22 (BK22). However, BK22-loaded nanocapsules suspended in an aqueous solution cannot be used directly in a polyurethane coating, as BK22, and metal catalysts in general, are mainly employed in solvent-borne coatings, in which water is to be avoided[1]. Therefore the synthesized nanocapsules need to be isolated. This has been intended by ultracentrifugation (Avanti J-26 XPI, Beckmann Coulter) at speeds varying from 10,000 to 18,000rpm during 15 to 60 minutes. This method is commonly used for the isolation of polymeric nanoparticles[2-4], however, all attempts of this work led to the formation of non-soluble aggregates of polymer at the bottom of the centrifugation tubes, making the ultracentrifugation not suitable.

It has therefore been decided to directly lyophilize the nanoparticle suspension, without further purification. The presence of Pluronic F-68 is not particularly problematic, as this surfactant sometimes plays the role of cryoprotectant in other applications[5, 6], but this will obviously impact the size of the lyophilized nanocapsules. In any case, the key parameter becomes the encapsulation efficiency (EE), as any non-encapsulated catalyst can be expected to be located at the surface of the nanocapsules after lyophilization, which would give a non-desired catalytic effect to the nanocapsules. Thus, this aim of this chapter is to maximize the EE of the nanoencapsulation process and to evaluate the usability of the nanocapsules as catalyst in an existing polyurethane coating formulation.

3.2. Materials & Methods

3.2.1. Materials

As described in the previous chapter, polycaprolactone (PCL) was used as the shell material. In this chapter, all the syntheses performed by nanoprecipitation were made with PCL-45kDa. In addition to the non-ionic surfactants Pluronic F-68 and Tween 80 previously introduced (Table 2.2), the ionic surfactants cetyltrimethylammonium bromide (CTAB, ≥98%) and sodium dodecyl sulfate (SDS, ≥99%), cationic and anionic respectively, were employed (Table 3.1). Their stabilizing properties are based on electrostatic repulsion and they were obtained from Sigma Aldrich.

Table 3.1. Ionic surfactant structures

Cetyltrimethylammonium bromide **CTAB** 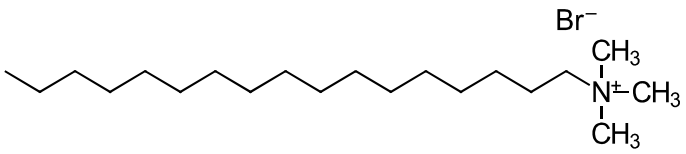
Sodium dodecyl sulfate **SDS** 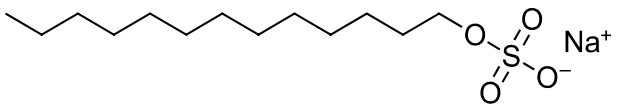

Glyceryl trioctanoate (GTO, ≥99%) and n-dodecane (≥99%) were supplied by Sigma Aldrich and dodecanal (≥95%) was obtained from Alfa Aesar. These products are highly hydrophobic compounds, hereinafter referred to as hydrophobic oils, with different structures and relative polarities (Table 3.2).

Table 3.2. Structure of the hydrophobic oils

Glyceryl trioctanoate **GTO** 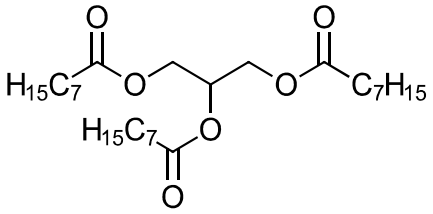 Water solubility: $0.4 mg/L$ at $37°C$[7]
n-dodecane  Water solubility: $3.7 \times 10^{-3} mg/L$ at $25°C$[8]
Dodecanal 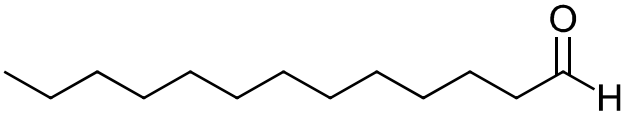 Water solubility: $4.7 mg/L$ at $25°C$[9]

The catalysts Borchi Kat 22 (BK22) and Borchi Kat 24 (BK24) (bismuth tri(2-ethylhexanoate); 23 – 25% bismuth content) were kindly donated by Borchers and previously described (Table 1.8). The nanocapsules were used in a coating formulation, which involved Setalux D A 665 BA (acrylic polyol; OH-content: 4.6%), obtained from Allnex, BYK 355 (polyacrylate-based surface additive), purchased from BYK, and Desmodur N 3300 (HDI trimer; NCO-content: 21.8%), directly provided by Covestro AG. Water was purified with a $0.22 \mu m$ Milipak® membrane filter. All other solvents and reagents were of analytical grade. All chemicals and materials were used as received.

3.2.2. Synthesis method

3.2.2.1. Nanoprecipitation

Nanocapsules encapsulating metal salt catalysts (Borchi Kat 22 or Borchi Kat 24) were synthesized via nanoprecipitation[10] with improved parameters as described in the previous chapter. Quickly, the PCL ($45kDa, 50mg$) was dissolved in acetone ($10mL$) at $50°C$ under moderate stirring, the catalyst ($50mg$) and eventually a hydrophobic oil (glyceryl trioctanoate, n-dodecane or dodecanal, 25-100mg) were added subsequently. This mixture was slowly added with a syringe pump to a water solution ($20mL$), containing one or two surfactants (0.1 to $2_{w/w}\%$), under magnetic stirring ($1200rpm$). The obtained nanocapsule suspension was stirred 10 more minutes after the addition was completed, filtered and kept overnight at room temperature to allow the evaporation of the remaining acetone. Finally, the suspension was freeze-dried (LyoAlpha, Telstar) for 3 days without further purification.

3.2.3. Characterization

3.2.3.1. Particle size analysis and zeta-potential measurements

The particle size was measured by Dynamic Light Scattering (DLS) as described in Chapter 2. The zeta-potential was measured by Electrophoretic Light Scattering using the Zetasizer Nano ZS (Malvern Instruments). All samples were diluted (1:10, v/v) in water and analyzed in triplicate at $25°C$. The zeta-potential measurements were performed in glass cells with a dip cell instrument (Zen 1002, Malvern Panalytical) made of palladium electrodes. All data were analyzed with the Zetasizer software.

3.2.3.2. Morphology and X-Ray microanalysis

Field Emission Scanning Electron Microscopy was used to observe the nanoparticles suspension, as well as the dried nanoparticles after freeze-drying; FESEM with Energy Dispersive X-Ray was used to qualitatively detect metals inside the nanoparticles and in solution, exactly as described in Chapter 2. In order to perform X-Ray microanalyses, the accelerated voltage was increased from $5kV$ to $15kV$, leading to low image quality. Most of the pictures associated with the measurements were of poor quality, as illustrated in Figure 3.1 and 3.2. Even though some pictures were of decent quality (Fig. 3.3), the microscopy pictures will not be shown unless they bring useful information.

3.2.3.3. Thermal analyses

The thermal properties of dried nanoparticles were observed by Differential Scanning Calorimetry (DSC; DSC821e, Mettler Toledo). Samples of approximately 3mg were weighed directly in an pierced aluminum pan on an analytical balance. The pan was heated under nitrogen atmosphere from $30°C$ to $200°C$ at a $10°C/min$ rate for DSC measurements.

3.2.3.4. Dynamic Mechanical Analysis

Dynamic Mechanical Analysis (DMA; Dynamic Mechanical Analyzer Model Q800, TA Instruments-Waters LLC) was performed to determine the cross-linking speed and behavior of 2K-coating formulations. Component A (polyol, solvent and eventually a catalyst) and component B (polyisocyanate) were added in a 8mL glass vial. The vial was mixed during two minutes with a IKA® VORTEX Shaker Genius 3 at maximum power. A thin film of the coating mixture was deposited on a glass support cloth (TA-Number 980228.902). The storage modulus was automatically calculated as a function of time or temperature. Three different analyses were performed: isotherm-DMA at $20°C$ or at $65°C$ during 120 minutes and a standard DMA analysis from $20°C$ to $250°C$ at a $10°C/min$ rate.

3.3. Results and Discussion

3.3.1. Improvement of the catalyst entrapment with hydrophobic oils

In this work, encapsulation efficiency (EE) defines the ratio of encapsulated catalyst to the total amount of catalyst used in the synthesis, and it is essential that the EE is maximized. In the literature, nanoprecipitation is known to synthesize nanoparticles with high encapsulation efficiency[11, 12], from more than 70% up to 99%[13]. Most of the encapsulated materials are hydrophobic, so only small amounts can be lost in the aqueous phase during the synthesis. The EE can be investigated by qualitatively estimating the amount of non-encapsulated catalyst, which can be done with a FESEM-EDX microscope. BK22 is a zinc-based catalyst and the presence of zinc inside the nanocapsules and in the aqueous phase (dried), where the non-encapsulated catalyst is located, can be investigated by X-Ray microanalysis. The FESEM-EDX allows to focus the microanalysis on a precise area of the sample as described in chapter 2. It is important to note that the amount of zinc detected inside the nanocapsules is not comparable from one experiment to another, as the amount of zinc in each measurement is directly related to the size of the nanocapsule. On the other side, the non-encapsulated zinc can be roughly compared in different experiments, as the non-encapsulated catalyst is evenly dissolved in the aqueous solution.

Figure 3.1 shows the X-ray microanalysis of nanocapsules synthesized in the previous chapter, i.e. nanocapsules containing pure catalyst. It confirms what has already been observed, that some catalyst is encapsulated in the polymer nanocapsules (Fig. 3.1; Pt. 1). However, the catalyst is also detected outside of the nanoparticles (Fig. 3.1; Pt. 2) where the aqueous phase has dried. This means some catalyst was not encapsulated and that the encapsulation is perfectible.

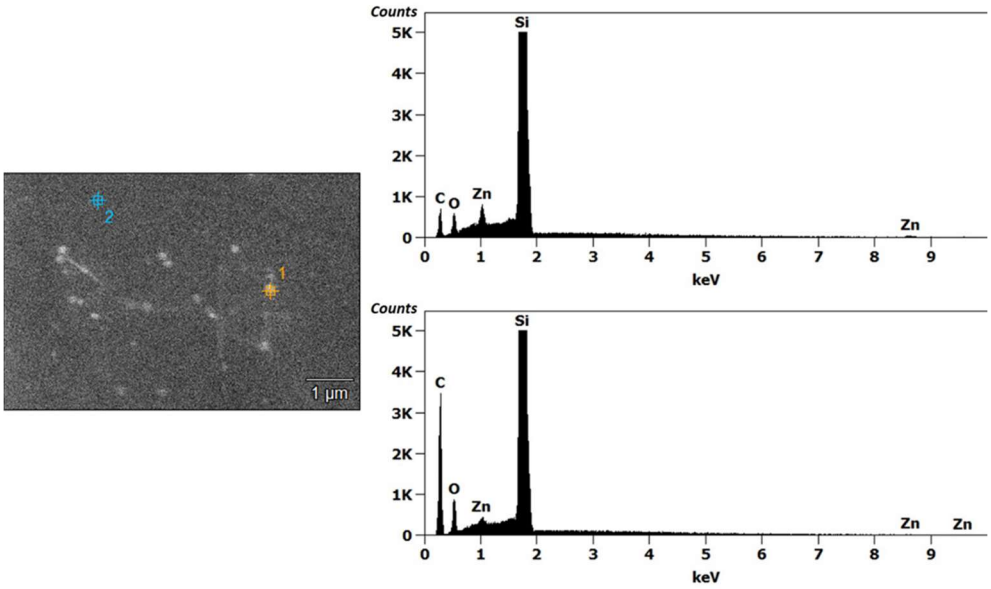

Figure 3.1. BK22-loaded nanocapsules: FESEM picture at ~x55k (left), X-ray microanalysis on a nanocapsule (point 1; top) and on the dried solution area (point 2; bottom)

It has been shown that the addition of an hydrophobic oil in the organic phase improves the EE[14, 15]. This phenomena is directly related to the affinity between the oil and the encapsulated material, regardless of the encapsulation method. The most common hydrophobic oils for nanoprecipitation are mixtures of fatty acids and/or triglycerides[15], hence, in this part, glyceryl trioctanoate (GTO) has been tested alongside dodecanal and n-dodecane for the encapsulation of metal salt catalyst (Table 3.3).

Table 3.3. Effect of the hydrophobic oil on the particle size and polydispersity index (PDI)

Oil concentration (mg/mL)	Type of oil	Particle size (nm)
-	-	202
5.0	GTO	225
	dodecanal	206
	n-dodecane	228
10.0	GTO	267
	dodecanal	230
	n-dodecane	182

The addition of hydrophobic oils in the formulation firstly impacted the particle size of the nanocapsules. The particle size increases proportionally to the amount of oil and more significantly when $10 mg/mL$ of oil was used in the formulation. This observation is consistent with the increase of particle size observed in the previous chapter for high concentrations of BK22 (Fig. 2.15). It can also be seen in the table that a higher amount of n-dodecane led to an unexpected decrease of the particle size, which remains unexplained so far. This experiment was reproduced two more times, leading to an average particle size of $262 \pm 80 nm$. Due to the high error on the particle size, it has been decided to not continue working with n-dodecane.

Figure 3.2 and 3.3 show the X-ray microanalyses of BK22/GTO-loaded and BK22/dodecanal-loaded nanocapsules respectively. In both cases, the amount of zinc detected outside of the nanocapsules seems lower than in Figure 3.1, when pure catalyst was encapsulated. In the case of the experiment with dodecanal (Fig. 3.3), no zinc peak was automatically shown, however, the software mentioned the presence of zinc as possible. The zinc peak was then manually added, as traces of zinc were supposedly detected. These observations seems to indicate that the EE was improved by addition of a hydrophobic oil.

The aluminum peak in Figure 3.3 has been observed in many other analyses even though no aluminum was added during the synthesis process. This could be explained by the fact that the EDX collimator is made of aluminum and the large peak of silica (support) can have a tendency to increase the nearby peaks[16]. Other unwanted peaks were sometimes detected, such as sulfur, potassium or calcium. They are believed to be impurities as no consistent observation could be made.

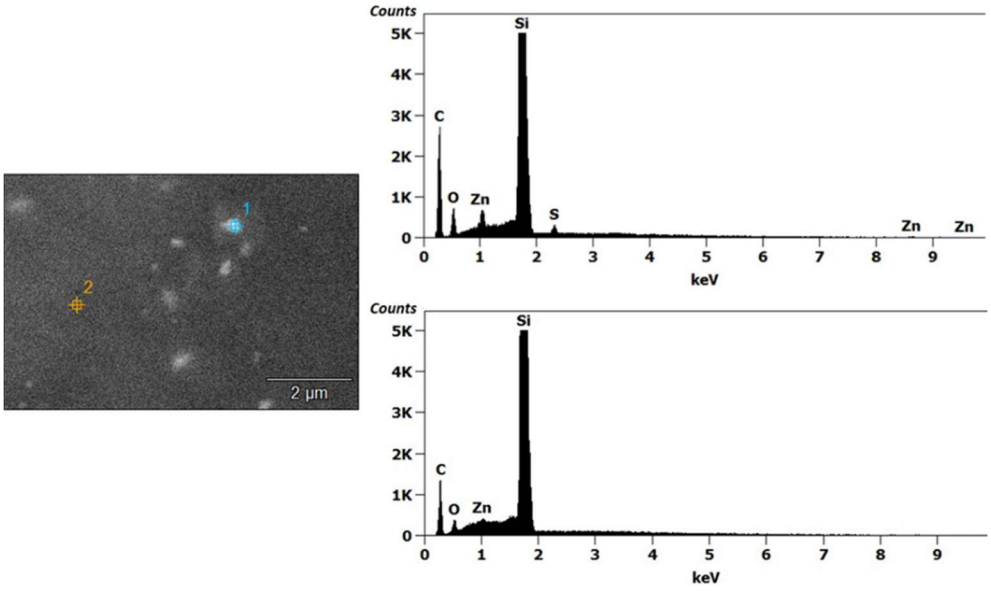

Figure 3.2. BK22/GTO-loaded nanocapsules: FESEM picture at ~x50k (left), X-ray microanalysis on a nanocapsule (point 1; top) and on the dried solution area (point 2; bottom)

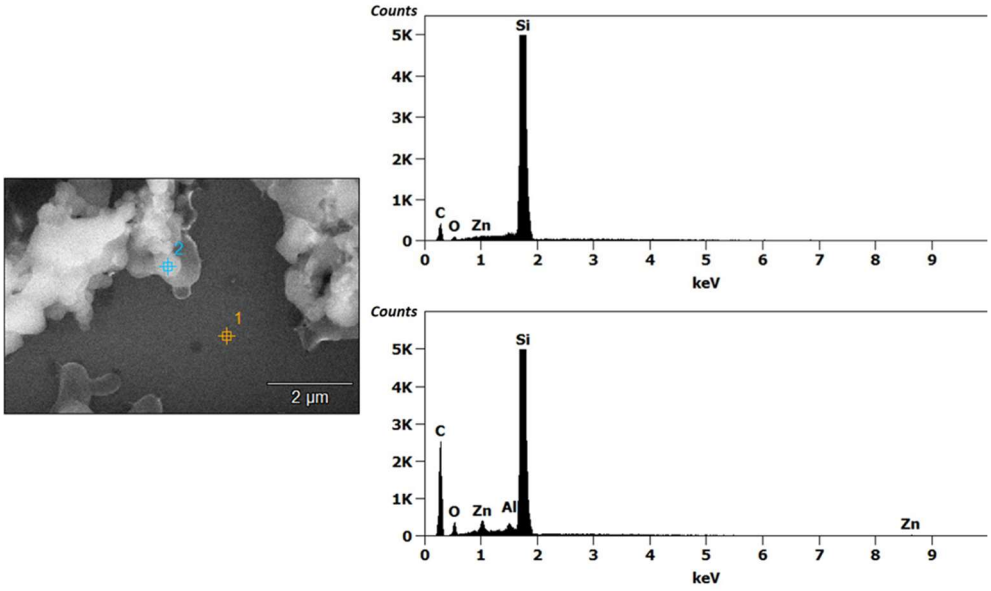

Figure 3.3. BK22/dodecanal-loaded nanocapsules: FESEM picture at ~x55k (left), X-ray microanalysis on the dried solution area (point 1; top) and on a nanocapsule aggregate (point 2; bottom)

3.3.2. Investigation of nanocapsules with charged outer surfaces

BK22 is a metal salt, therefore it has been hypothesized that charged nanocapsules could possibly increase the EE. A charged surface could stabilize the catalyst inside the nanocapsules via electrostatic repulsion. Both positively and negatively charged nanoparticles were successfully synthesized using as surfactant CTAB and SDS respectively.

The replacement of the surfactant deeply impacted the particle size of the nanocapsules. In order to be comparable with the particle sizes measured in the previous chapter, the nanoparticle sizes measured in Figure 3.4 were exceptionally synthesized with PCL-80kDa. This figure shows that both surfactants could properly stabilize the nanocapsules. Moreover, no modifications of the particle size were detected when the surfactant concentration was increased. This means the nanocapsules can be stabilized with a very low amount of surfactant which is very convenient for the lyophilization step.

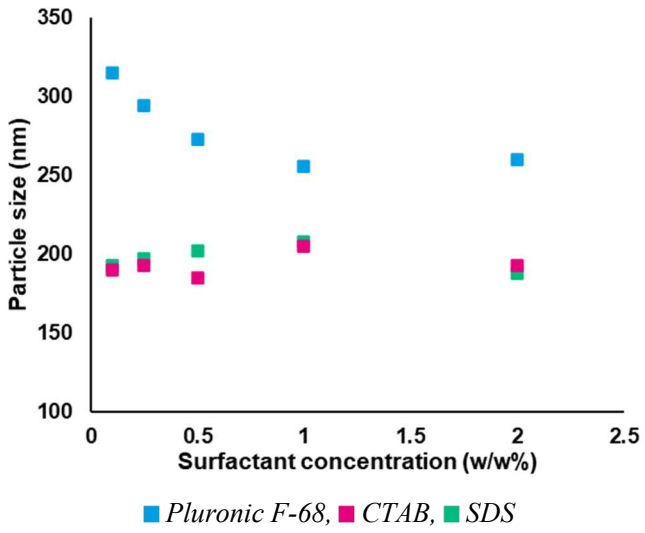

Figure 3.4. Effect of the surfactant type and concentration of the particle size of nanocapsules

Due to the PCL being hydrophobic, SDS and CTAB are adsorbed onto the PCL with their ionic head facing toward the aqueous phase[17]. So SDS-nanocapsules have shown negative zeta-potentials whereas CTAB-nanocapsules have shown positive zeta-potentials. Values near zero were detected for the Pluronic F-68 nanocapsules, which was expected as Pluronic F-68 is a neutral polymer whose surfactant properties are based on steric hindrance. It is commonly accepted that particles charged with a zeta-potential of $\pm 30 mV$ are perfectly stable.

The measured zeta-potentials are displayed in Figure 3.5 in absolute value to facilitate the reading. SDS and CTAB as surfactants for polymeric nanoparticles were rarely studied, but it is mentioned in some works that the zeta-potential is independent from the surfactant concentration[15, 18]. This is exactly what was observed here for CTAB-stabilized nanocapsules. On the other hand, the SDS concentration showed direct influence on the zeta potential, which suggests favorable interactions between the surfactant and the polymer. Overall, nanocapsules with good stability were synthesized with only $0.1_{w/w}\%$ of ionic surfactants.

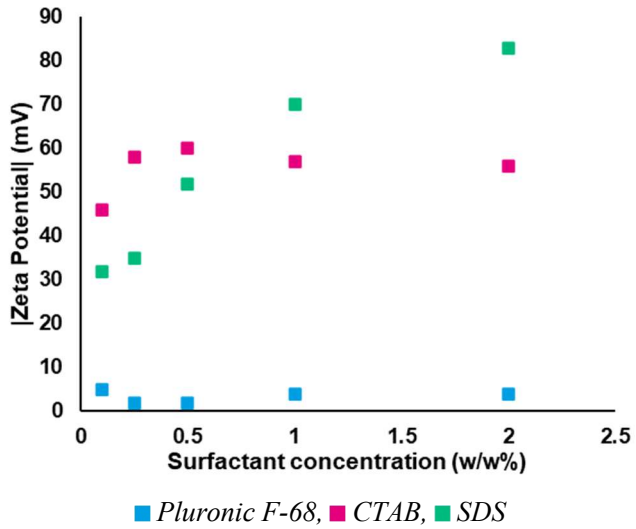

Figure 3.5. Effect of the surfactant type and concentration of the | zeta potential | of nanocapsules

Charged nanocapsules can also be obtained indirectly from non-ionic surfactants when they have high amount of charged groups as for example Tween 80. This surfactant bears a high number of hydroxyl groups, which, in water, can bring a negative charge to the polymer surface of the nanoparticles. However, it has been mentioned in Chapter 2 that Tween 80 as single surfactant would not be suitable for the synthesis of nanoparticles. This is why a combination of Pluronic F-68 and Tween 80, $1_{w/w}\%$ and $0.5_{w/w}\%$ respectively, was used to synthesize new nanoparticles. The obtained nanocapsules do not show remarkable results in terms of particle size ($317 nm$, PDI=0.202) but the nanocapsules have an interesting zeta-potential of $-21 mV$.

All three systems (CTAB, SDS, Pluronic F-68+Tween 80) were analyzed by FESEM-EDX in order to study their EE. The CTAB-stabilized nanocapsules X-ray microanalyses showed that no zinc was detected outside of the nanoparticles (Fig. 3.6). However, several crystal-like solids of different sizes were observed (Fig. 3.7, (a), (b)). The microanalysis of these solids revealed that, besides carbon and oxygen, it is essentially composed of zinc and bromine. Therefore, it has been hypothesized that the non-encapsulated zinc cations crystallize with the bromine anions from the surfactant during the drying process. Consequently, no conclusion can be drawn about the EE of this system. No problem of crystallization can occur with the SDS-stabilized system, as no anion is available in the nanocapsule suspension. However, the X-ray microanalyses of SDS-stabilized nanocapsules exposed another issue (Fig. 3.7, (c), (d)).

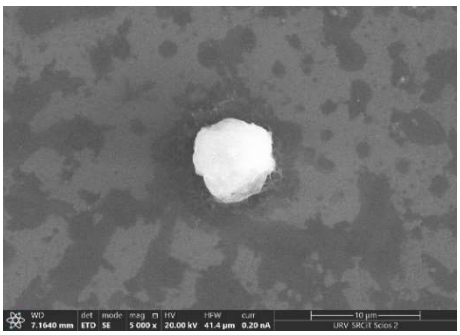

Figure 3.6. Cristal observed in a CTAB-stabilized nanocapsules formulation at ~x5k

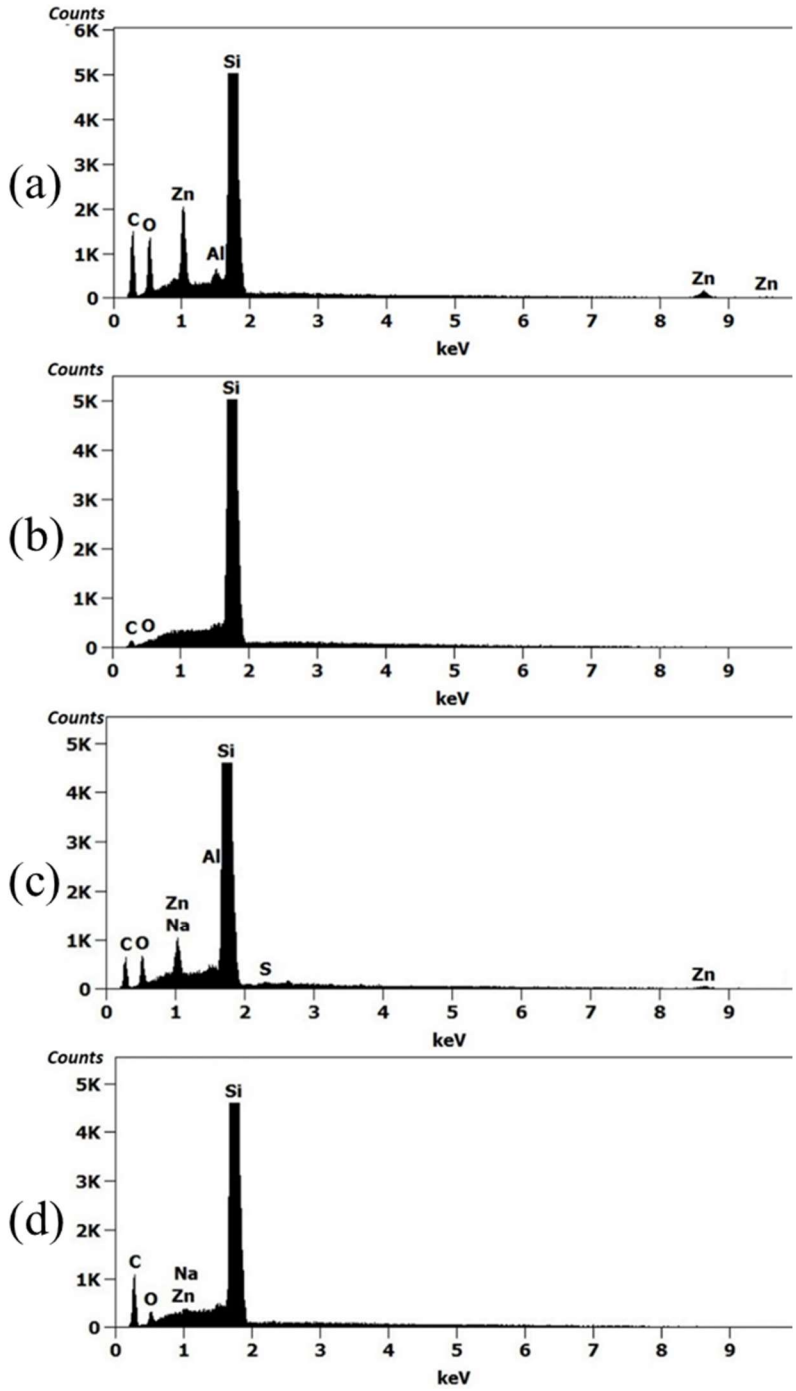

Figure 3.7. CTAB-stabilized BK22-loaded nanocapsules: X-ray microanalysis on a nanocapsule (a) and on the dried area (b); SDS-stabilized BK22-loaded nanocapsules: X-ray microanalysis on a nanocapsule (c) and on the dried area (d)

The zinc peak and the sodium peak, from the surfactant, are merged into one single peak due to very similar energies (1.01 and 1.04 keV respectively). It is then impossible to determine which atom causes the peak observed at about 1keV in both spectra. This issue is easily solved by replacing the zinc catalyst with its bismuth alternative (BK24). SDS-stabilized BK24-loaded nanocapsules have been synthesized and analyzed by FESEM-EDX. The X-ray analyses (Fig. 3.8) show that the nanocapsules are loaded with BK24, and a (very) small amount of BK24 was detected outside of the nanocapsules. In fact, the bismuth was not automatically detected and was manually added afterwards due to the small peak at 2.4keV. The bismuth peak has the advantage to be in an area with less background noise and its measurement is more precise but no other experiments were previously performed with BK24 and it is complicated to conclude about the efficiency of charged surfaces with this experiment.

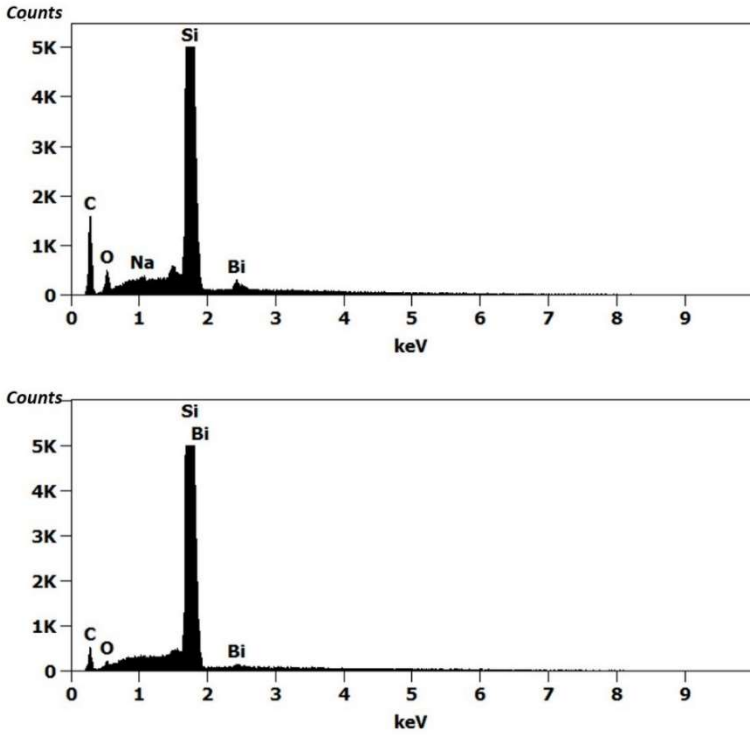

Figure 3.8. SDS-stabilized BK24-loaded nanocapsules: X-ray microanalysis on a nanocapsule (top) and on the dried area (bottom)

The most valuable comparison was finally obtained by doing the X-ray microanalyses of the Pluronic-Tween system. The only difference with the first experiment (Fig. 3.1) is that by using Tween 80, a charged surface has been obtained. Figure 3.9 displays the results of the X-ray microanalyses of this system. The catalyst is detected in large amount in the nanocapsules whereas close to no zinc is detected outside of the nanocapsules. The zinc peak detected where the aqueous solution has dried was first attributed to sodium and has been manually modified, as no sodium is supposed to be in the formulation. This result suggests that the encapsulation is improved by a charged surface of the nanoparticles, but the EE is still not high enough for applications in coatings.

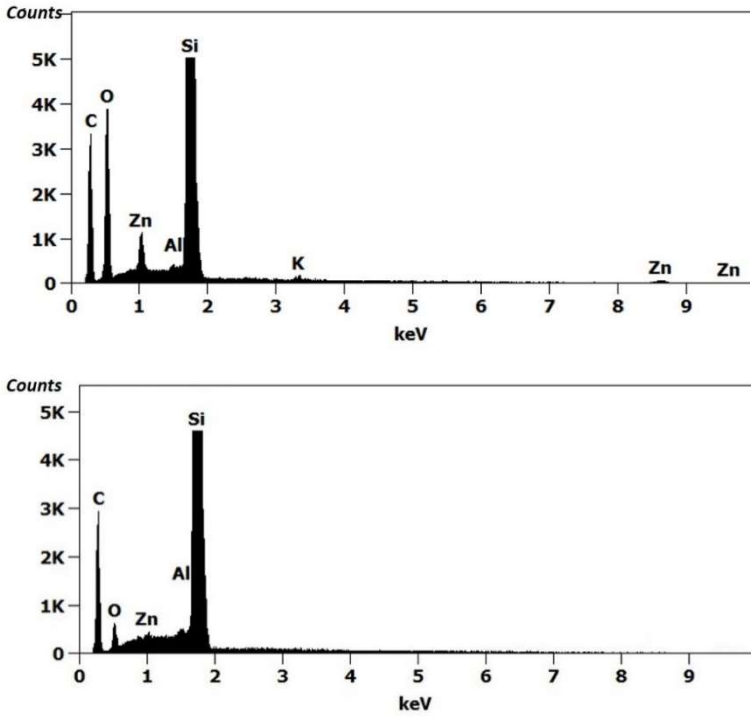

Figure 3.9. BK22-loaded nanocapsules stabilized with a mixture of Pluronic F-68 and Tween 80: X-ray microanalysis on a nanocapsule (top) and on the dried area (bottom)

3.3.3. Combination of hydrophobic oils and charged surfaces

To further improve the EE, additional syntheses were performed, combining hydrophobic oils and charged surfaces. Firstly, the concentration of GTO in the organic phase was incremented up to 10.0 mg/mL into a CTAB-stabilized formulation ($0.1_{w/w}\%$). The particle size was logically affected and increased proportionally to the increase of GTO reaching more than $300nm$ (Fig. 3.10)

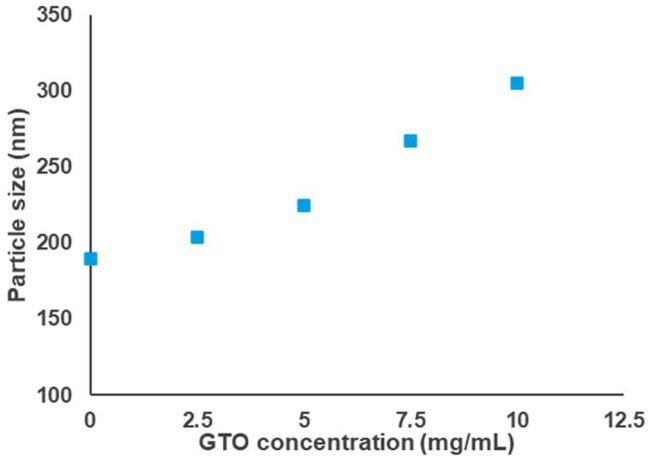

Figure 3.10. Effect of the amount of GTO on the particle size of CTAB-stabilized nanocapsules

All these different formulations were analyzed by FESEM-EDX. The results for the formulation with 2.5mg/mL of GTO are shown in Figure 3.11. In the FESEM picture of this figure (and of Fig. 3.12 as well), the darker area corresponds to agglomeration of nanocapsules whereas light grey areas are the silica support.

Similarly to the formulation without any GTO studied in the previous part, several crystal-like solids were also observed. The X-ray microanalysis of one of these crystals (Fig. 3.11, top) revealed that it is made of very high amounts of zinc and bromine, as well as many impurities (sulfur, chlorine, potassium). This reinforces the hypothesis of formation of zinc-bromine crystals during the drying process.

Then, the presence of zinc was detected inside the nanocapsules (Fig. 3.12, bottom) and its absence was observed outside of the nanocapsules (Fig. 3.12, middle). Overall, this formulation showed the exact same results as the formulation without any GTO.

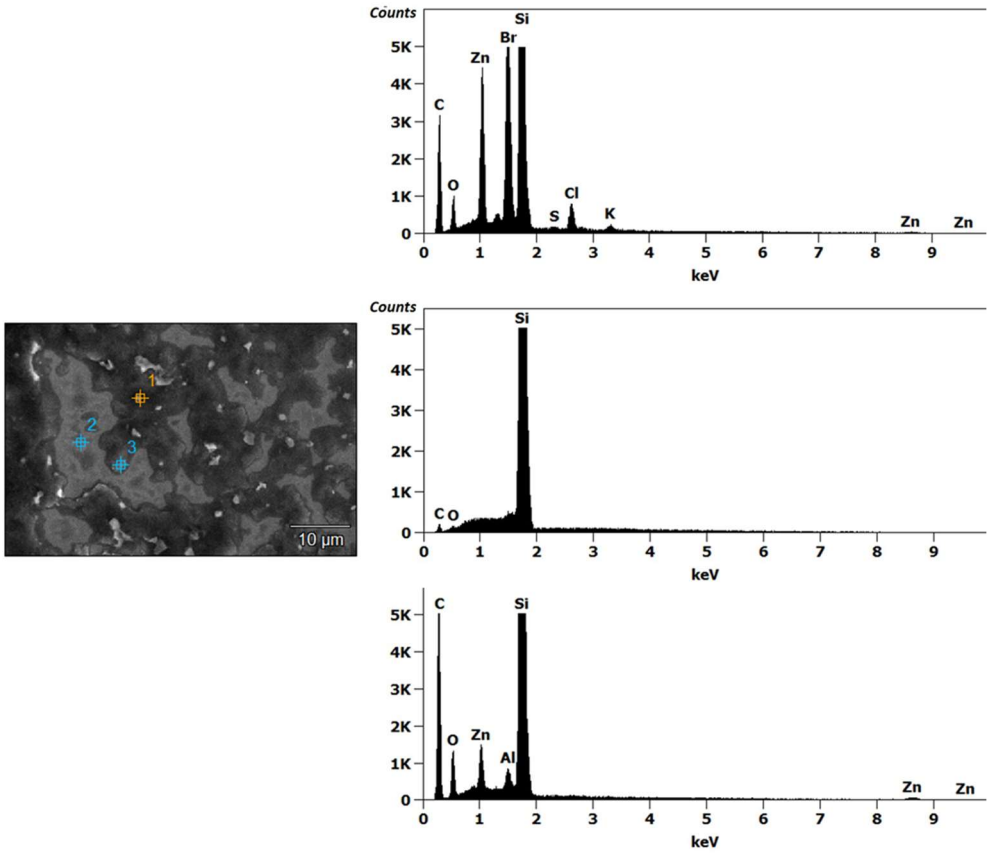

Figure 3.11. BK22/GTO2.5-loaded nanocapsules: FESEM picture at ~x7k (left), X-ray microanalysis on a crystal (point 1; top), on the dried solution area (point 2; middle) and on a nanocapsule aggregate (point 3; bottom)

The increase of GTO in the formulation to $5.0 mg/mL$ led to a different observation on the FESEM picture (Fig. 3.12, left). Crystals were still observed, however in much smaller amount, and for concentrations of GTO of $7.5 mg/mL$ and higher (Fig. 3.12, right), no crystals were spotted on the sample. In these formulations, the concentration of BK22 in the organic phase was kept constant at $5.0 mg/mL$, and, due to GTO and BK22 having a similar density, $0.96 g/mL$ and $1.07 g/mL$ respectively, the volume of GTO and BK22 can be compared using their concentration.

This previous observation could be due to the volume ratio between the GTO and the catalyst. Indeed, if the volume of GTO is lower than the volume of the catalyst, then the system has barely changed. The catalyst is still present in large amounts at the droplet interface and the GTO does not play any role in the encapsulation of the catalyst. This explains why no differences were observed between the formulations with no GTO and 2.5mg/mL of GTO. On the other hand, at high concentration of GTO (>7.5mg/mL), the catalyst is mixed in the GTO. This improves the catalyst retention into the nanocapsules, as a limited amount of catalyst is at the droplet interface. Therefore the losses are limited and close to no catalyst is available outside of the nanocapsules to make crystals. Lastly, when the concentrations are identical (5.0mg/mL), the local concentration from one capsule to another can change and a few crystals are observed.

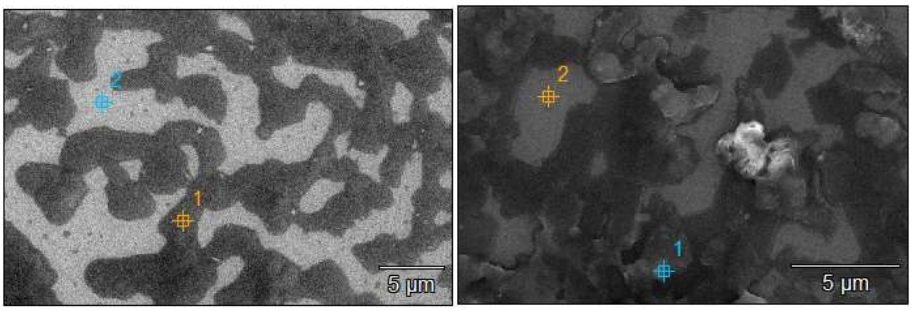

Figure 3.12. FESEM pictures of CTAB-stabilized nanocapsules with 5.0mg/mL (~x12k, left) and 7.5mg/mL (~x20k, right) of GTO

No non-encapsulated catalyst was detected neither in the formulation with 5.0 and 7.5mg/mL of GTO (Annex A.2 and A.3 respectively), nor with 10.0mg/mL of GTO as displayed in Figure 3.13 (a) and (b). This indicates that nanoparticles with a charged surface increases the EE and that an even higher EE can be reached by using both a hydrophobic oil and an ionic surfactant. This statement veracity is confirmed by Figure 3.13 (c) and (d), which illustrates the X-ray microanalyses of a SDS-stabilized BK24/GTO-loaded nanoparticle system, in which bismuth was not detected outside of the nanocapsules.

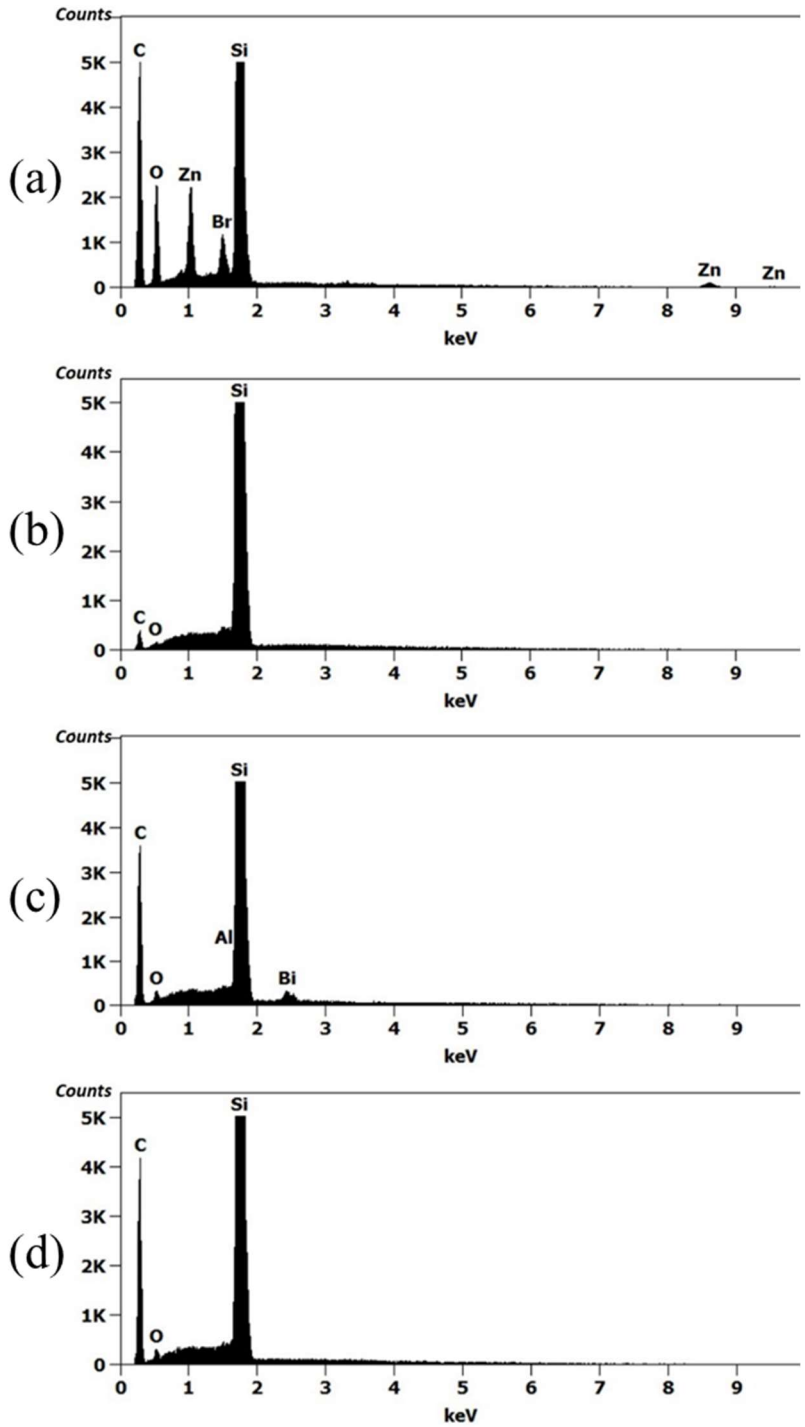

Figure 3.13. CTAB-stabilized BK22/GTO10.0-loaded nanocapsules microanalysis on a nanocapsule (a) and on the dried area (b). SDS-stabilized BK24/GTO-loaded nanocapsules microanalysis on a nanocapsule (c) and on the dried area (d)

The same experiment was performed with the Pluronic-F68/Tween80 system. However, no nanoparticles could be synthesized by using Tween 80 and GTO simultaneously. Tween 80 and GTO are perfectly miscible with each other and it is supposed that this high affinity causes the complete aggregation of the polymer. This issue has been overcome by replacing the GTO by dodecanal and nanocapsules were obtained. The X-ray microanalysis of this formulation was performed and can be found in Figure 3.14. The results are the same as with the ionic surfactants which confirms that it is the charges on the nanocapsule surface that favorizes its encapsulation. Finally, neither zinc nor bismuth were detected outside of the nanocapsules in any of the optimized formulations combining charges on the particle surface and hydrophobic oils. This indicates that the EE has been greatly improved, as the EDX allow trace measurements with concentrations of 0.001 weight fraction, up to eventually 0.0001 weight fraction[16, 19].

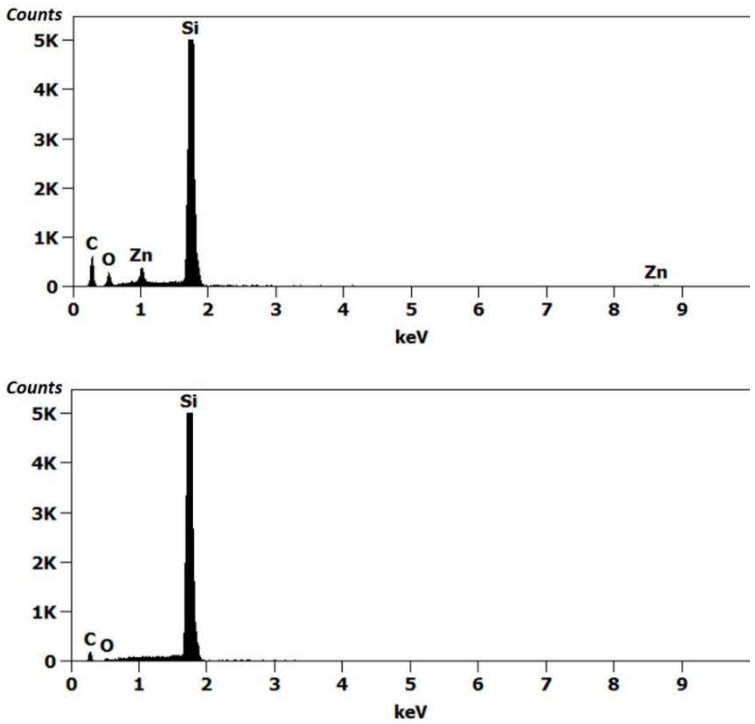

Figure 3.14. BK22/dodecanal-loaded nanocapsules stabilized with a mixture of Pluronic F-68 and Tween 80: X-ray microanalysis on a nanocapsule (top) and on the dried area (bottom)

3.3.4. Implementation in a coating formulation

The nanocapsule suspensions were lyophilized for 3 days in order to obtain nanocapsule powders. It could be observed that the formulations containing only $0.1_{w/w}$% of ionic surfactant were not perfectly stable. Therefore, $0.5_{w/w}$% of Pluronic F-68 was added to the formulation to play the role of cryoprotectant. This allowed the formation of stable nanocapsules in solid state. Figure 3.15 below shows FESEM pictures of the nanocapsule suspension and the lyophilized nanocapsules.

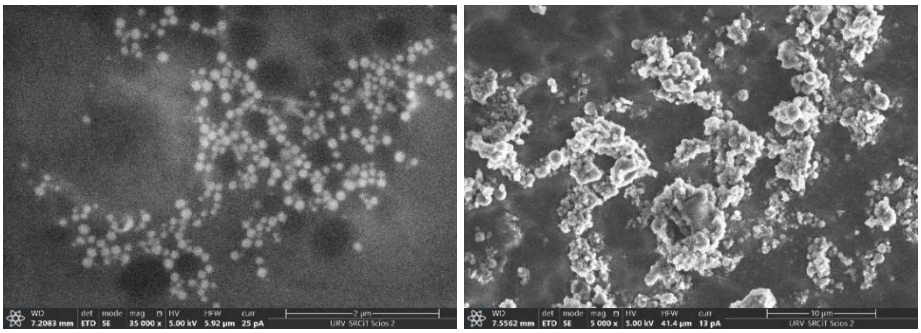

Figure 3.15. FESEM Pictures: nanocapsule suspension, x35k (left) and lyophilized nanocapsules, x8k (right)

The lyophilized nanocapsules were then analyzed by DSC to determine their melting point. At first, the pure polymeric materials Pluronic F-68 and PCL-45kDa were analyzed (Fig. 3.16).

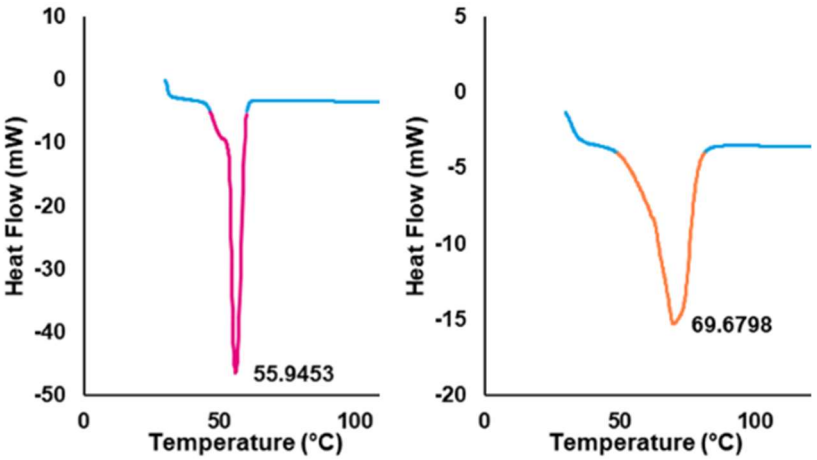

Figure 3.16. DSC thermograms: Pluronic F-68 (left) and PCL-45 (right)

Due to their range of molecular weights, the peak of energy is usually considered as the melting temperature of the polymers[20]. Therefore, it has been measured that Pluronic F-68 and PCL-45 kDa have a melting point of 55.9 $°C$ and 69.7 $°C$ respectively, which are slightly higher than their theoretical melting point, 52$°C$ and 60$°C$ respectively.

For the dried nanocapsules, two different DSC thermograms were obtained depending of the formulation. The nanocapsule formulations, which only contain PCL as polymer material, displayed a DSC with one peak as shown in Figure 3.17 (left). In these nanocapsules, the PCL melting point was measured between 54$°C$ and 58$°C$, slightly lower than the pure PCL. Nanocapsule formulations containing PCL and Pluronic F-68 as polymer materials exposed two peaks (Fig. 3.17, right). The first peak corresponds to the melting of the Pluronic F-68, which happened between 52$°C$ and 55$°C$, and the second peak is the melting of the PCL in the range from 55$°C$ to 58$°C$. The melting points of nanocapsules are lower than those of the pure polymers, however they remain into a good range of temperature for the assumed application. In both cases, the nanocapsules are completely melted above 60$°C$, which means the catalyst is released for temperatures higher than 60$°C$.

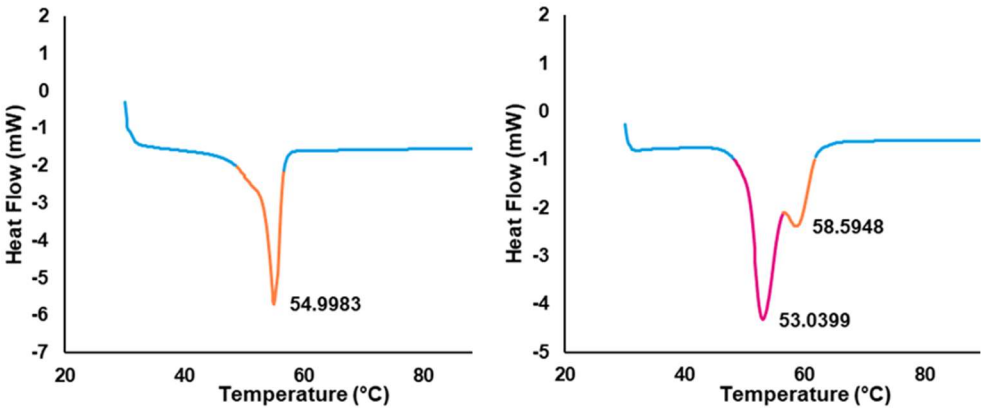

Figure 3.17. DSC thermograms of nanocapsules containing PCL (left) or containing PCL and Pluronic F-68 (right)

One nanocapsule sample could be entirely investigated in a coating formulation. The selected nanocapsule sample was loaded with BK22 (zinc-based catalyst) and GTO ($10.0 mg/mL$) and was stabilized with Pluronic F-68 ($0.5_{w/w}\%$) and CTAB ($0.1_{w/w}\%$). Three different coating formulations were tested on DMA: the normally catalyzed system, the non-catalyzed system and the nanoparticle system, in which the catalyst is replaced by nanocapsules of catalyst. The formulations are described in Table 3.4.

Table 3.4. Formulations for DMA analysis

Coating formulation		Catalyzed system	Nanoparticle system	Non-catalyzed system
Component A	Setalux D A 665 BA	3.04	3.04	3.04
	BYK 355 52%	0.012	0.012	0.012
	Solvent mixture MPA:BA 1:1	1.52	1.52	1.52
	Borchi Kat 22, 10% in MPA	0.06	-	-
	Nanoparticles	-	0.04	-
Component B	Desmodur N 3300 MPA	1.02	1.02	1.02

BA: butyl acetate; MPA: methoxopropyl acetate

The cross-linking speed of the coating formulations was observed at $20°C$ and at $65°C$ for two hours. At the lowest temperature, the nanoparticle system is supposed to behave like the non-catalyzed system, whereas at $65°C$, the nanoparticle system should resemble the catalyzed system. It can be seen in Figure 3.18 that the nanoparticle formulation cross-links much slower than the catalyzed system, however not as slow as the non-catalyzed system. The cross-linking speeds can be read in Table 3.5. The slight catalytic effects of the nanoparticle system could be explained by a small amount of catalyst deposited at the surface of the nanocapsules, by a possible slow diffusion of the catalyst from inside to outside of the nanocapsules, or due to a stability issue, as the nanocapsules were used more than a month after their syntheses. Further investigations are needed to understand the behavior of the nanocapsules at room temperature. The same experiment was then performed at $65°C$ and the results are presented in Figure 3.19. It can be seen that the nanoparticle system behaves exactly like the catalyzed system. This means that, at this temperature and higher, the nanoparticle system is perfectly suitable to replaces the normal catalyst. This is also confirmed by the cross-linking speeds in Table 3.5.

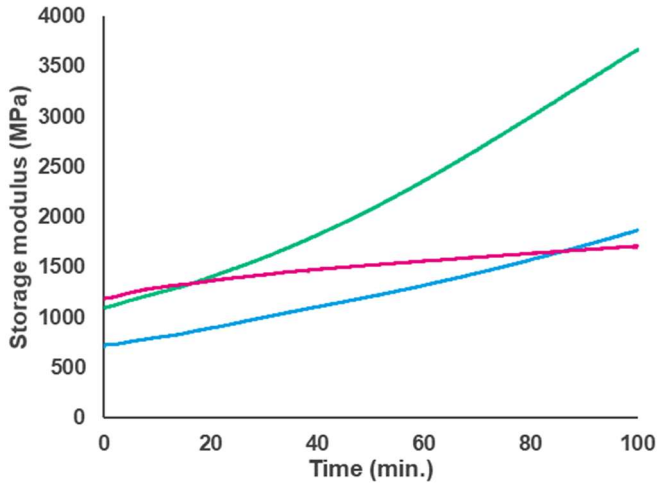

■ *Catalyzed system,* ■ *Nanoparticle system,* ■ *Non-catalyzed system*

Figure 3.18. Evaluation of the cross-linking speed by DMA at 20°C

Table 3.5. Data extracted from the DMA measurements

DMA measurements		Catalyzed system	Nanoparticle system	Non-catalyzed system
Cross-linking Speed (MPa/min.)	at 20°C	28.7	10.5	5.1
	at 65°C	348.9	378.1	183.1
Cross-linking Temperature (°C)	at 10°C/min.	57.3	58.4	73.9

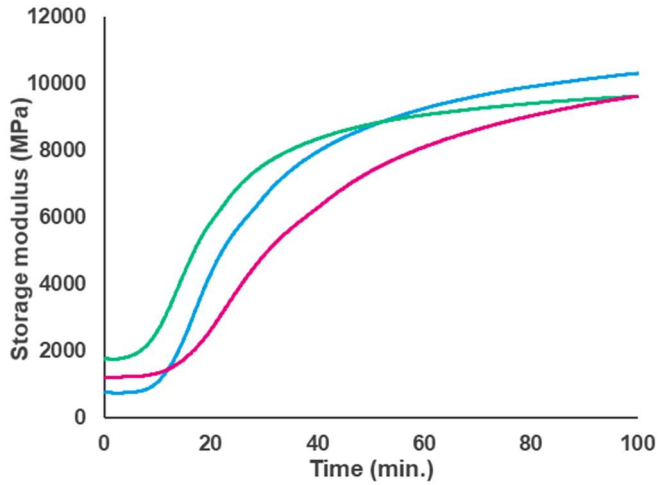

■ *Catalyzed system,* ■ *Nanoparticle system,* ■ *Non-catalyzed system*

Figure 3.19. Evaluation of the cross-linking speed by DMA at 65°C

Finally, the coatings were tested in a standard DMA from $20°C$ to $250°C$ at a $10°C/min.$ rate to compare their behavior. The curves can be found in Annex A.4. The temperatures at which the cross-linking starts could be measured (Table 3.5). As expected from the two previous experiments, the catalyzed system and the nanoparticle start cross-linking at similar temperatures, whereas the non-catalyzed system requires a higher temperature to start cross-linking.

In summary these experiments showed that PCL-nanoparticles are suitable candidates for the replacement of the catalyst in coating formulation, and therefore the increase of the pot-life, however, a deep investigation of several parameters that can impact the catalyst release must be done, such as the polycaprolactone shell thickness or the amount of Pluronic F-68 used as cryoprotectant.

3.4. Conclusion

It has been demonstrated that the addition of a hydrophobic oil in the formulation improves the retention of the catalyst within the nanocapsule, leading to an increase of the EE. In that purpose, glyceryl trioctanoate was shown to be particularly effective. The increase of the EE was also demonstrated in nanocapsules with charged outer surfaces, whether they were obtained by the intermediate of ionic surfactants or by smart uses of non-ionic surfactants having a large amount of charged groups. The addition of a hydrophobic oil inside the nanocapsules coupled with the increase of the nanocapsule zeta-potential led to nanocapsules with maximized EE, as no metal catalyst was detected outside of the nanoparticles. After lyophilization of the nanocapsule suspensions using Pluronic F-68 as cryoprotectant, the melting point of the dried nanocapsules was recorded between $50°C$ and $60°C$, as desired. Primary experiments of the implementation of the nanocapsules into a coating formulation were performed, in order to determine if the nanocapsules could be a suitable replacement of the catalyst. The first results demonstrated that polymeric nanocapsules are appropriate to be used in coating formulations. However, it will require further investigations to make such a system reliable.

This synthesis of nanocapsules could be applied to a wide range of polyurethane polymerization catalyst, as long as they are hydrophobic. Even solid-state catalysts, such as zinc neodecanoate, can be considered as they can be dissolved in the hydrophobic oil. The information learnt in this chapter could also be applied to the nanoencapsulation by emulsion-solvent diffusion, as it would have the advantage to synthesize size-tunable nanoparticles. It would also be very interesting to adapt this encapsulation technique for the encapsulation of hydrophilic substances. The synthesis of nanoparticles loaded with catalysts for water-borne polyurethane formulation, such as the very common DBU, would of great interest. This could be intended by inverting the organic phase and the aqueous phase, or by working with double emulsions, but it would in any case be complicated, as the encapsulation of hydrophilic substances remains challenging in many fields.

3.5. References

1. U. Meier-Westhues, et al., *Polyurethanes: Coatings, Adhesives and Sealants*. 2nd Revised Edition. 2019: Vincentz Network GmbH & Co. KG, Hanover, Germany.
2. Fraj, A., et al., *A comparative study of oregano (Origanum vulgare L.) essential oil-based polycaprolactone nanocapsules/ microspheres: Preparation, physicochemical characterization, and storage stability.* Industrial Crops and Products, 2019. **140**: p. 111669 DOI: 10.1016/j.indcrop.2019.111669.
3. Hernández-Giottonini, K.Y., et al., *PLGA nanoparticle preparations by emulsification and nanoprecipitation techniques: effects of formulation parameters.* RSC Advances, 2020. **10**(8): p. 4218-4231 DOI: 10.1039/c9ra10857b.
4. Alshamsan, A., *Nanoprecipitation is more efficient than emulsion solvent evaporation method to encapsulate cucurbitacin I in PLGA nanoparticles.* Saudi Pharmaceutical Journal, 2014. **22**(3): p. 219-222 DOI: 10.1016/j.jsps.2013.12.002.
5. Doğan, A., et al., *Effect of F68 on Cryopreservation of Mesenchymal Stem Cells Derived from Human Tooth Germ.* Applied biochemistry and biotechnology, 2013. **171** DOI: 10.1007/s12010-013-0472-z.
6. Lowe, K., et al., *Beneficial effects of Pluronic F-68 and artificial oxygen carriers on the post-thaw recovery of cryopreserved plant cells.* Artificial cells, blood substitutes, and immobilization biotechnology, 2001. **29**: p. 297-316 DOI: 10.1081/BIO-100104232.
7. Funasaki, N., S. Hada, and K. Suzuki, *The Dissolution State of a Triglyceride Molecule in Water and Its Orientation State at the Air-Water Interface.* CHEMICAL & PHARMACEUTICAL BULLETIN, 1976. **24**(4): p. 731-735 DOI: 10.1248/cpb.24.731.
8. Shaw, D.G., et al., *IUPAC-NIST Solubility Data Series. 81. Hydrocarbons with Water and Seawater—Revised and Updated. Part 10. C11 and C12 Hydrocarbons with Water.* Journal of Physical and Chemical Reference Data, 2006. **35**(1): p. 153-203 DOI: 10.1063/1.2134730.
9. The Good Scents Company. October 2021; Available from: thegoodscentscompany.com/data/rw1000371.html.
10. Fessi, H., et al., *Nanocapsule formation by interfacial polymer deposition following solvent displacement.* International Journal of Pharmaceutics, 1989. **55**(1): p. R1-R4 DOI: 10.1016/0378-5173(89)90281-0.
11. Jummes, B., et al., *Antioxidant and antimicrobial poly-ε-caprolactone nanoparticles loaded with Cymbopogon martinii essential oil.* Biocatalysis and Agricultural Biotechnology, 2020. **23**: p. 101499 DOI: 10.1016/j.bcab.2020.101499.
12. Granata, G., et al., *Essential oils encapsulated in polymer-based nanocapsules as potential candidates for application in food preservation.* Food Chem, 2018. **269**: p. 286-292 DOI: 10.1016/j.foodchem.2018.06.140.
13. Ameller, T., et al., *Polyester-Poly(Ethylene Glycol) Nanoparticles Loaded with the Pure Antiestrogen RU 58668: Physicochemical and Opsonization Properties.* Pharmaceutical Research, 2003. **20**(7): p. 1063-1070 DOI: 10.1023/A:1024418524688.
14. Mora-Huertas, C.E., et al., *Nanocapsules prepared via nanoprecipitation and emulsification-diffusion methods: comparative study.* Eur J Pharm Biopharm, 2012. **80**(1): p. 235-9 DOI: 10.1016/j.ejpb.2011.09.013.

15. Mora-Huertas, C.E., H. Fessi, and A. Elaissari, *Polymer-based nanocapsules for drug delivery.* International Journal of Pharmaceutics, 2010. **385**(1): p. 113-142 DOI: 10.1016/j.ijpharm.2009.10.018.
16. Newbury, D., et al., *SEM/EDS Trace Analysis: Limits Imposed by Fluorescence of the Detector.* Microscopy and Microanalysis, 2017. **23**(S1): p. 1026-1027 DOI: 10.1017/S1431927617005797.
17. Joo, H.H., et al., *Colloidal stability and in vitro permeation study of poly(ε-caprolactone) nanocapsules containing hinokitiol.* Journal of Industrial and Engineering Chemistry, 2008. **14**(5): p. 608-613 DOI: 10.1016/j.jiec.2008.03.007.
18. Hajduová, J., et al., *Structure of polymeric nanoparticles in surfactant-stabilized aqueous dispersions of high-molar-mass hydrophobic graft copolymers.* Colloids and Surfaces A: Physicochemical and Engineering Aspects, 2014. **456**: p. 10-17 DOI: 10.1016/j.colsurfa.2014.04.059.
19. Nasrazadani, S. and S. Hassani, *Chapter 2 - Modern analytical techniques in failure analysis of aerospace, chemical, and oil and gas industries*, in *Handbook of Materials Failure Analysis with Case Studies from the Oil and Gas Industry*, A.S.H. Makhlouf and M. Aliofkhazraei, Editors. 2016, Butterworth-Heinemann. p. 39-54.
20. Schindler, A., et al., *Identification of polymers by means of DSC, TG, STA and computer-assisted database search.* Journal of Thermal Analysis and Calorimetry, 2017. **129**(2): p. 833-842 DOI: 10.1007/s10973-017-6208-5.

Part 2 – Encapsulation of polyurethane polymerization cross-linkers

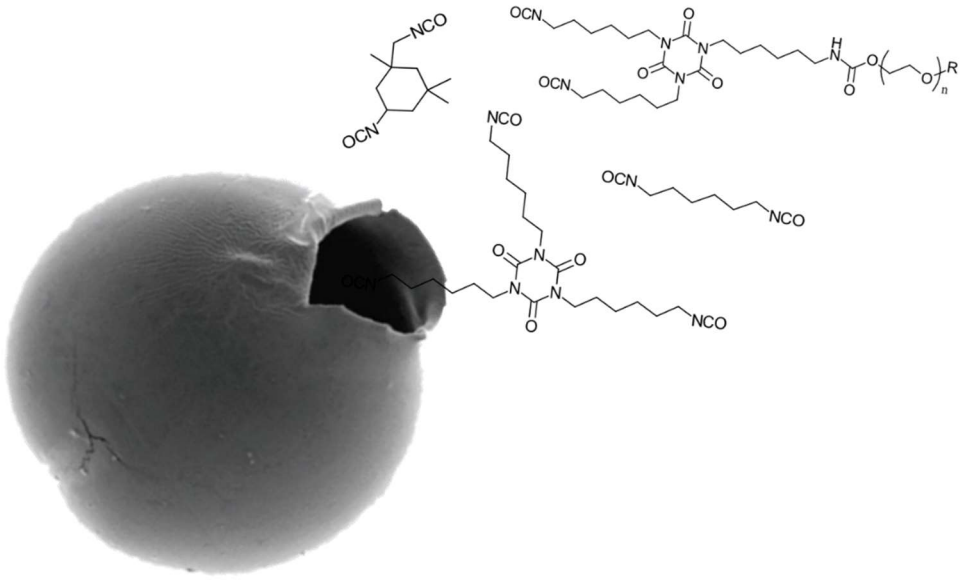

Adapted with permission from [1]. © 2019 WILEY-VCH Verlag GmbH & Co. KGaA, Weinheim

Chapter 4. Microencapsulation of aliphatic polyisocyanates by interfacial poly-condensation

4.1. Introduction

Isocyanates are extensively used since decades for the preparation of all types of polyurethanes (foams, coatings, adhesives and so on). Despite that isocyanates have been studied for the preparation of polyurethane/polyurea shell since the 1990s, the microencapsulation of the isocyanates themselves is relatively new, as the first papers were published at the beginning of the 2000s. Since then, microencapsulation of isocyanates has been further developed, focusing almost exclusively on one application, namely self-healing materials.

In 2008, Rawlins and coworkers[2] filed a patent on the nanoencapsulation of blocked isocyanates in aqueous media. The same year, the same team published the first paper on microencapsulation of isocyanates (Yang and coworkers)[3]. They prepared polyurethane microcapsules containing reactive isophorone diisocyanate (IPDI) for use in self-healing polymers via the interfacial polycondensation method. A toluene diisocyanate (TDI) prepolymer solution and IPDI were mixed and emulsified in a gum Arabic (surfactant) solution in water. The mixture was heated to 70°C with slow addition of 1,4-butanediol when the temperature reached 50°C, which led to the formation of a polyurethane shell at the interface. The polyurethane shell is obtained through a reaction between the polyol crosslinker and the TDI prepolymer. These capsules were filled with up to 70% of liquid core-content, determined by TGA analysis.

In 2010, Sondari and coworkers[4] choose to encapsulate IPDI with glycerol as a polyol crosslinker. In 2011, Huang and Yang[5] encapsulated successfully hexamethylene diisocyanate (HDI) as self-healing agent within a polyurethane shell made of methyl diphenyl diisocyanate (MDI) prepolymer and 1,4-butanediol. Microcapsules size range and core content showed similar results to Yang and coworkers' microcapsules. Two years later, Di Credico and coworkers[6] prepared microcapsules containing IPDI with different types of polymeric shells: polyurethane, poly(urea-formaldehyde) and double layer polyurethane/poly(urea-formaldehyde) for self-repairing coatings. Their capsules showed increased properties due to urethane/urea-formaldehyde shell. In 2014, Nguyen and coworkers[7] prepared polyurea microcapsules whose shells were functionalized with hydrophobic monoamines, such as 2-ethylhexylamine. They showed an increase of the lifetime during immersion in water while increasing the shell hydrophobicity.

Kardar and coworkers[8] studied the influence of the polyol crosslinker for the preparation of isocyanate-filled microcapsules in 2015. The same work with increased number of crosslinkers was published by Attaei and coworkers[9] in 2018. Their work resulted in optimized impermeable microcapsules of IPDI made of polyurea/polyurethane-silica hybrid shell obtained In 2017, He and coworkers[10] synthesized microcapsules containing IPDI and obtained through a reaction between diethylenetriamine (DETA) and polymethylene polyphenylene isocyanate (PAPI). They used polyvinyl alcohol as surfactant to stabilize the emulsion, as well as a crosslinker for the microcapsule. The prepared microcapsules are constituted of an inner polyurea shell and an outer polyurethane shell.

What all these works commonly show is that the chemical composition of the shell surrounding the isocyanates is vital to obtain stable microcapsules. Most of these microcapsules were synthesized by interfacial polycondensation with polyurethane or polyurea as shell material, but the shell composition differs in the isocyanate or in the alcohol/amine employed. Hence, the objective of this chapter is to encapsulate aliphatic polyisocyanates, by interfacial polycondensation of polyurethane or polyurea, for a new application: cross-linkers in polyurethane adhesive formulations.

4.2. Materials & Methods

4.2.1. Materials

The microcapsules were loaded with Desmodur N 3600 (DN36; HDI trimer, solvent free, NCO-content: 23.0%), whose shells were made of different types of polyisocyanates: Desmodur L 75 (TDI prepolymer, 75% solution in ethyl acetate, NCO-content: 13.3%), Desmodur IL EA (TDI trimer, 51% solution in ethyl acetate, NCO-content: 8.0%), Desmodur RE (triphenylmethane-4,4',4''-triisocyanate, 27% solution in ethyl acetate, NCO-content: 7.2%) and Desmodur VL R 20 (Polymeric MDI, solvent free, NCO-content: 31.5%). They were all directly provided by Covestro AG. To form the shell of the microcapsules, the polyisocyanates were cross-linked with different polyamines. Diethylenetriamine (DETA), tetraethylenepentamine (TEPA), 2,4,6-triaminopyrimidine (TAP), melamine, polyethylene imine (PEI, M_w=800Da) were purchased from Sigma-Aldrich while Jeffamine T-403 (J403; polyoxypropylenetriamine) was obtained from Huntsman.

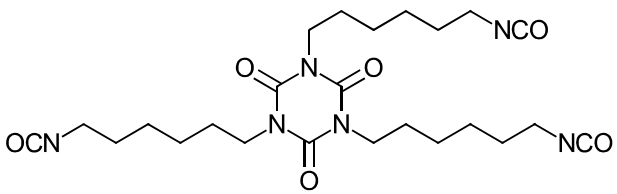

Figure 4.1. Structure of Desmodur N 3600 (idealized structure)

Several surfactants were used to stabilize the emulsion during the synthesis process: gum Arabic from acacia tree (GA), gelatin type A strength 300, poly(vinyl alcohol) (PVA; M_w=31kDa), and sodium dodecyl sulfate (SDS, ≥99%) were bought from Sigma-Aldrich. Deionized water was used for the synthesis of microcapsules. All other solvents and reagents were of analytical grade. All chemicals and materials were used as received.

4.2.2. Synthesis methods

4.2.2.1. Synthesis of hydrophilically-modified polyisocyanates

Hydrophilically-modified Desmodur N 3600 (HD36) was successfully synthesized following a literature known method[11]. First, DN36 (435.0g) was put in a round bottom flask and heated to 90°C. Methoxypolyethylene glycol-500 (MPEG, 65.0g) was added to the isocyanate solution in 30 minutes under mechanical stirring (300rpm). The reaction was followed by measurements of the NCO-content every ten minutes until the NCO-content reached 18.7±0.1%, which corresponds to the completion of the reaction. NCO titrations were performed in triplicate 24 hours after the end of the reaction in order to confirm the final NCO-content of the newly synthesized hydrophilically-modified polyisocyanate (18.7%), in which roughly 10% of NCO groups are turned into urethane bonds bearing hydrophilic chains.

The particularity of this isocyanate is its ability to behave as a surfactant (Fig. 4.2). Indeed, the isocyanate now possesses both a hydrophobic and a hydrophilic part. Such isocyanates are used in water-borne formulations, in which the isocyanate is turned into micelles, and its pot-life within the water-based formulation is increased. HD36 is used in this work precisely for its surfactant-like behavior.

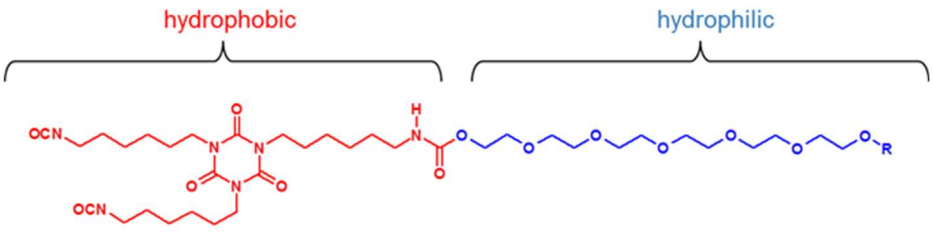

Figure 4.2. Structure of hydrophilically-modified Desmodur N3600 (idealized structure)

4.2.2.2. Interfacial Polycondensation

DN36-loaded and HD36-loaded microcapsules were synthesized by interfacial polycondensation (Fig. 1.21) as described by Nguyen and coworkers[7]. This method involves the polymerization of two monomers at the oil/water interface of an emulsion. Firstly, the core material ($20.0g$) was mixed with an aromatic isocyanate (20-50% NCO-equivalents to the amount of core material) during 3 minutes at $3500rpm$ in a high-speed homogenizer (DAC 150.1 FVZ, SpeedMixer). The mixture was slowly added to a water solution containing a surfactant (1 to $13_{w/w}\%$). A stable emulsion was formed with a high-speed mixer at $3600rpm$ during 10 minutes (Ultra-Turrax T25, IKA). A polyamine (50 to 100% equivalent of aromatic isocyanates) was dissolved in water and added dropwise to the emulsion. The polyamine reacts almost exclusively with the aromatic isocyanate, as it is much more reactive than the aliphatic isocyanate. The polyurea cross-linking is completed by heating the mixture up to $75°C$ during 20 minutes to 2 hours. The obtained suspension was filtered under vacuum and washed three times with water. The solid was dried at room temperature for 24 hours before further analysis.

4.2.3. Characterization

4.2.3.1. NCO-content measurement

The NCO-content was determined by back titration according to the standard test method ASTM D2572-97. The sample is put in acetone with a known excess of N-dibutylamine (NDBA). The isocyanates react quickly with the amines and the remaining NDBA is titrated with hydrochloric acid. The NCO-content is obtained via the following equation:

$$NCO\ content(\%) = \frac{(C_{NDBA} \times V_{NDBA} - C_{HCl} \times V_{equivalent}) \times 4.2}{m_{sample}} \quad (4.1)$$

4.2.3.2. Core-content measurement

The microcapsules core-content was obtained using Fourier-Transform Infrared Spectroscopy (FT-IR, Spectrum Two, Perkin Elmer)[7]. Beforehand, a calibration curve (Fig. 4.3) was made by measuring the maximum absorbance of the NCO groups at 2270cm^{-1} of DN36 and HN36 solutions in dimethylformamide (DMF), with concentrations from 0.01 to 0.20 weight fraction (Fig. 4.3 and Annex B.1, respectively). A known amount of microcapsules was sonicated with a known amount of DMF and the maximum absorbance at ~2270cm^{-1} was measured. The isocyanate concentration was obtained thanks to the calibration curve, and the core-content was calculated with Equation 4.2:

$$Core\ content(\%) = \frac{\frac{C_{DN36} \times m_{DMF}}{1 - C_{DN36}}}{m_{sample}} \times 100 \quad (4.2)$$

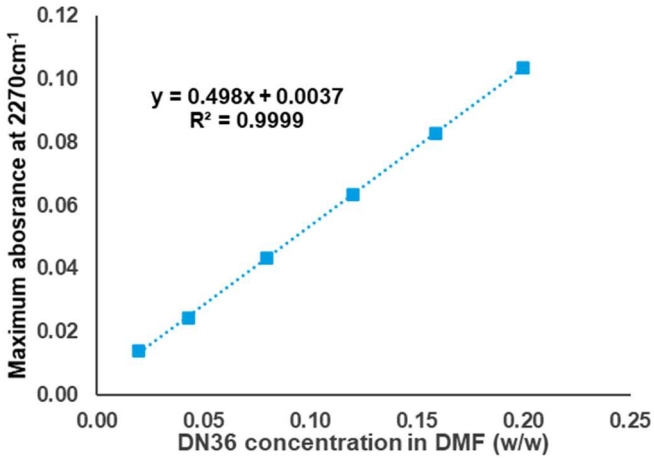

Figure 4.3. Calibration curve of Desmodur N 3600 absorbance at 2270cm^{-1} in DMF

4.2.3.3. Morphology

The microcapsules morphology was observed by optical microscopy (Digitalmikroskop VHX-600, Keyence). The sample was mixed with a small amount of water using a IKA® VORTEX Shaker Genius 3 at moderate power. The microcapsule suspension was observed in between glass supports. Solid samples were observed directly on the glass support. Scanning Electron Microscopy (SEM) was also used but independently performed by a Covestro AG specific department.

4.3. Results and Discussion

4.3.1. Synthesis of HD36-loaded microcapsules

As the polymerization occurs at the oil/water interface of each emulsion droplets, the synthesized microparticles are exclusively microcapsules. The core material is the aliphatic isocyanate, DN36 or its hydrophilically-modified version HD36, which is encapsulated in a polyurea shell, obtained by a reaction between an aromatic isocyanate and a polyamine. Firstly, HD36 was encapsulated in microcapsules, while playing simultaneously the role of core material and surfactant. Pictures of the successfully obtained microcapsules are displayed in Figure 4.4 and show sizes from 1 to 100μm, which is in accordance the microcapsule size of other works. It can be seen in the picture of dried microcapsules that both white and transparent spherical microcapsules were obtained. This observation remains unclear, but it is assumed that the reaction was incomplete and some microcapsules were not fully formed.

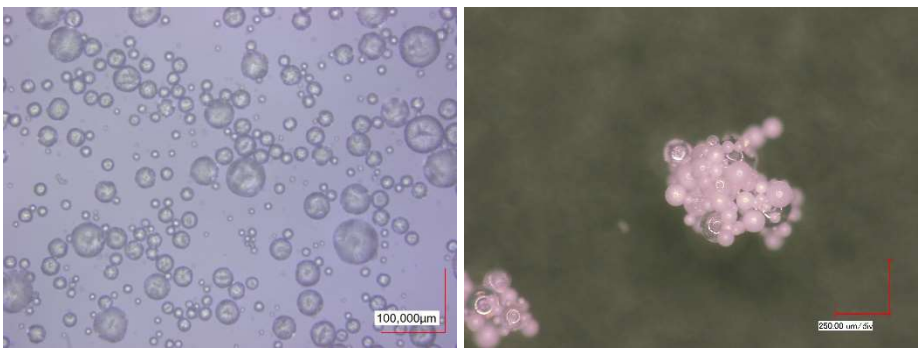

Figure 4.4. Digital microscope pictures of a suspension of HD36-loaded microcapsules at x20 (left) and of dried HD36-loaded microcapsules at x150 (right)

The encapsulation of isocyanate inside these microcapsules was confirmed by crushing some microcapsules on the FTIR device. The crushed microcapsules were compared with pure HD36 and the spectra are presented in Figure 4.5. The typical NCO bond of the isocyanates at 2270cm^{-1} can be observed in the crushed microcapsules, as well as the C-N bond (~1200cm^{-1}) and the C-O-C (~1600cm^{-1}) group of the polyurea network.

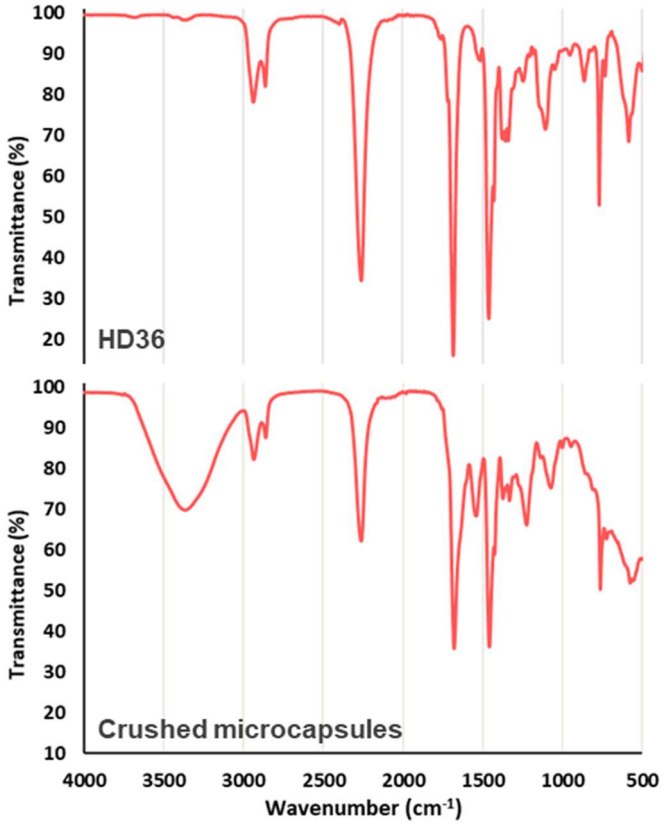

Figure 4.5. FTIR spectra: HD36 (top) and crushed microcapsules (bottom)

The NCO-content and the core-content of these microcapsules were measured. It revealed that the core-content was only of 30% and the NCO-content was below 6%, while up to 70% and 13% of core-content and NCO-content could be expected, respectively. The microcapsules also showed a poor stability, as no isocyanate was detected inside the microcapsules after 7 days. Even by optimization of this system, the core-content barely reached 50%, whereas on the other hand, the microencapsulation of DN36 using a surfactant easily exceeded these 50% core-content with a better stability. Therefore, it was concluded that the surfactant properties of HD36 are insufficient to synthesize efficiently microcapsules, and that focusing on the development DN36-loaded microcapsules would be more relevant.

4.3.2. Synthesis and optimization of DN36-loaded microcapsules

Microcapsules containing DN36 were successfully obtained via the interfacial polycondensation technique with a higher core-content and NCO-content (>12%) than the HD36-loaded microcapsules previously synthesized. However, they also showed a very limited stability, as the microcapsules were NCO-free after 14 days. Therefore, several parameters are here investigated in order to improve the long-term stability of the microcapsules, which is followed by measuring their core-content over time.

As the syntheses are performed in water, the reaction time is a crucial parameter to form stable microcapsules. The isocyanates are very reactive toward water, therefore, the reaction time needs to be kept short, but long enough to allow the good formation of the polyurea shell. Any reaction time below 20 minutes led to the formation of one large aggregate during the purification step. On the other side, after 30 minutes of reaction, bubbles started appearing in the flask. They suggest that the isocyanates started reacting with water, as this reaction releases CO_2 before quickly forming polyurea. The measurements of the DN36 core-content over time for microcapsules synthesized during 20 to 120 minutes are displayed in Figure 4.6.

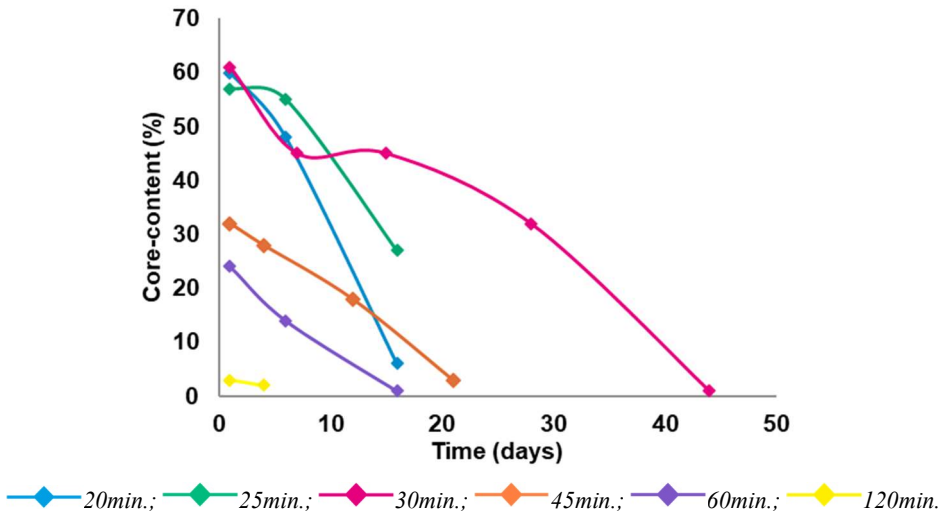

Figure 4.6. Stability of the core-content over time for different reaction times

The core-content measurements at $t = 1\ day$ show that the increase of the reaction time above 30 minutes leads to an important decrease of the core-content, and the microcapsules contain close to no isocyanates after 2 hours of reaction. This confirms that, for long reaction times, the aliphatic isocyanate can react with water, which is not desired. On the other side, it can be seen that the initial core-content for reactions lasting 20 to 30 minutes remains constant, however, the long term stability improves as a function of the reaction time and reaches its maximum at 30 minutes. This also confirms the previous observations, as the efficiency of the shell is improved with a longer reaction time. All further experiments were performed with a reaction of 30 minutes.

Most the papers describing the encapsulation of isocyanates use prepolymers as shell material, which can be based on MDI[5-7, 9] or TDI[3, 12]. It has also be mentioned that high NCO-content prepolymers are preferred to obtain stable and robust microcapsules[3]. This is why the effect of the isocyanate wall was studied and the stability of the core-content over time is shown in Figure 4.7.

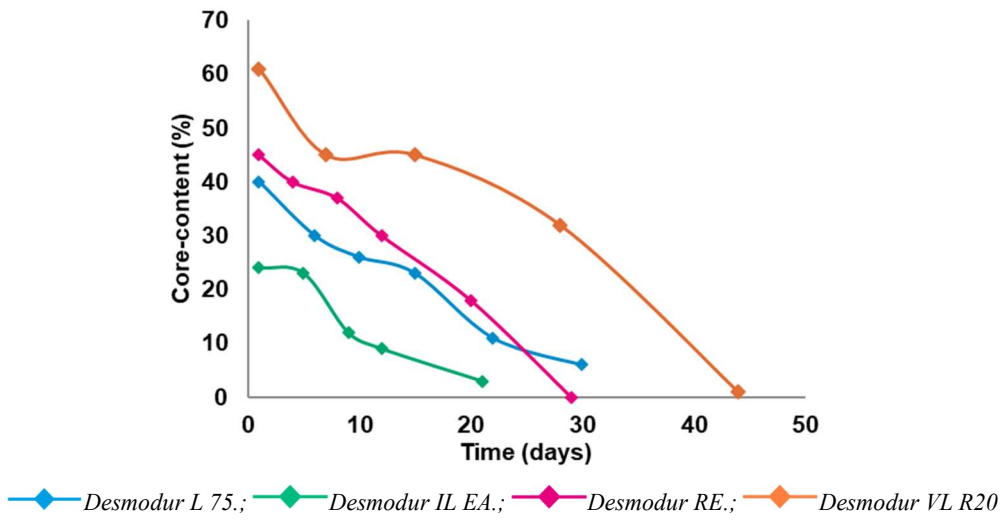

Figure 4.7. Stability of the core-content over time for different isocyanates

The results show that the type of isocyanate used to make the polyurea wall has a large impact on the core-content. However, the core-content at day 1 is not entirely proportional to the NCO-content of these isocyanates, which are summarized in Table 4.1. The microcapsules made with Desmodur RE show better results than those made with Desmodur L 75, despite a higher NCO-content for the latter. This difference is believed to come from the structure of these isocyanates. Due to its very hydrophobic structure, Desmodur RE is able to make a more hydrophobic and tighter polyurea, which increases the entrapment of the core inside the microcapsules and prevents the side-reaction with water. In any case, the highest core-content was obtained when using Desmodur VL R 20, which is highly hydrophobic and also solvent-free.

Desmodur VL R 20 is also the only aromatic polyisocyanates of this work with a solid-content of a 100%, which means that the isocyanate is not dissolved in any solvent. For example, Desmodur L 75 has a solid-content of approximatively 75%, the other 25% being ethyl acetate. The presence of ethyl acetate in the emulsion droplets could have an impact on the stability of the microcapsules, as this solvent is partially soluble in water and could disrupt the emulsion stability by diffusing to the aqueous phase. However, no stability issue were observed, as Desmodur RE has a solid-content of only 27% and showed better results than Desmodur IL EA (51% solid-content).

Table 4.1. Aromatic isocyanate structures and NCO-contents

Isocyanate	Structure	Properties
Desmodur L 75	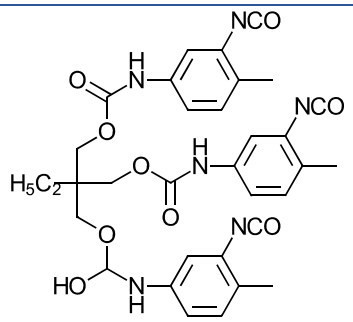	NCO-content (%) 13.3 ± 0.4 Solid-content (%) 75.0 ± 2.0
Desmodur IL EA	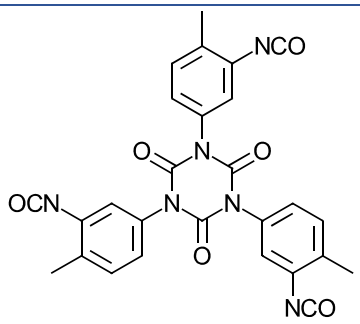	NCO-content (%) 8.0 ± 0.2 Solid-content (%) 51.0 ± 2.0
Desmodur RE	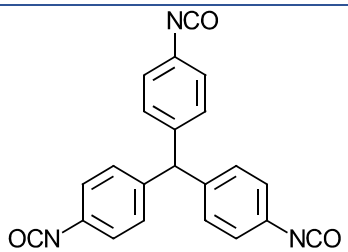	NCO-content (%) 9.3 ± 0.2 Solid-content (%) ~27
Desmodur VL R 20	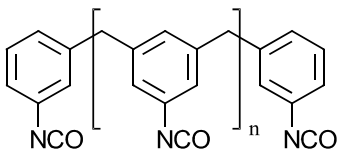	NCO-content (%) 31.5 ± 0.1 Solid-content (%) 100

Several surfactants can be used for the synthesis of polyisocyanate microcapsules. The most common are GA and PVA which were used in this work, but they were also compared with other common surfactants: Gel and SDS. The microcapsules which were internally stabilized with HD36 are also presented in Figure 4.8 for comparison with the experiments using a surfactant. The effect of the surfactant was firstly investigated respectfully to their concentration used in the literature: $13_{w/w}$% for GA[3, 7, 13] and $5_{w/w}$% for PVA[10, 14]. SDS[15] and Gel are employed with a wide range of concentrations for other applications, and were investigated with a $1_{w/w}$% concentration.

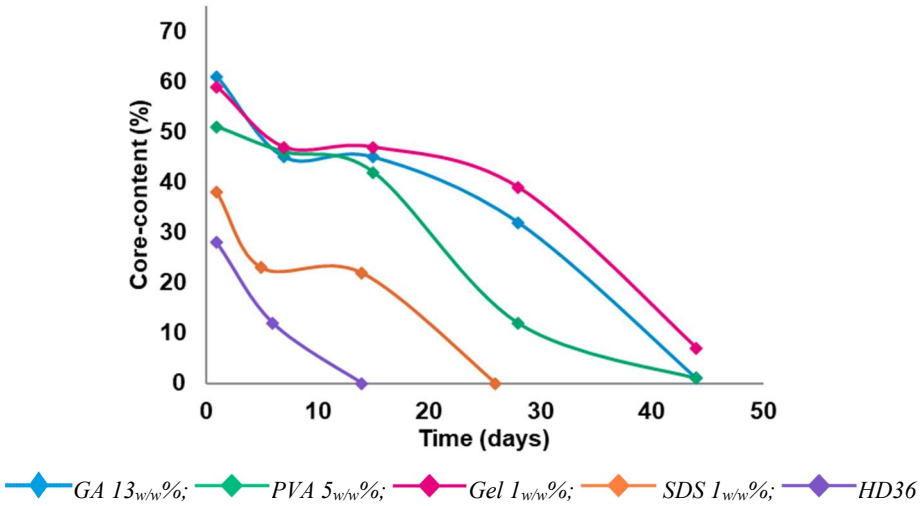

Figure 4.8. Stability of the core-content over time for different surfactants (Desmodur VL R 20)

The data in Figure 4.8 clearly demonstrates that HD36, as both the surfactant and the encapsulated material, is not a suitable option for the encapsulation of isocyanates, as previously stated. The initial core-content of microcapsules stabilized by SDS is also significantly lower and overall, SDS-stabilized syntheses did not show consistent results. It can also be seen that the initial core-content and its stability over time is similar for the microcapsules stabilized with GA, PVA and Gel. This is not surprising, as all three surfactants have a similar structure, i.e. long chains with large amount of hydroxyl groups.

The same study was conducted with the other type of isocyanates and can be found in Annex (B.2, B.3 and B.4). The combination of PVA as surfactant and any other type of isocyanates did not allow the formation of stable microcapsules. The viscosity of the aqueous phase is particularly high when PVA is used as surfactant, which could explain why microcapsules were difficulty obtained, unless the NCO-content is particularly high.

A lower viscosity is more convenient for the purification of the microcapsules, therefore, the effect of the concentration of the surfactant has been studied for GA and Gel. Figure 4.9 shows that the impact of the surfactant concentration on the core-content and the long-term stability is limited, but a difference of about 15% of core-content after 28 days can still be observed between the GA at $1_{w/w}$% and $13_{w/w}$%. This indicates that a solution of GA with a concentration higher than $10_{w/w}$% is preferred.

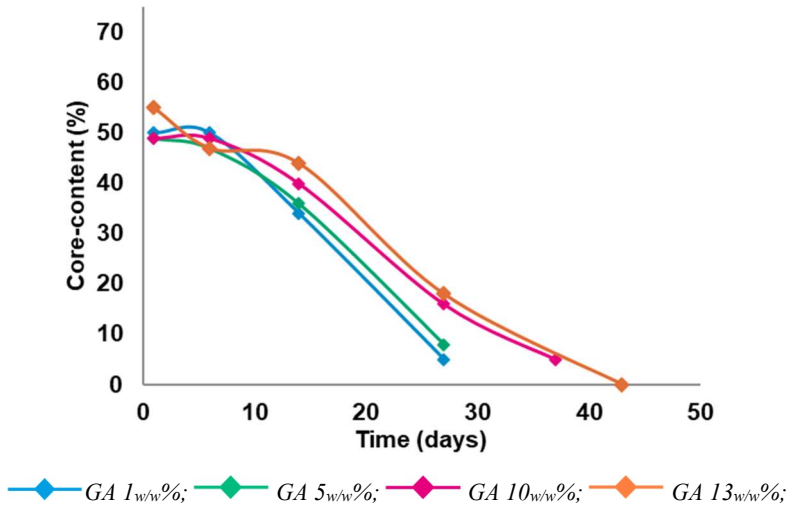

Figure 4.9. Stability of the core-content over time for different concentration of GA

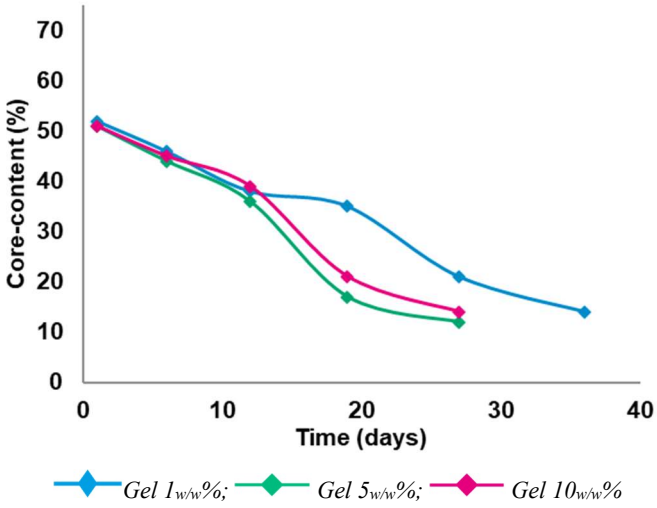

Figure 4.10. Stability of the core-content over time for different concentration of Gel

On the other side, Figure 4.10 demonstrates that the concentration of Gel has close to no influence on the core-content and the long-term stability of the microcapsules. This means the synthesis can be properly performed with a smaller, and more appropriate, amount of surfactant. The concentration of surfactant is an important parameter, not only because of the purification step, but also because of the reaction than can occur between the surfactant and the isocyanates. These surfactants possess a very high number of hydroxyl groups and/or amine groups (Table 4.2) which are able to react with the isocyanates at the droplet interface, especially with the aromatic isocyanate. It is very likely that a thin layer of polyurethane and/or polyurea is obtained during the emulsification step. A lower concentration of surfactant will reduce its interaction with the isocyanates and, therefore, a better control of the encapsulation can be expected. Moreover, some surfactant will remain after purification, either because it has reacted with the isocyanates or because it is trapped in the polyurea network. These hydroxyl groups will be able to react with the isocyanates upon release, thus decreasing the surfactant concentration could also help to reduce this side reaction. Gel $1_{w/w}$% has been selected as surfactant for future experiments.

Table 4.2. Gum Arabic and Gelatin type A main structures

Gum Arabic (main backbone) **GA** 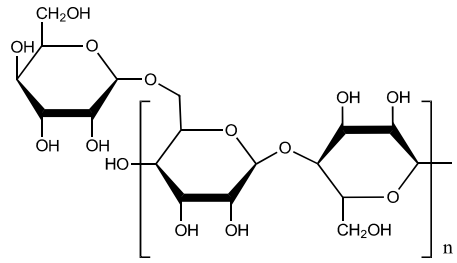
Gelatin type A (main backbone) **Gel** 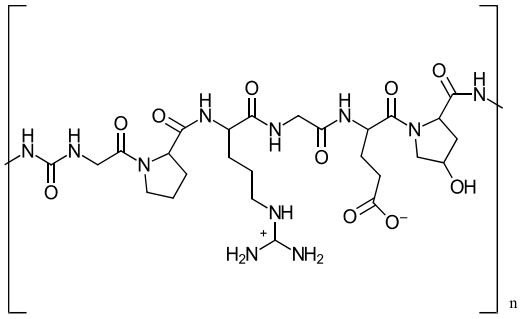

Another important parameter for the long-term stability of microcapsules is the shell thickness. Therefore, different amounts of shell materials were investigated. The amount of shell material was measured as NCO-equivalents relatively to the encapsulated material, which was kept constant. In the previous experiments, the aromatic isocyanate was used as 40% of NCO-equivalents. The increase of this amount means that the shell around the microcapsule is larger. Figure 4.11 illustrates the results obtained for different shell thickness.

With 20% of NCO-equivalents, no stable microcapsules were produced and one large polyurea aggregate was obtained. The synthesis with 30% of NCO-equivalents has a higher initial core-content, whereas the synthesis with 50% of NCO-equivalents has a lower core-content. This is consistent with the formulation of those microcapsules, as a thicker (thinner) polyurea wall means the core-content decreases (increases).

Figure 4.11 also shows that the long-term stability worsen with a thinner shell, however it does not improve with a thicker shell. This means the maximum stability that the capsule can provide is already reached with 40% of NCO-equivalents.

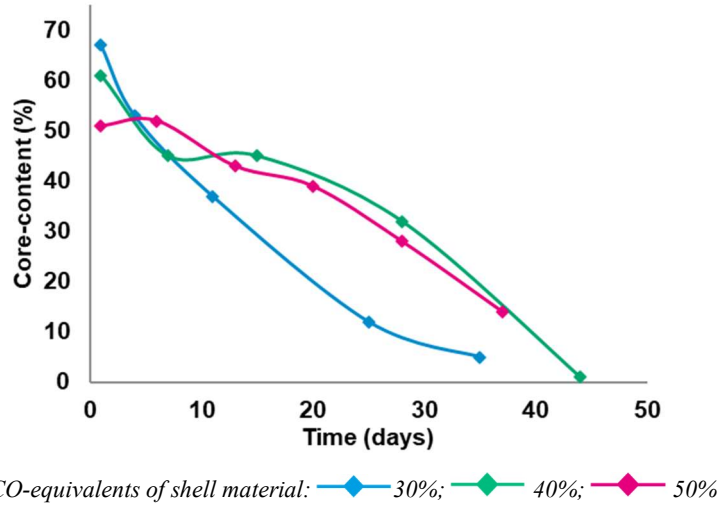

Figure 4.11. Stability of the core-content over time for different NCO-equivalents of wall material in Gel $1_{w/w}$%

As mentioned earlier, the polyisocyanates can react with water and with the surfactant as side-reactions of the shell formation. Therefore, it has been intended to purposely involve the water and/or the surfactant in the microcapsule synthesis, similarly to the work of He and coworkers[10].

The syntheses were so far accomplished with a 1:1 equivalent ratio of aromatic isocyanates to amines. The amount of amines was decreased and the excess of isocyanates reacted with the surfactant or water to form a hybrid polyurea/polyurethane shell. The effect of this parameter is illustrated in Figure 4.12. It can be observed that no consistent evolution was detected when the amount of amine was decreased, but all formulations showed a reduced long-term stability in comparison to the 1:1 equivalent ratio, which is therefore preferred.

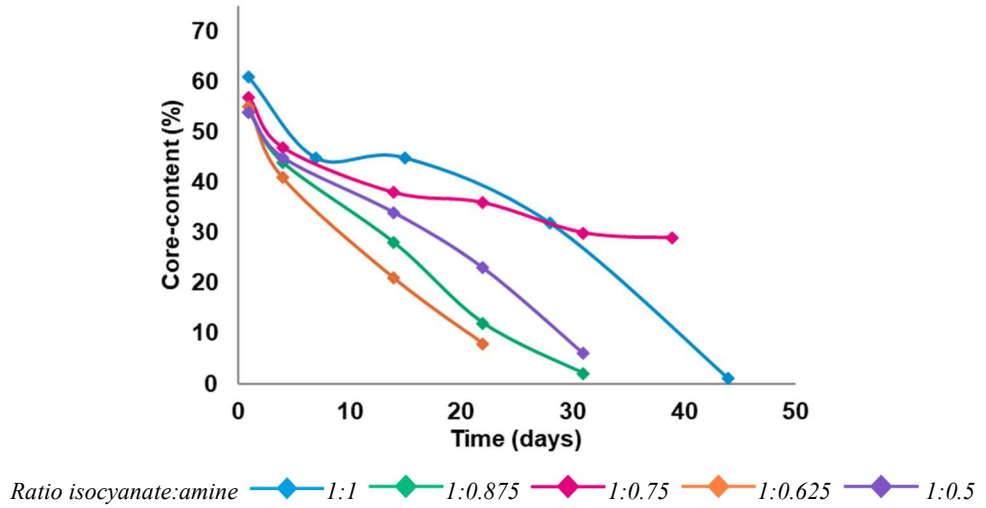

Figure 4.12. Stability of the core-content over time for different isocyanate to amine ratio in Gel $1_{w/w}$%

Finally, the influence of the amine functionality and structures was investigated with the optimized formulation. Three types of amines were examined: aliphatic polyamines (DETA and TEPA), aromatic polyamines (TAP and melamine) and high functionality polyamines (JT-403 and PEI). Their structures are shown in Table 4.3.

Table 4.3. Polyamine structures

DETA 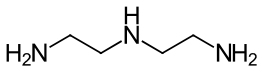	**TEPA** 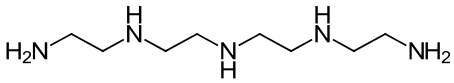
TAP 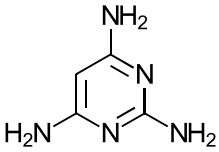	**Melamine** 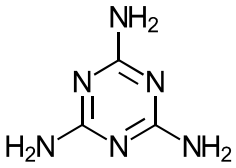
JT-403 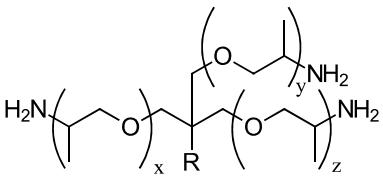	**PEI** 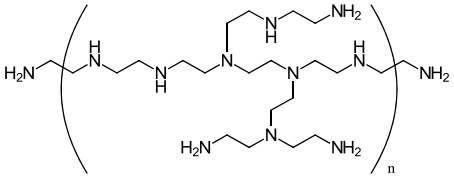

Microcapsules were successfully synthesized with all the polyamines just mentioned. The stability over time of these microcapsules can be found in Figure 4.13. As expected, DETA and TEPA led to similar microcapsules, as TEPA is just a longer version of DETA, which might explain why TEPA has a slightly better core-content after 40 days.

Aromatic polyamines are more hydrophobic and should allow the formation of more hydrophobic polyurea microcapsules. This is what can be observed with TAP, but not in the case of melamine. In the synthesis with melamine, a white solid was deposited on the flask, which is believed to be some recrystallized melamine, as it has a very poor solubility in water. This means that the shell was not properly formed and a poor stability is observed.

The high-functionality polyamines are more hydrophilic than the other amines presented here, however, it was hypothesized that a tighter shell could be made due to their high-functionality. The results indicate that the hydrophobicity of the shell has more impact than the cross-linking network.

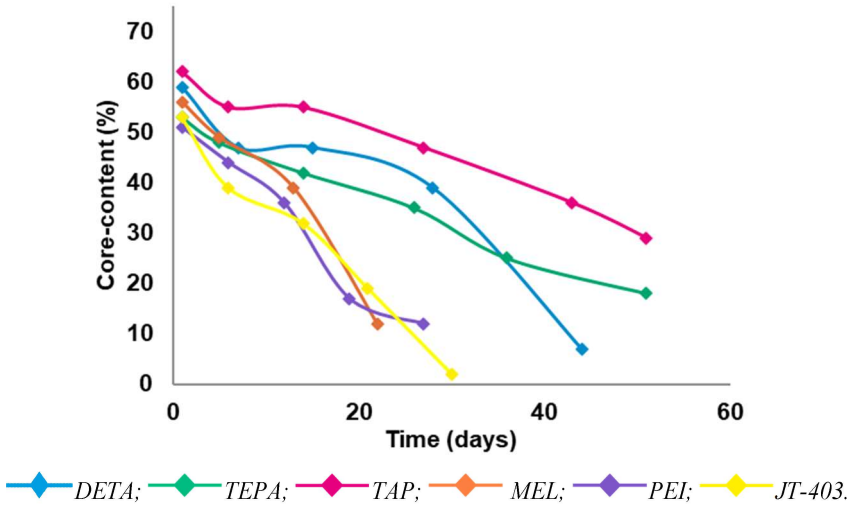

Figure 4.13. Stability of the core-content over time for different amines in Gel $1_{w/w}$%

The microcapsules were observed with a digital microscope and the pictures can be seen in Figure 4.14. The microcapsules are spherical and their sizes, between 1 and 100μm, are consistent with other works[3, 5, 7].

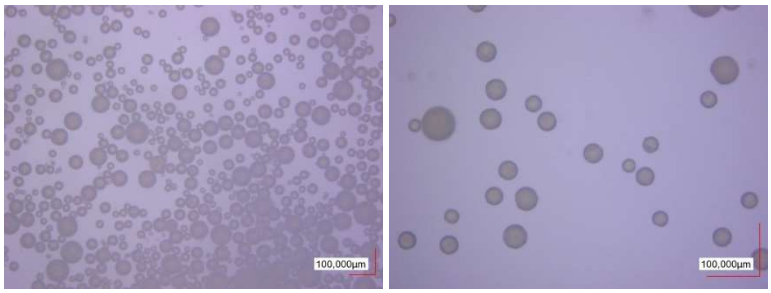

Figure 4.14. Digital microscope pictures of microcapsules stabilized with GA 13$_{w/w}$% at x10 (left) and with Gel 1$_{w/w}$% at x20 (right)

Figure 4.15 and 4.16 show SEM pictures of GA-stabilized and Gel-stabilized microcapsules respectively. They show spherical microcapsules with a relatively smooth outer surface. In fact, the GA-stabilized microcapsules have a smoother surface whereas the surface of Gel-stabilized is a bit more wrinkled. GA-stabilized are visually yellowish, which is due to some GA remaining at the surface (GA is naturally orange), and Gel-stabilized are simply white. The different concentration of surfactant could also explain the difference between the surfaces.

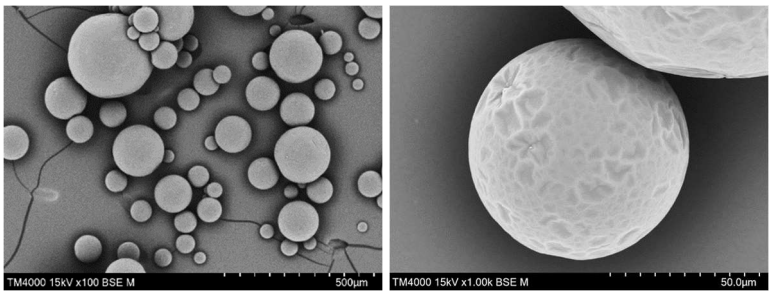

Figure 4.15. SEM pictures of microcapsule stabilized with GA 13$_{w/w}$% at x100 (left) and at x1k (right)

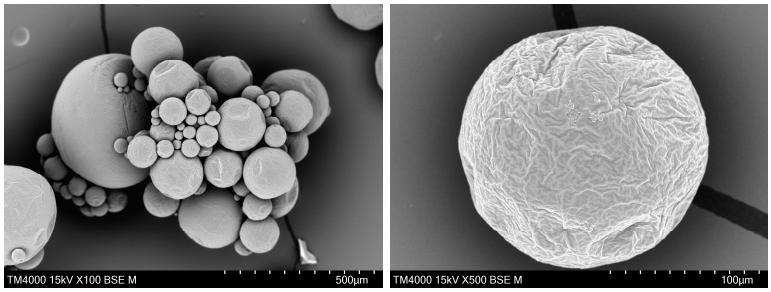

Figure 4.16. SEM picture of microcapsules stabilized with Gel $1_{w/w}$% at x100 (left) and at x500 (right)

4.4. Conclusion

A wide range of microcapsules were successfully synthesized by interfacial polycondensation. The synthesis process was shown to have a large impact on the microcapsules core-content and NCO-content. In particular, the materials used to prepare the microcapsule shell were of high importance; aromatic isocyanates and amines with high hydrophobicity showed improved core-content and long-term stability. Overall, the microcapsules were enhanced from 50% to close to 70% core-content, which corresponds to more than 15% of NCO-content. The core-content would decrease of 10% within the first month, which is similar to some other polyisocyanate-loaded microcapsules[5], but relatively far from the 10% loss in 6 months of other works[3, 6], despite using comparable set-up.

These microcapsules could possibly be used for self-healing materials, but they are however not suitable as cross-linkers for adhesive polyurethane formulations. The primary implementation of these microcapsules in an adhesive formulation did not show more than a hardly noticeable cross-linking at $120°C$. This supports the idea that the isocyanates can react with the surfactant before and after being released. It also suggest that this approach, i.e. interfacial polycondensation, is probably not the best approach to synthesize polyisocyanate-loaded microcapsules for this type of applications. One other approach will be experimented in the next chapter, and some other possibilities will also be discussed.

In any case, the encapsulation of materials into polyurethane/polyurea remains very effective, as close to the maximum core-content was obtained, as well as high yields. This technique can be applied to encapsulate a variety of other materials, preventing that they are not reactive toward isocyanates.

4.5. References

1. Zhang, W., et al., *Controllable Fabrication of Inhomogeneous Microcapsules for Triggered Release by Osmotic Pressure.* Small, 2019. **15**(42): p. 1903087 DOI: doi.org/10.1002/smll.201903087.
2. Rawlins, J.W., H. Yang, and S.K. Mendon, *Nanoencapsulation of Isocyanates Via Aqueous Media.* 2008. **US20080234406A1**.
3. Yang, J., et al., *Microencapsulation of Isocyanates for Self-Healing Polymers.* Macromolecules, 2008. **41**(24): p. 9650-9655 DOI: 10.1021/ma801718v.
4. Sondari, et al., *Polyurethane microcapsule with glycerol as the polyol component for encapsulated self healing agent.* International Journal of Engineering and Technology, 2010. **2**.
5. Huang, M. and J. Yang, *Facile microencapsulation of HDI for self-healing anticorrosion coatings.* Journal of Materials Chemistry, 2011. **21**(30): p. 11123-11130 DOI: 10.1039/C1JM10794A.
6. Di Credico, B., M. Levi, and S. Turri, *An efficient method for the output of new self-repairing materials through a reactive isocyanate encapsulation.* European Polymer Journal, 2013. **49**(9): p. 2467-2476 DOI: 10.1016/j.eurpolymj.2013.02.006.
7. Nguyen, L.-T.T., et al., *Efficient microencapsulation of a liquid isocyanate with in situ shell functionalization.* Polymer Chemistry, 2015. **6**(7): p. 1159-1170 DOI: 10.1039/C4PY01448K.
8. Kardar, P., *Preparation of polyurethane microcapsules with different polyols component for encapsulation of isophorone diisocyanate healing agent.* Progress in Organic Coatings, 2015. **89**(Complete): p. 271-276 DOI: 10.1016/j.porgcoat.2015.09.009.
9. Attaei, M., et al., *Isophorone Diisocyanate (IPDI) Microencapsulation for Mono-Component Adhesives: Effect of the Active H and NCO Sources.* Polymers, 2018. **10**(8) DOI: 10.3390/polym10080825.
10. He, Z., et al., *Facile and cost-effective synthesis of isocyanate microcapsules via polyvinyl alcohol-mediated interfacial polymerization and their application in self-healing materials.* Composites Science and Technology, 2017. **138**: p. 15-23 DOI: 10.1016/j.compscitech.2016.11.004.
11. Laas, H.-J., et al., *Water-dispersible polyisocyanate mixtures* 1991. **EP0540985B1**.
12. Haghayegh, M., S.M. Mirabedini, and H. Yeganeh, *Preparation of microcapsules containing multi-functional reactive isocyanate-terminated-polyurethane-prepolymer as healing agent, part II: corrosion performance and mechanical properties of a self healing coating.* RSC Advances, 2016. **6**(56): p. 50874-50886 DOI: 10.1039/C6RA07574F.
13. Budd, M.E., et al., *Exploiting thermally-reversible covalent bonds for the controlled release of microencapsulated isocyanate crosslinkers.* Reactive and Functional Polymers, 2019. **135**: p. 23-31 DOI: 10.1016/j.reactfunctpolym.2018.12.008.
14. Sun, Y., et al., *Optimized synthesis of isocyanate microcapsules for self-healing application in epoxy composites.* High Performance Polymers, 2020. **32**(6): p. 669-680 DOI: 10.1177/0954008319897745.
15. Torini, L., J.F. Argillier, and N. Zydowicz, *Interfacial Polycondensation Encapsulation in Miniemulsion.* Macromolecules, 2005. **38**(8): p. 3225-3236 DOI: 10.1021/ma047808e.

Chapter 5. Nanoencapsulation of aliphatic polyisocyanates by nanoprecipitation

5.1. Introduction

The work performed in Chapter 4 has illustrated that the microencapsulation of polyisocyanates could be performed, but that, despite improvements, stability issues remain due to unwanted side-reactions. To be used as cross-linkers, isocyanate-loaded microcapsules would be preferred over nanocapsules, as the latter would mean that a high amount of polymer will be introduced in the formulation. However, it is believed that the study of nanoencapsulation of isocyanates could give important information toward a more successful microencapsulation.

The nanoencapsulation of polyisocyanates was rarely performed in the literature, with the only mention being the work of Rawlins, Yang and coworkers[1, 2]. They filed a patent and published a paper on the nanoencapsulation of blocked isocyanates in aqueous media. Such isocyanates are unreactive, as they are protected with different types of blocking groups, such as butanone oxime or dimethylpyrazole[3]. Therefore, they could encapsulate the isocyanates in emulsion polymerization techniques (similar to Chapter 4) without being concerned about the reactivity of the isocyanates. This is why their work cannot be directly applied to the encapsulation of reactive isocyanates, and, thanks to the knowledge acquired in Part 1, polyisocyanate-loaded nanocapsules made of PCL will be synthesized by nanoprecipitation in this chapter.

5.2. Materials & Methods

5.2.1. Materials

Desmodur N 3600 (DN36, NCO-content: 23.0%) and hydrophilically-modified Desmodur N 3600 (HD36, NCO-content: 18.7%, synthesis described in Chapter 3) were encapsulated in polycaprolactone (PCL, $45kDa$). If necessary, the nanocapsules were stabilized with Pluronic F-68. Water was purified with a $0.22\mu m$ Milipak® membrane filter. All other solvents and reagents were of analytical grade. All chemicals and materials were used as received.

5.2.2. Nanoparticle synthesis

Nanocapsules encapsulating polyisocyanates (were synthesized via nanoprecipitation[4] as described in Chapter 3. Briefly, the PCL (50-100mg) was dissolved in acetone ($10mL$) at $50°C$ under moderate stirring and the isocyanate (50-200mg) was added subsequently at room temperature. This mixture was slowly added with a syringe pump to a water solution ($20mL$) under magnetic stirring ($1200rpm$), containing no surfactant or Pluronic F-68 ($0.5_{w/w}\%$), when HD36 and DN36 were used respectively. The suspension was then freeze-dried (LyoAlpha, Telstar) for 3 days without further purification.

5.2.3. Characterization

The nanoparticle sizes and polydispersity index (PDI) were measured with Dynamic Light Scattering (DLS) and their morphologies were observed by Field Emission Scanning Electron Microscopy (FESEM), as described in Chapter 2. The nanoparticle thermal properties were studied by Differential Scanning Calorimetry (DSC), as previously presented in Chapter 3. Finally, the core-content of the nanoparticles was measured using Fourier Transform Infrared Spectroscopy (FTIR) exactly as explained in Chapter 4, except that the calibration and measurements were performed in xylene, that is able to dissolve PCL. The calibration curve can be found in Annex B.5.

5.3. Results and Discussion

Synthesis of nanocapsules

Nanoparticles containing DN36 and HD36 were successfully synthesized by nanoprecipitation. Due to limited interactions between the PCL and the isocyanates, the nanoparticles are necessarily nanocapsules: the isocyanates are surrounded by the PCL shell.

The effect of the PCL concentration on the nanocapsule sizes was studied, and similar results were obtained depending on the encapsulated isocyanates. This effect on the encapsulation of DN36 can be found in Figure 5.1.

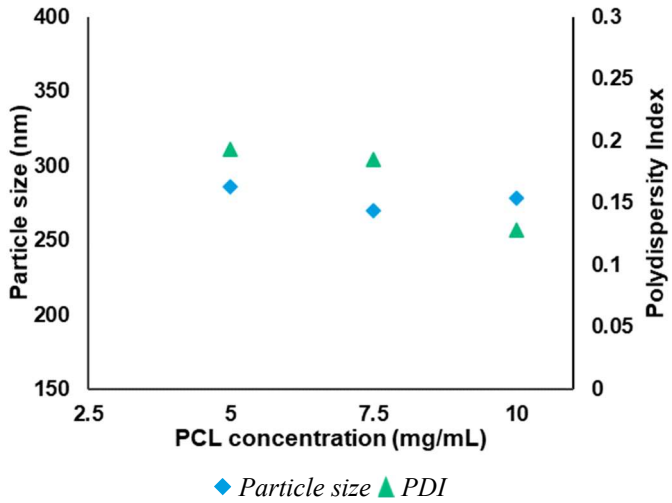

Figure 5.1. Effect of the PCL concentration on the particle size of DN36-loaded nanocapsules

It can be seen that the average particle remains overall constant when the PCL concentration increases. This is similar to what was observed for catalyst nanocapsules in Chapter 2, in which the use of PCL 45kDa led to a very small increase of the particle size. The PDI also remains in the same range, from 0.1 to 0.2.

The nanocapsules loaded with HD36 show an increase of the particle size, and of the PDI, proportionally to the increase of the PCL concentration (Fig. 5.2). This is also slightly different to what was observed in Chapter 2 and 3. The increase of the polymer means that diffusion rate of the acetone into water is reduced, which therefore leads to larger particles. However, this was not observed previously for PCL with lower molecular weights (Fig. 2.15).

The simultaneous increase of the PDI and the particle size indicates that the stability of the nanocapsules is reduced for higher concentrations of PCL. This could be explained by the difference of surfactant. This formulation is internally stabilized by HD36 but its surfactant capabilities are limited. For high amounts of PCL, the nanoparticle system needs to decrease its overall surface in order for the surfactant to work efficiently, therefore the particle size increases. This can also lead to the formation of more aggregates and to a higher PDI.

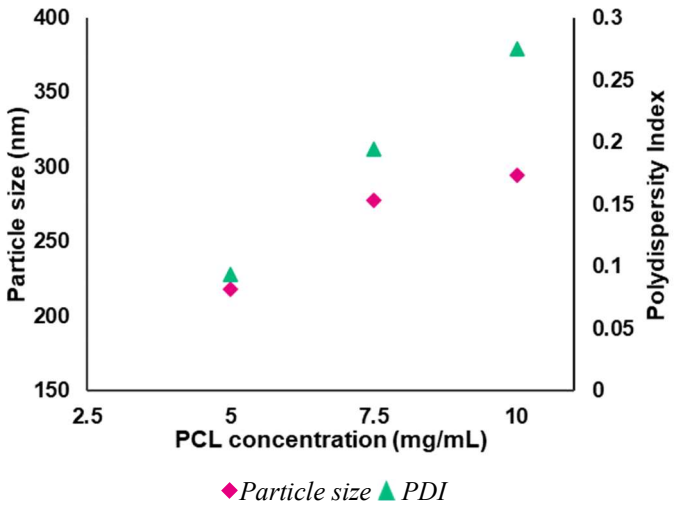

Figure 5.2. Effect of the PCL concentration on the particle size of HD36-loaded nanocapsules

The influence of the isocyanate concentration on the particle size was then studied; the PCL concentration was kept constant at $5.0 mg/mL$. Both nanocapsule systems showed a similar trend (Fig. 5.3). It can be observed that the particle size increases as a function of the isocyanate concentration. This was expected, as a higher concentration of isocyanates in each droplets means that each particle will be larger. It is also interesting to note that the system stabilized internally by HN36 leads to smaller nanocapsules. This is due to the outer layer made of Pluronic F-68 around DN36-loaded nanocapsules, whereas the HN36 stabilizes the system from inside the droplets.

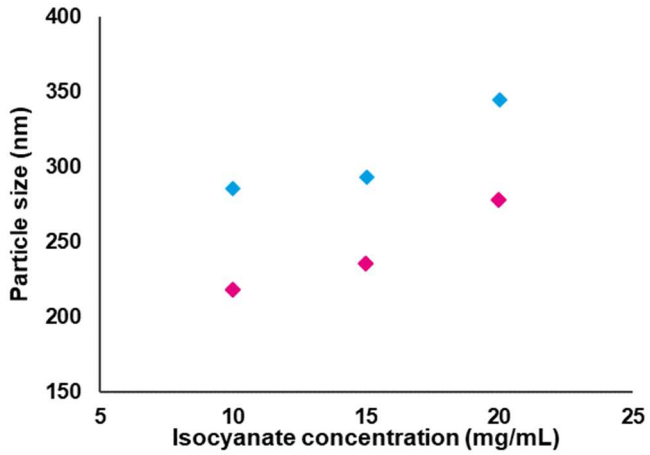

Figure 5.3. Effect of the isocyanate concentration on the particle size

In any case, the nanoparticle size is not an important parameter for the synthesis of polyisocyanate capsules. In fact, larger particles can have a higher core to shell ratio and would therefore be more suitable for applications in which they are used as cross-linkers. The study of the particle size was made in order to gain understanding of the nanocapsule synthesis. It revealed that both systems behave differently, probably because of the ability of the isocyanate to react with water, but they are both suitable for the encapsulation of polyisocyanates in terms of process.

The nanocapsule were then observed by FESEM, either as a suspension (Fig. 5.4) or lyophilized (Fig. 5.5). In the nanocapsule suspension, spherical nanocapsules can be observed in the same size range as measured by DLS, i.e. 200-400nm.

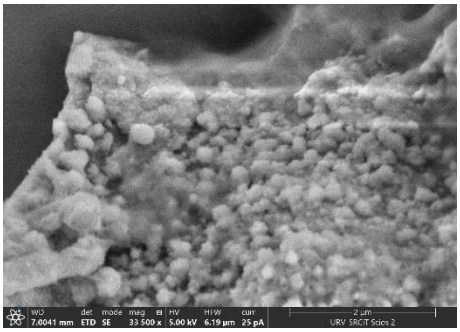

Figure 5.4. FESEM picture of a HD36-loaded nanocapsule suspension at ~x33k

The pictures of the lyophilized nanocapsules could not be of high quality. DN36-loaded nanocapsules melted very quickly when placed under the electron beam. This melting seems to be due to the Pluronic F-68 layer, as HD36-loaded nanocapsules were relatively stable. However, the HD36-loaded nanocapsule aggregates were compact, but it is still possible to guess the shape of each nanocapsule in the aggregate.

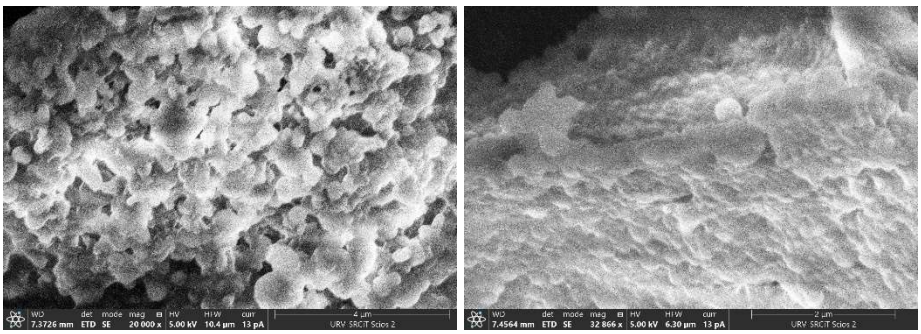

Figure 5.5. FESEM pictures of lyophilized DN36-loaded (left, x20k) and HD36-loaded nanocapsules (right, ~x33k)

The thermal behavior of the nanocapsules was investigated by DSC. Figure 5.6 illustrates the DSC thermograms of HD36-loaded nanocapsules at different concentrations of PCL and HD36. They all show that the polycaprolactone shells melt at about 60°C, close to the PCL melting point as anticipated[5], but another unexpected peak was detected between 100 and 150°C.

It can be seen that the peak intensity increases while the PCL concentration decreases and while the HD36 concentration increases. This peak is endothermic, which suggests the melting or the glass transition of another polymer, and corresponds probably to polyurea. Polyurea can be obtained by reaction between the isocyanates and water and this reaction is favorized at high isocyanate concentrations and also at low concentration of PCL, as the polymer is thinner. Shahabudin and coworkers reported that polyurea-formaldehyde microcapsules showed a melting point between 130 and 155°C[6] which matches the observation of this work. However, polyurea can have a wide range of melting temperature and glass transition temperature, therefore the nature of this endothermic peak could not be determined.

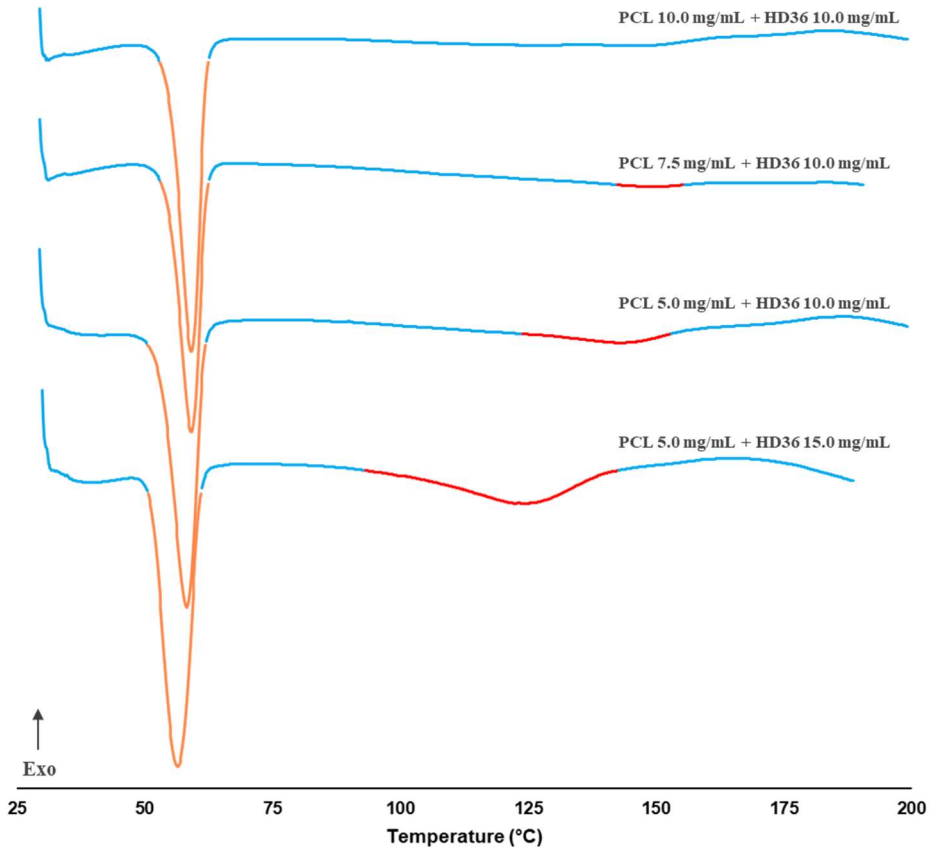

Figure 5.6. DSC thermograms of HD36-loaded nanocapsules

DN36-loaded nanocapsules were also analyzed by DSC. It was expected that the DSC thermograms would expose two peaks for Pluronic F-68 and the PCL, similar to what was seen in Chapter 3 (Fig. 3.19). This is indeed what can be viewed in Figure 5.7, but it is not the case for all thermograms. The intensity of the PCL peak logically reduces as the PCL concentration decreases, but it seems that the PCL and Pluronic F-68 peaks merge into one single peak at high concentrations of DN36.

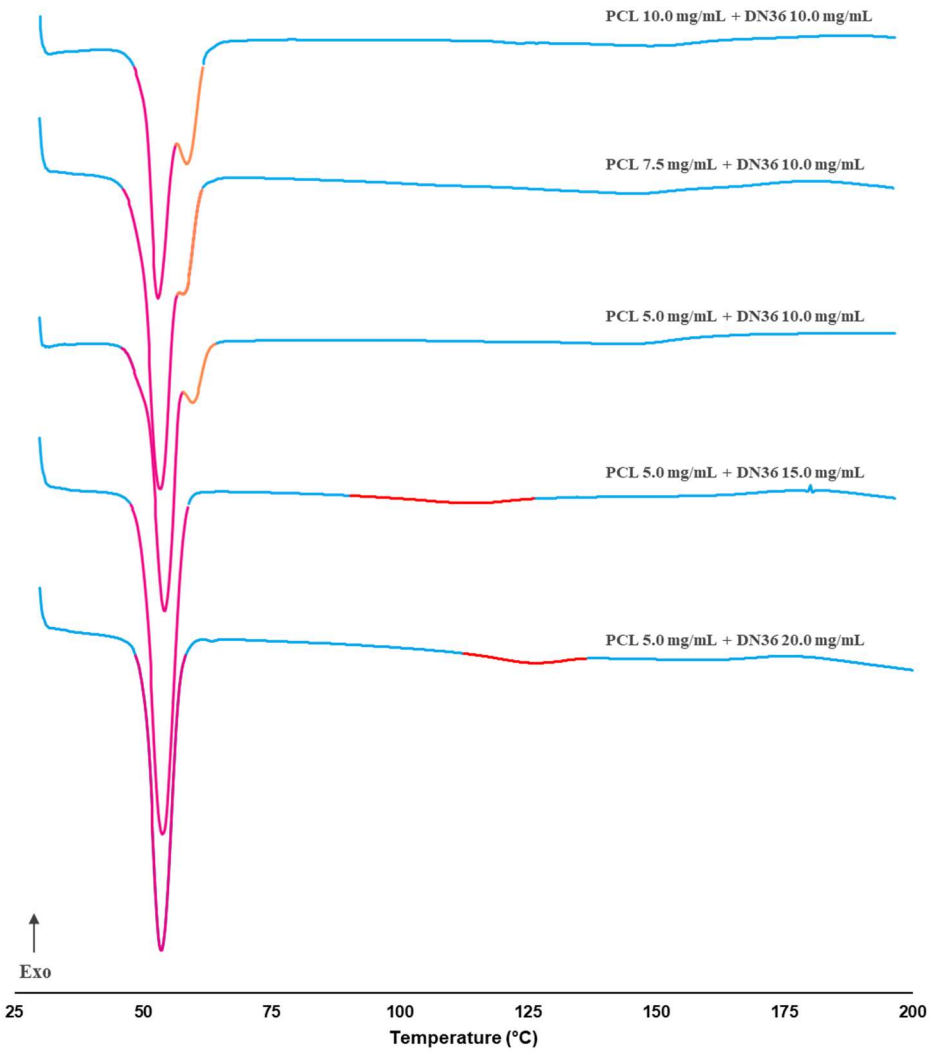

Figure 5.7. DSC thermograms of DN36-loaded nanocapsules

Some polyurea is also detected but only for high concentrations of DN36 and the peaks are less intense than for the previous nanocapsules. This can be explained by a better protection of the core material, thanks to Pluronic F-68 surfactant properties, which confirms what was observed earlier with the particle size. Moreover, HD36 behaves as a surfactant and its hydrophilic parts are located near the droplet interface, therefore some NCO-groups are also located near to the droplet interface in comparison to the nanocapsules stabilized with Pluronic F-68. This explains why more polyurea can be formed in the self-stabilized system.

These thermal analyses show that the ratio polymer to isocyanate is extremely important in order to limit the isocyanate-water side reaction. Therefore, an efficient encapsulation of polyisocyanates can be done at low concentrations of isocyanates or high concentrations of PCL. In both cases, it considerably limits the core-content of the nanocapsules.

Evaluation of the core-content and stability

The core-content of several nanocapsule formulations was measured by FTIR, 7 days after their synthesis (Table 5.1). Due to the relatively large amount of sample necessary to perform the analysis and the small amount obtained from each synthesis, the measurement could be performed only once, and the obtained core-content values could also be under-estimated.

Table 5.1. Core-content measured after 7 days for 6 formulations

PCL concentration (mg/mL)	Isocyanate	Isocyanate concentration (mg/mL)	Maximum Core-content (%)	Experimental Core-content (%)	Process efficiency (%)
5.0	DN36	5.0	25.0	19.4	77.6
5.0	DN36	10.0	40.0	31.3	78.3
10.0	DN36	10.0	33.3	27.6	82.9
5.0	HD36	5.0	50.0	32.7	65.4
5.0	HD36	10.0	66.7	34.8	52.2
10.0	HD36	10.0	50.0	37.4	74.8

Table 5.1 shows that HD36-loaded nanocapsules can in theory have a higher core-content than DN36-loaded nanocapsules, because they are not using any surfactant. Despite that, a higher process efficiency is obtained for the Pluronic F-68-stabilized nanocapsules. It can also be observed that the increase of the PCL concentration leads to slightly better process efficiency, which is consistent with the observations made from the thermal analyses.

The sample leftovers were kept for 2 months at room temperature. They were then crushed and analyzed by FTIR spectroscopy, which revealed that none of these nanocapsules had NCO remaining. This confirms that the encapsulated isocyanates can still react slowly with moisture. Therefore, in future works, the core-content could be measured over time, and especially in a dry environment, which could give to these nanocapsules a long-term stability. That would also allow to observe if the isocyanates are reacting with the surfactant or the PCL itself, as it has hydroxyl as ending groups. This lead to the conclusion that the nanoprecipitation is a reliable technique to perform the encapsulation of isocyanates, however, and similarly to Chapter 4, the long-term stability remains an issue, because of the water involved in the synthesis as well as the other materials isocyanates can potentially react with.

5.4. Conclusion

Nanocapsules loaded with aliphatic isocyanates were successfully synthesized. It was shown that the polymer to isocyanate ratio is a key parameter for this synthesis, as low concentrations of PCL or high concentrations of isocyanates led to the formation of undesired polyurea. These results can also be used to improve the encapsulation of catalysts, as it can be assumed that the encapsulation can be even greater at higher concentrations of PCL. It has been shown in this chapter that the encapsulation of polyisocyanates is challenging, mainly because of the high reactivity of isocyanates toward a lot of species. Therefore, new approaches of polyisocyanates should focus on limiting these possible side-reactions. Some chemical or physico-chemical encapsulation techniques could be considered, especially those adaptable with double emulsion. Such systems would avoid direct contact with water and could largely improve the long-term stability.

Nevertheless, encapsulation techniques based on physico-mechanical concepts might be even more adapted. Any extrusion techniques, such as centrifugal extrusion (Fig. 1.10), can be used to prepare microparticles with a polymer dissolved in a solvent, or even directly from a melt polymer such as in spray congealing. This technique would probably be the most relevant to explore, as the isocyanates could simply be mixed in a polymer with a low melting point, such as poly(ethylene adipate) ($T_m = 52°C$)[7], PCL ($T_m = 60°C$)[5] or high molecular weight poly(ethylene oxide) ($T_m > 60°C$)[8] and transformed into microparticles via atomization and cooling. This would have the advantage to be water-free, as well as very simple in terms of process.

5.5. References

1. Rawlins, J.W., H. Yang, and S.K. Mendon, *Nanoencapsulation of Isocyanates Via Aqueous Media.* 2008. **US20080234406A1**.
2. Yang, H., S.K. Mendon, and J.W. Rawlins, *Nanoencapsulation of blocked isocyanates through aqueous emulsion polymerization.* Express Polymer Letters, 2008. **2**: p. 349-356.
3. U. Meier-Westhues, et al., *Polyurethanes: Coatings, Adhesives and Sealants*. 2nd Revised Edition. 2019: Vincentz Network GmbH & Co. KG, Hanover, Germany.
4. Fessi, H., et al., *Nanocapsule formation by interfacial polymer deposition following solvent displacement.* International Journal of Pharmaceutics, 1989. **55**(1): p. R1-R4 DOI: 10.1016/0378-5173(89)90281-0.
5. McKeen, L.W., *13 - Environmentally Friendly Polymers*, in *Permeability Properties of Plastics and Elastomers (Third Edition)*, L.W. McKeen, Editor. 2012, William Andrew Publishing: Oxford. p. 287-304.
6. Shahabudin, N., R. Yahya, and S.N. Gan, *Microcapsules of Poly(urea-formaldehyde) (PUF) Containing alkyd from Palm Oil.* Materials Today: Proceeding, 2016. **3** DOI: 10.1016/j.matpr.2016.01.012.
7. Mitchell, G.R. and A. Tojeira, *Controlling the morphology of polymers : multiple scales of structure and processing*. 2016, Switzerland: Springer.
8. Pielichowski, K. and K. Flejtuch, *Differential scanning calorimetry studies on poly(ethylene glycol) with different molecular weights for thermal energy storage materials.* Polymers for Advanced Technologies, 2002. **13**(10-12): p. 690-696 DOI: 10.1002/pat.276.

Chapter 6. General conclusion

Polyurethane is one of the most common material for the preparation of coatings and adhesives, thanks to its excellent mechanical and chemical properties. However, they have a limited pot-life due to the high reactivity of the polyisocyanates. Therefore, smart systems in which the polyurethane formation can be triggered by external stimulus are highly valuable and this thesis investigated the preparation of such systems via the encapsulation of polyurethane formulation components.

The microencapsulation of polyisocyanates is a process which was already known for the preparation of self-healing materials and was applied in this work to the preparation of thermoresponsive adhesives. Polyisocyanates-loaded microcapsules were successfully obtained but, and despite great improvements, these microcapsules are not suitable to be used in polyurethane adhesives due to their limited long-term stability. Nanocapsules containing polyisocyanates were also successfully obtained and their thermal analyses also exposed a limited stability, due to the reaction of the encapsulating material with water. This suggests that new water-free approaches to encapsulate polyisocyanates should be considered, such as the spray-congealing encapsulation technique which stands out, as it would solely involve the polyisocyanates and the polymer material.

On the other hand, the encapsulation of polyurethane polymerization catalysts was a completely new approach for the preparation of thermoresponsive polyurethane systems. Catalyst-loaded nanocapsules were efficiently synthesized and their implementation in polyurethane coatings revealed the great usefulness of such formulations. The entrapment of the catalyst in nanocapsules reduces the polymerization reaction rate to a minimum, providing a significantly longer pot-lifes to polyurethane formulations, which is a direct improvement of their main drawback. Moreover, the controlled release of the catalyst by thermal activation at low temperatures offers a wide range of applications, including the coating of thermosensitive materials.

Annex A – Supporting information for Part 1

Annex A.1. Effect of the addition on the particle size (nanoprecipitation)

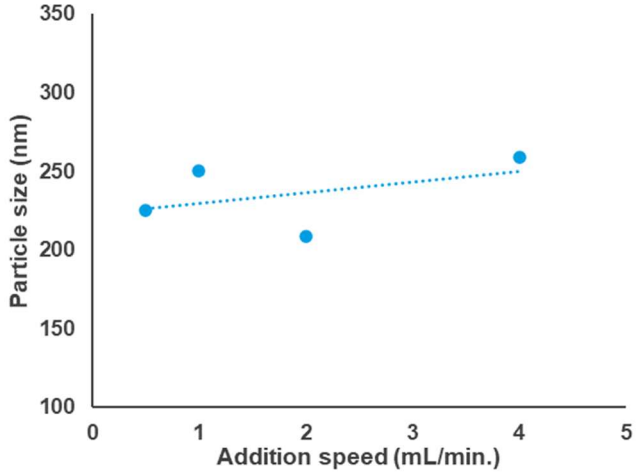

Annex A.2. CTAB-stabilized BK22/GTO5.0-loaded nanocapsules X-ray microanalysis on a nanocapsule (top) and on the dried area (bottom)

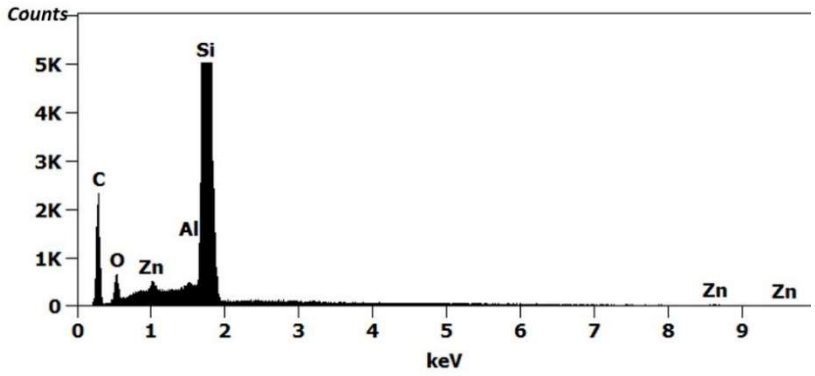

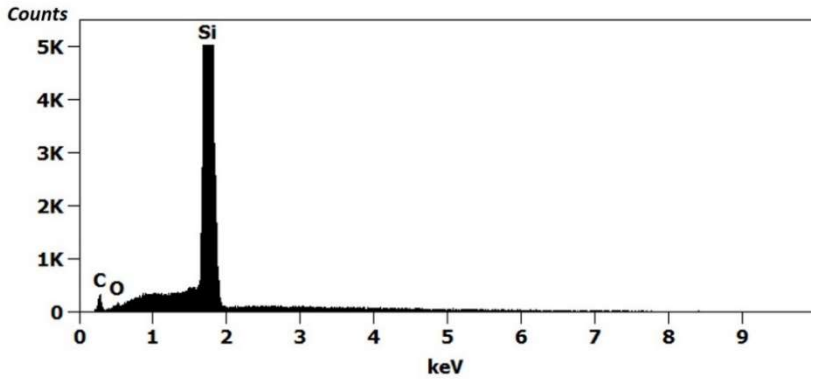

Annex A.3. CTAB-stabilized BK22/GTO7.5-loaded nanocapsules X-ray microanalysis on a nanocapsule (top) and on the dried area (bottom)

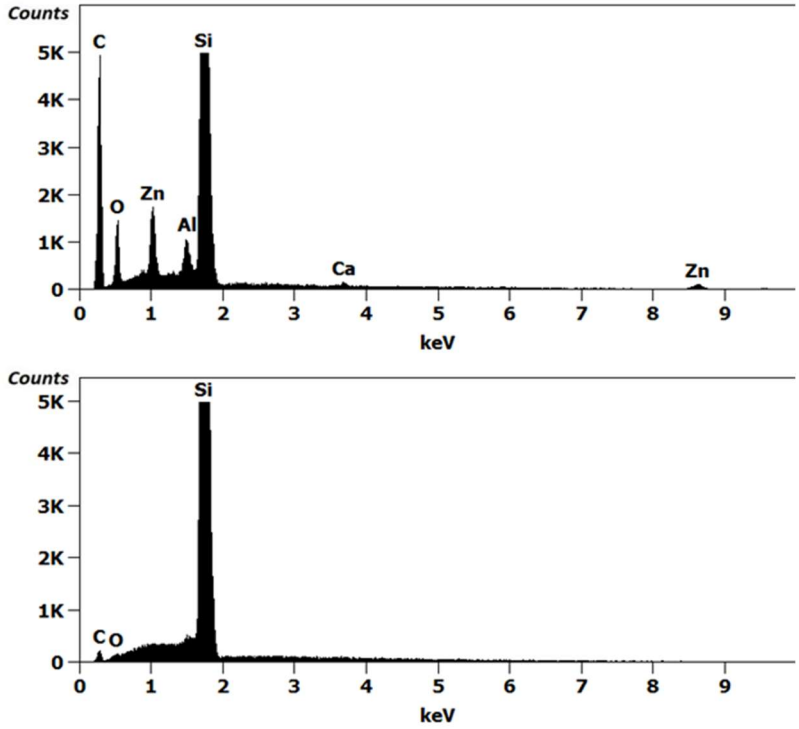

Annex A.4. Evaluation of the cross-linking temperature by DMA

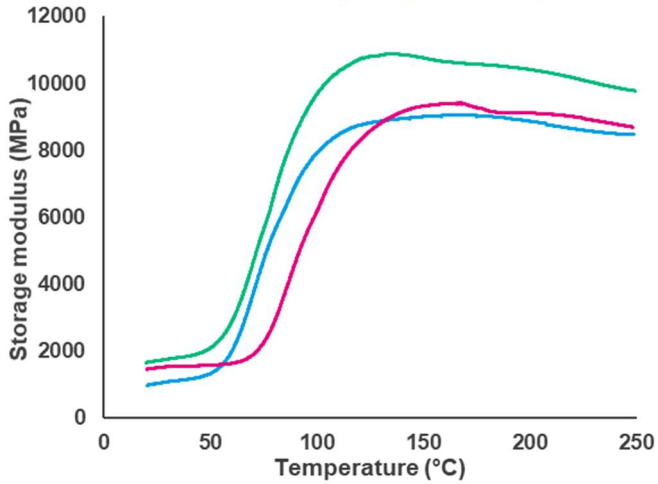

Catalyzed system, Nanoparticle system, Non-catalyzed system

Annex B – Supporting information for Part 2

Annex B.1. Calibration curve of HD36 in DMF

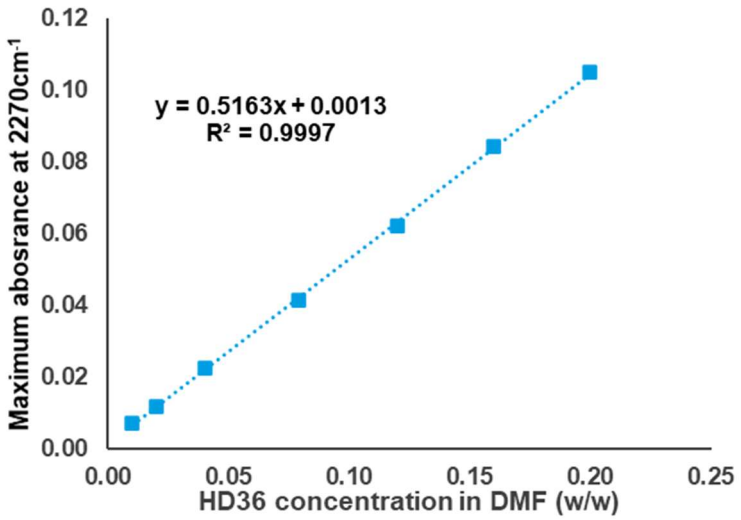

Annex B.2. Stability of the core-content over time for different surfactants (Desmodur IL EA)

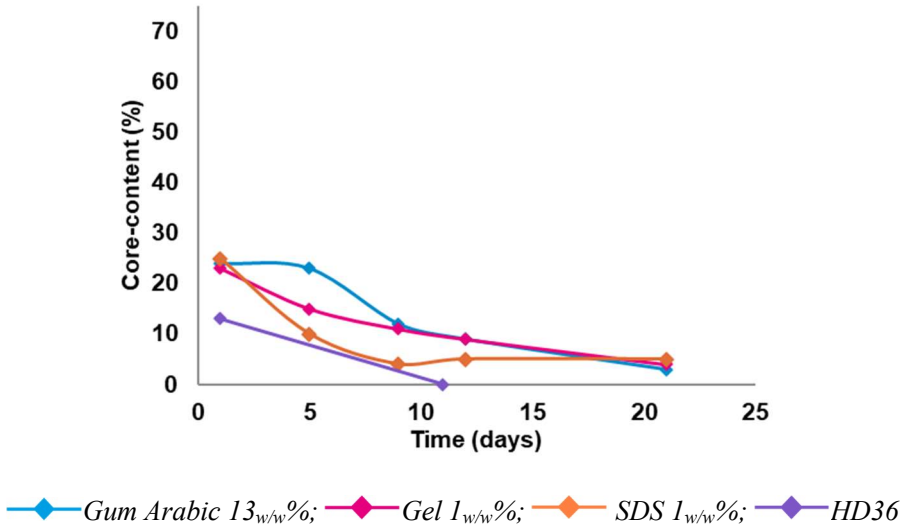

Annex B.3. Stability of the core-content over time for different surfactants (Desmodur RE)

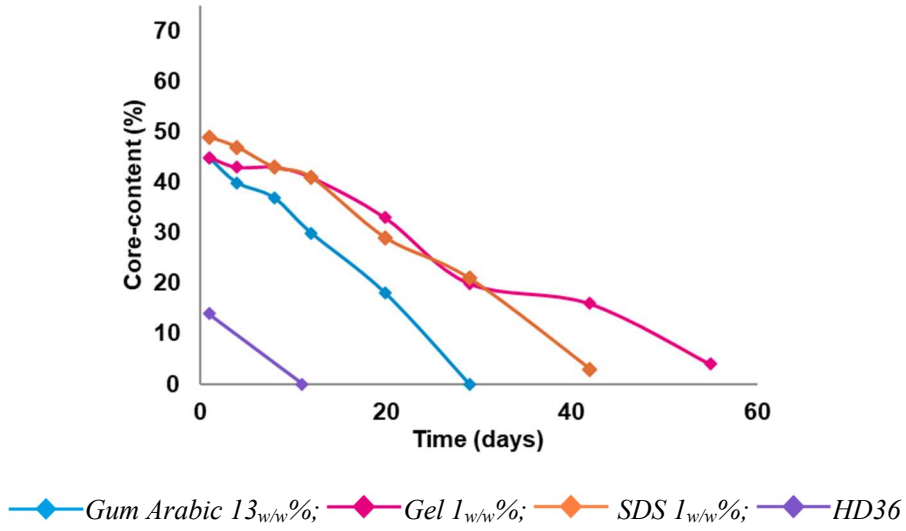

Annex B.4. Stability of the core-content over time for different surfactants (Desmodur L75)

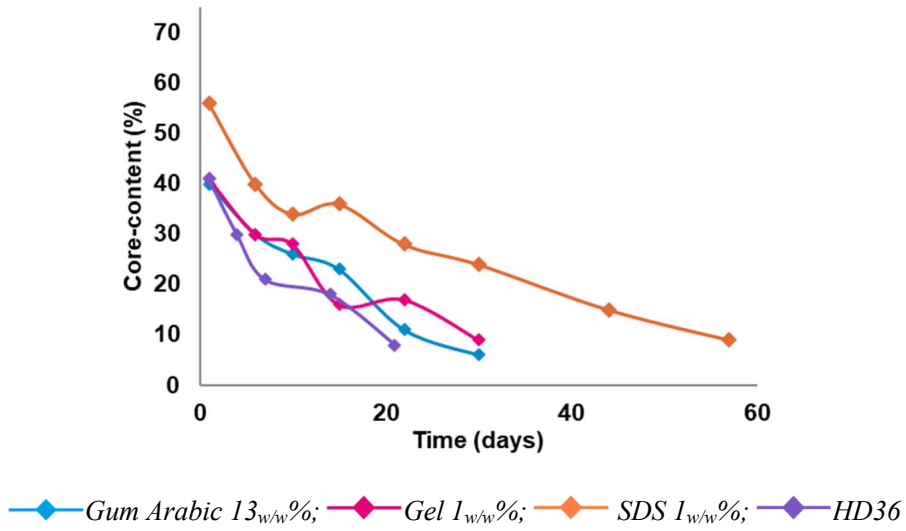

Annex B.5. Calibration curve of DN36 absorbance at 2270cm^{-1} in xylene

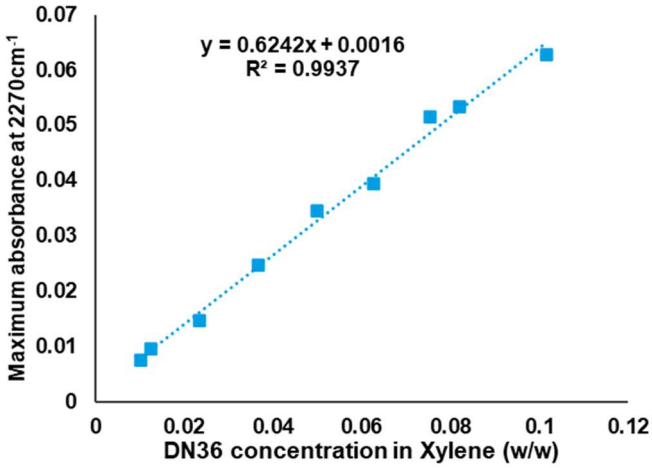

UNIVERSITAT
ROVIRA i VIRGILI